Intuitive Chemical Topology Concepts

Eugene V. Babaev

Moscow State University, Moscow 119899, *RUSSIA*

1. Introduction

During last two decades, chemistry underwent a strong influence from nonroutine mathematical methods. Chemical applications of graph theory [1–10], topology [11–18], and related fields of fundamental mathematics [21–27] are growing rapidly. This trend may indicate the birth of a novel interdisciplinary field, mathematical chemistry, imperceptibly flourishing on the border of chemistry and pure mathematics. The term "chemical topology" (the title of this volume) has become frequent in papers, books, and scientific conferences. Similarly, the term *molecular topology* (differing in its sense from *molecular geometry*) has become frequently used, although there may exist diverse viewpoints on the meaning of this concept. The key difference between topology and geometry is that in geometry the concepts of distances and angles are important, whereas in topology they are not. Instead, the essential topological properties are connectedness and continuity. Chemical structural formulas are good examples of topological models of molecules: the pattern of connectivity between atoms is essential, whereas the interatomic distances and angles are less important and may be neglected.

A colloquial definition of topology is "rubber" geometry. Indeed, one may consider a topological object made of an ideal elastic material, so that any deformation (like stretching or distortion) retains points of this elastic object "close enough" one to another. In contrast, cutting separates previously close points, and any joining of parts makes points "closer" one to another. Such a continuous transformation of an object without cutting and joining any parts is called *homeomorphism*. (The term should not be confused with homomorphism.) The study of properties that are invariant to homeomorphic transformations is the fundamental goal of topology. Molecules are nonrigid objects: they may undergo conformational changes and bond stretching (as evident from molecular spectroscopy) without deterioration of their integrity. Hence, these "inessential" geometrical changes of the same molecule may be clearly related to the homeomorphism [28].

The concept of homeomorphism has one more meaning. It is not only a change of the *same object* (to itself), but it is also a continuous, reversible mapping of one topological object to another. In other words, it is a sort of a global identification of *different objects.* In contrast to the geometrical equivalence of figures (congruency), topological equivalence (homeomorphism) is a finer and more general relationship. The homeomorphism differs from isotopy, a manner of embedding of an object into a space; thus, an ordinary torus and a knotted torus are homeomorphic but not isotopic. The homeomorphism concept offers a fascinating liberty of identifying apparently different objects, like a needle and a pipe or a doughnut and a coffee cup. These objects with quite different geometrical properties have homeomorphic 2*D* surfaces, which can be continuously deformed one to another or to the same surface of a torus. The hole (or tunnel or cavity) in every one of these objects is preserved upon deformations. Another, less evident, example of homeomorphism is the equivalence between a punctured sphere, a hemisphere (with no boundary around the hole), and a plane. The hole in the hemisphere and the hole (of another type) in the torus are topological invariants preserved in homeomorphic transformations. Equality in the number of topological invariants may indicate that the objects are homeomorphic.

The interpretation of the homeomorphism concept just discussed may be suitable for chemistry. Equalization of different molecules by arranging them in series is a long-standing chemical tradition, and periodical and homological classifications are examples. In these classifications, the sets of related atoms or structures are grouped together into similarity classes according to some important numerical invariants (number of valence electrons, saturation degree, etc.). Are these invariants topological? Is it possible to treat chemical similarity as a sort of homeomorphism of molecular models? This aspect of the homeomorphism concept has never been comprehensively investigated in chemistry, at least as a global phenomenon. The difficulty is evident: how to relate *discrete* chemical structures by *continuous* mapping? The complementary 2*D* models of molecules are apparently more suitable, and there is no difficulty to imagine continuous mapping of one 2*D* model to another. However, a serious question arises, whether the topological invariants of such surfaces are unequivocally defined. For instance, some fundamental chemical concepts (free radicals, centers of Lewis basicity and acidity, multiple and multicentered bonds) are ill-defined in terms of 2*D* models and even in terms of molecular graphs.

In the present paper we treat chemical similarity in terms of the homeomorphism concept and electron count rules. We suggest a novel interrelationship between molecular graphs and molecular 2*D* surfaces by direct mapping of chemical structures (like the Lewis dot formulas) to the specific 2*D* manifolds and pseudomanifolds. We define this mapping in such a way that the lone pairs, free radical centers, and multiple and multicentered bonds serve as the intrinsic topological invariants of the 2*D* models. This approach (a generalization of our earlier works [29-33]) allows us to apply the homeomorphism concept to chemical problems in a new way, classifying molecular structures and reactions from the viewpoint of the topology of surfaces.

The structure of the paper is the following. Section 2 recalls several concepts of the graph theory and topology of surfaces, necessary for further discussion, and Section 3 is the overview of the common types of molecular graphs and molecular surfaces used in chemistry. In Section 4 we treat the concepts of free radicals, lone pairs, and multiple bonds as *intuitively topological* concepts, whereas Section 5 provides an explicit definition and visualization of their topology on the graph-theoretical level. In Section 6 we suggest an explicit mathematical concept of *molecular topoid*, which visualizes the lone pairs, free radicals, and multiple bonds as sorts of "holes" in an appropriate 2*D* surface. The topoid (a "rubber 2*D* molecule" without geometry) is a novel combinatorial 2*D* image of molecule, intermediate between ordinary surfaces and graphs. Operations on topoids (resembling cut-and-paste operations of a topologist with imaginary 2*D* manifolds) reflect the key types of formation and cleavage of chemical bonds. In Section 7 we suggest a novel conservation law, the invariance of Euler characteristic of molecular topoids, and use it for classifying the chemical reactions. Section 8 has the goal to illustrate, how the homeomorphism of topoids brings together diverse molecular similarity types in a unique manner. In Section 9 we prove that the explicit 2*D* image of a graph should be a surface with embedded Jordan curves, and in Section 10 the nonequivalent types of embedding are used to expand the common principles of 2*D*

modeling in chemistry. In Section 11 we use the generalized concept of *hypertopoids* to classify the structure and reactivity of molecules with multicentered and delocalized bonds on the 2*D* level. Finally, in Section 12 we investigate the possibility of 2*D* modeling of the excited states of molecules with several unpaired electrons by using nonorientable surfaces.

2. Some Useful Concepts of Visual Topology

Expecting that the audience of the readers will be diverse (and may equally include chemists and topologists), the author provides an elementary introduction into the concepts of graph theory and of the topology of surfaces. A mathematician may ignore this section and go directly to the Section 3, whereas a chemist is advised to accept some important topological terms and concepts presented below, because they are necessary in our further discussion. Considering the tradition of *visual topology* useful in education [34-37], we substitute (wherever possible) the complex algebraic expressions by visual images. As Hermann Weyl stated, "The angel of topology and the devil of abstract algebra fight for the soul of every individual discipline", and we may add to this, "the angel of *visual* topology". More advanced discussions may be found in handbooks on graph theory [38-41], topology of surfaces [41-46], and general topology courses [46-49].

2.1. Graphs

A *graph* may be treated either as an abstract or a topological object. An abstract graph G is an ordered pair (V,E), where V is nonempty set of elements (*vertices*) and E is a set of pairs of vertices, called edges. In the topological sense, a graph is a finite set of V points (vertices) connected by E edges (represented as curved uncrossed arcs homeomorphic to a closed interval). Any graph may be embedded in the space R^3 so that its edges are not self-crossed, although this may not always be possible for a graph embedded in the plane. A *multigraph* has several edges between a pair of vertices. A *loop* is a specific curved edge adjacent to the same vertex, and a *pseudograph* is a multigraph with loops, (Figure 1).
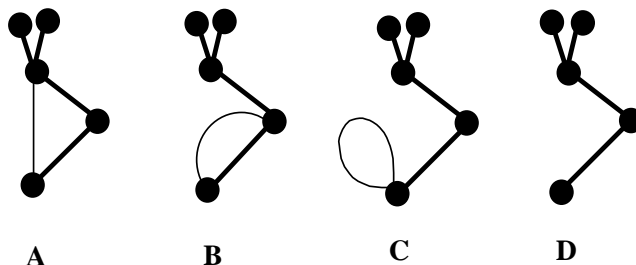

$$ \textbf{A} \qquad \textbf{B} \qquad \textbf{C} \qquad \textbf{D} $$

Figure 1.   Examples of graph (A), multigraph (B), and pseudograph (C) with cyclomatic number C = 1. Removal of a cyclic edge results in a tree (D). All four diagrams together form a single disconnected pseudograph having 4 components and 3 cycles.

The *degree of vertex* v_i (denoted as deg v_i) is the number of edges adjacent to this vertex; each loop adds 2 to the degree of the vertex. Therefore, the sum of degrees of vertices is twice the number of all edges (including loops):

(1) Σ deg v_i = 2 E

A graph may be *connected* or *disconnected* (consisting of K components). A *cycle* is a closed path in the graph (a sequence of edges ending with the initial vertex). A cycle in a graph is homeomorphic to a circle. A loop is also a cycle of unit size, and the simplest multiple edge (two edges joining two vertices) forms a cycle of size two. A graph without cycles is a *tree*. The *cyclomatic number* C of a connected graph is the integer:

(2) $C = E - V + 1$,

The value C is not the total number of cycles one may find in a graph, rather it is the number of *independent* cycles. (If C edges are removed step-by-step keeping the intermediate graph(s) connected, the remainder is a tree.) The cyclomatic number is an additive property, and for the set of disconnected graphs with K components and total C cycles (see Figure 1) formula (2) may be rewritten as (3):

(3) $C = E - V + K$

Graphs are *isomorphic* if there is a one-to-one correspondence between their vertices, edges, and adjacencies of vertices. Graphs may also be *homeomorphic*. To obtain a homeomorphic graph, subdivide any edge of a graph by a vertex (giving rise to pair of adjacent edges) or shrink (if possible) two edges adjacent to a vertex of degree 2 to a new edge.

In a *bipartite* graph, vertices may be labeled by two colors, so that no vertices of the same color are adjacent. The colors of vertices in a bipartite graph alternate, therefore, the cycles are of even size only. Any graph can be converted to a certain bipartite graph by a (homeomorphic) subdivision of *every* edge by a vertex.

2.2. Hypergraphs

The concept of the *hypergraph*, a generalization of the graph concept, was introduced in 1970s by Berge [50] and Zykov [51]. A hypergraph is a pair (V, E) of vertices and (hyper)edges, where a hyperedge is any subset (not only a pair, as in a graph) of the set of vertices V. The hypergraph H(V,E,R) has an *incidentor* R(V,E), that assigns adjacency of a vertex to an edge. Hence, in hypergraphs not only several edges may be adjacent to the same vertex (as in pseudographs), but also any number of vertices (not only two, as in a graph) may be adjacent to the same edge. Any hypergraph has the König representation by a usual bipartite graph (a König graph) with two colors standing for vertices and hyperedges of the hypergraph. A hypergraph has a planar representation (Figure 2A), where a hyperedge is homeomorphic to a bounded 2*D* disk containing incident vertices. The adjacency of

hyperedges is an overlapping of two disks in the neighborhood of a vertex (Figure 2A).
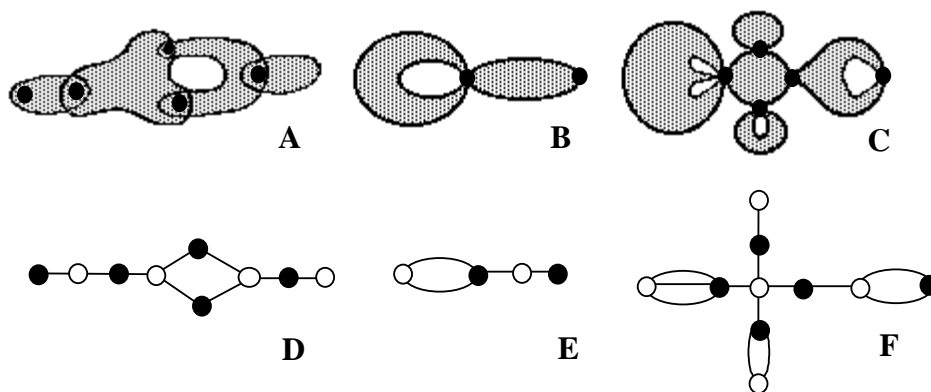

Figure 2. (A) Example of a hypergraph; (B) Example of a pseudograph (with edges represented by 2D disks) treated as a pseudo-hypergraph graph. (C) Example of a pseudo-hypergraph with three different hyperloops and one terminal hyperedge. (D), (E), (F): Representation of (pseudo)hypergraphs for cases (A), (B), (C) by bipartite graphs (König graphs). Black color is used for vertices in (A) -- (F). Vertices of white color in (D), (E), (F) represent images for hyperedges and hyperloops in (A), (B), (C).

It is possible to assign a cyclomatic number to a hypergraph (either to its planar representation or to the corresponding König graph). However, this concept has a serious limitation in respect of considering pseudographs with loops as particular cases of hypergraphs. The possibility of the existence of loops in hypergraphs is completely ignored [50,51], and the only suitable analog of a loop is a "terminal" edge. Let us assume that the adjacency of two disks (hyperedges) occurs precisely at one point, which coincide with a vertex. Then it is possible to imagine a "self-incident" hyperedge (a *hyperloop*) as a deformed disk mutually adjacent to the same vertex. A simple example is shown in Figure 2B; here the "usual" pseudograph is drawn as a planar hypergraph with edges substituted by deformed disks. Hence, the concept of hypergraphs may be further generalized, and let us call a hypergraph with hyperloops a *pseudo-hypergraph*. This concept (introduced by the present author in 1987 [32]) opens the possibility of counting cycles (including hyperloops) using an analog of formula (3) for graphs. Of course, a self-touching hyperloop is also homeomorphic to a disk (as usual hyperedge), but it has "holes" (degenerate cycles) and cannot be shrunk into a terminal edge. By contrast to usual edges and loops (in pseudographs), a hyperloop may serve as an edge, multiple edge, and a loop in the same time. The König graph of a pseudo-hypergraph should have multiple edges (Figure 2F).

2.3. Surfaces

A closed 2D *surface* is an example of connected 2D *manifold.* Generally, an n-dimensional manifold is a (Hausdorff) space, such that the neighborhood of every point is homeomorphic to an open n-dimensional disk. Thus, an object is a 2D-manifolds if an imaginary 2D disk can be drawn around *any* point. Such a disk can be further deformed to a planar disk, and therefore, a closed 2D surface (2D manifold) is "locally flat" in all its points. Examples of *closed* connected surfaces are a sphere and a torus, as well as a sphere with any number of pasted *handles* (like surfaces of a pretzel or a rotary telephone disk). These surfaces are *orientable*, since one may define an orientation in 2D neighborhood of a point, consider a closed path of this point around the surface, and prove that initial orientation is preserved. The well-known theorem states that the total set of orientable closed surfaces is exhausted by the family of spheres S_C with C pasted handles. The number of handles is also known as the *genus* of the surface. Some familiar examples of surfaces are presented in Figure 3.
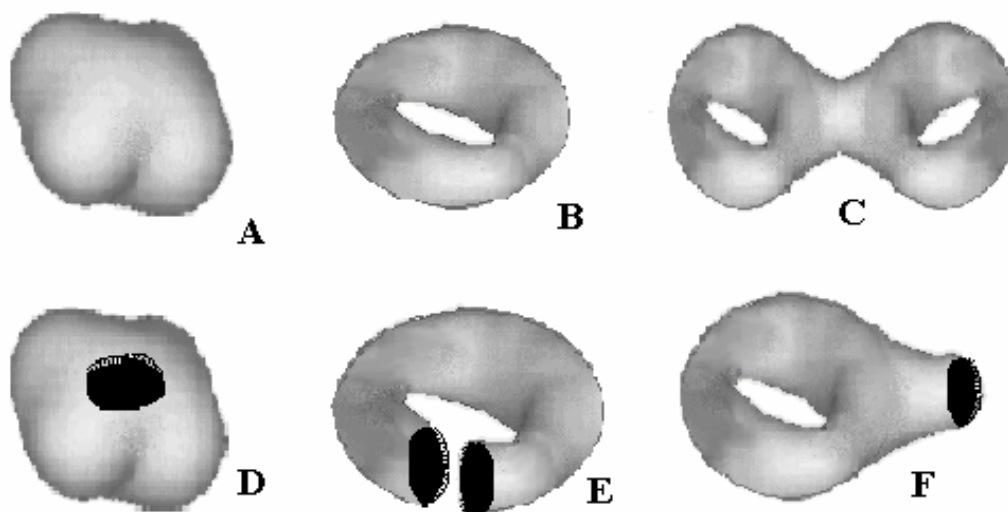

Figure 3. Examples of closed (A, B, C) and open (D, E, F) orientable 2D surfaces.

A sphere with L *punctures* or round *holes* (^{L}S) is orientable, but it is open (nonclosed) surface. We can make the puncturing larger by "stretching" the puncture to a hole. The points on the border of the hole no longer belong to the remaining surface. The punctured sphere ^{1}S is homeomorphic to a hemisphere (without equator points), to an open disk (without $1D$ boundary), and to a plane, as evident from the stereographic projection of punctured sphere onto other surfaces. The sphere with two punctures ^{2}S is equivalent to the cylindrical surface of a tube or to an annulus (of course, without $1D$ borders).

An operation called the *connected sum* of surfaces allows one to construct new surfaces. To visualize this idea, consider two surfaces, remove a disk (make round hole) in each surface, and connect disjoint surfaces by pasting a cylindrical tube onto the boundary of each hole. The number of punctures and handles are additive with respect to this operation. Thus, $^mS_p\#^nS_q\sim^{m+n}S_{p+q}$ (symbol # designates the connected sum operation, and symbol ~ means homeomorphic).

The genus and punctures of orientable surfaces are numerical invariants preserved upon topological transformations. Finally, the full family of compact orientable surfaces (closed or not) with a finite number of handles and punctures is completely classified by surfaces ^LS_C. (The canonical form for such a family may be a sphere with C+L holes, of which C holes are pasted by handles.)

A Möbius band (or Möbius strip), like a cylinder, is an open surface. However, this is an example of a *nonorientable* surface (see Figure 4). The projective plane (4A) and the Klein bottle (Figure 4D) are also nonorientable surfaces, but they are closed in the same sense as a sphere or a torus. The projective plane is the self-crossed surface in the R^3 space, but not in R^4, and it can be also imagined as the Möbius band (4C) pasted around boundary of a hemisphere. Therefore, the projective plane may be equivalently drawn as a hemisphere with pasted "self-crossed cap" (Figure 4B).
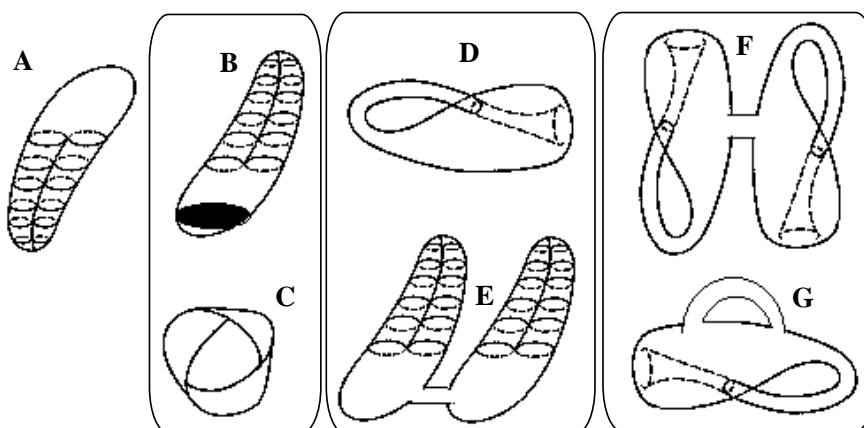

Figure 4. Nonorientable surfaces and their homeomorphisms. Homeomorphic pairs of surfaces are placed in rectangles.

The Klein bottle is a connected sum of two projective planes or a sphere with two holes pasted by self-crossed caps (4E). A connected sum of two Klein bottles (4F) is the Klein bottle with a handle (4G). The complete family of closed nonorientable surfaces is exhausted by sphere with L holes each pasted by self-crossed cap.

2.4. Euler Characteristic

The architecture of topological objects may be better understood in terms of their subdivision (or partition) into *cells*, a set of joint "primordial" elements. The e^n cell is homeomorphic to an open n-dimensional disk without its $(n-1)$ boundary, and it is required that the boundary of a cell in such a partition belongs to the union of these cells. The e^0 cells are points, and the e^1 cells are the open intervals (like edges in graphs and polyhedrons with e^0 boundary points removed). The e^2 cells are open disks (like internal parts of polygons without any $1D$ boundary), and the e^3 cells are open "solid balls" without the $2D$ boundary (like a milk inside a carton). Of course, the e^n cells are homeomorphic to R^n spaces (line R^1, plane R^2, or usual space R^3), and the elements from R^{n-1} space may serve as cells for the subdivision of space R^n. For instance, the usual Cartesian coordinate system (considered as three crossed orthogonal planes R^2) is a subdivision of space R^3 into cells.

The most important property of any subdivision into cells is the alternating sum (4) known as the *Euler characteristic* χ

(4) $\chi = a_0 - a_1 + a_2 - a_3 + ... = \Sigma (-1)^n a_n$,

where a_n is the number of e^n cells. The value of alternating sum (4) is independent on the number and mutual arrangement of elements used for subdivision. The simplest example is the subdivision of a line (space R^1) by any number of points: evidently, a_0 points (cells e^0) always subdivide a line into $a_1 = a_0 + 1$ segments (cells e^1), so that $\chi(R^1) = -1$. Partitions of a plane by several lines (shown in Figure 5) are more diverse. However, the value χ remains invariant either for the case of parallel lines ($a_0 = 0$) or for the case of lines crossed at any number of points (appearance of e^0 cells). Therefore, $\chi(R^2) = 1$. For the Cartesian coordinate system (taken as a partition of space R^3) there are: one cell e^0 (center of the coordinate system), six cells e^1 (semi-axes from 3 axis), twelve cells e^2 (quarters of 3 planes) and eight cells e^3 (octants of space). Finally, $\chi(R^3) = 1 - 6 + 12 - 8 = -1$.
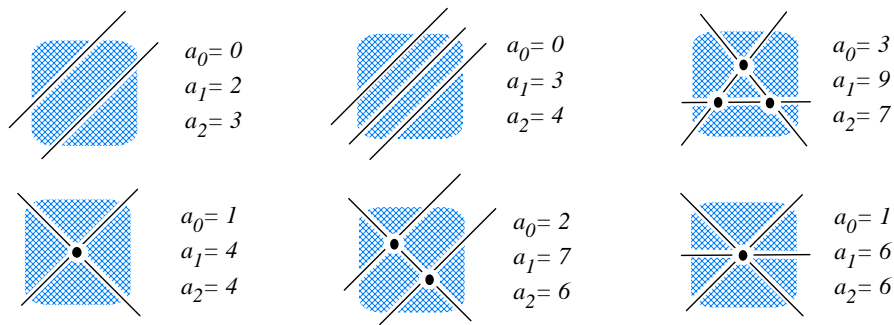
Figure 5. Arrangement of two and three lines on the plane as different subdivisions of the space R^2 (plane) into cells (e^0, e^1, e^2); a_i is the number of elements e^i. The alternating sum $\chi(R^2) = a_0 - a_1 + a_2 = 1$ is invariant to the number and arrangement of lines.

The Euler characteristic is one more intrinsic topological invariant. A graph consists of only e^0 and e^1 elements, and its Euler characteristic is defined by formula (5):

(5) $\chi(G) = a_0 - a_1 = V - E = K - C$

The Euler characteristic of an orientable closed surface S_C may also be defined in terms of a partition of the surface into e^0, e^1, and e^2 elements. The simplest idea of such a partition is the *triangulation* of a surface. For instance, consider a hollow tetrahedron or octahedron (with removed faces) each inside a sphere. A triangulation appears when such a hollow polyhedron is projected outwards onto the sphere that surrounds it. (Alternatively, a polyhedron with curved edges may simply be drawn on a surface.) For the sphere $\chi(S_0) = 2$, and this result is the famous Euler theorem:

(6) $\chi(S_0) = a_0 - a_1 + a_2 = V - E + F = 2,$

where V, E, and F are the numbers of vertices, edges, and faces of the convex polyhedron. (The polygons on the faces of a polyhedron generally may differ from triangles, but may be further triangulated without changing χ.)

The triangulation of a torus S_1 results in $\chi(S_1) = 0$. (An example of the torus triangulation is a prismatic block with a tunnel.) The closed surface S_C with C pasted handles has $\chi(S_C) = 2 - 2C$. To calculate χ for sphere ^LS with L punctures or holes, one should consider that some elements (e^0 for punctures and e^2 for holes) are removed, and the Euler characteristic is decreased by this value. The presence or absence of the 1D border around a hole is inessential for calculating of χ. Since this boundary is a circle (with $a_0 = a_1$) it does not contribute to the χ value. Therefore, for a punctured sphere ^LS (or sphere with holes bounded or not), $\chi(^LS) = 2 - L$. For disconnected sets, χ value is additive over the set, and the disconnected union of K orientable surfaces { ^LS_C }$_K$ has the following value of χ:

(7) $\chi (\{ ^LS_C \}_K) = 2 K - 2C - L$

The total value of χ does not uniquely characterize the given surface or set of surfaces. There may be degeneracy in χ for nonhomeomorphic connected surfaces as in the case of a torus or a cylinder, where $\chi (S_1) = \chi (^2S) = 0$. Similarly, the χ value of a connected surface may coincide with that of a disconnected set. Evidently, $\chi = 2$ for a sphere, for a pair of disconnected hemispheres, and for a disjoint ensemble of a sphere and torus.

A specific type of topological objects is represented by *pseudomanifolds* (or *wedges* of surfaces), where the parts of different surfaces (or the same surface) are pasted one to another. The simplest examples of such object are the spaces with *base point(s)*, like the *bouquets of spheres* (several spheres joined by only one point) or a "pinched" torus (a stretched and bent sphere that touches itself at a single point), see Figure 6.
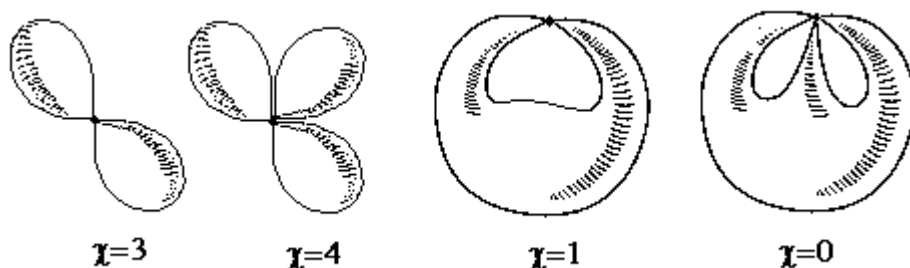

Figure 6.   Examples of pseudomanifolds: bouquets of spheres and self-touching 2D surfaces.

Of course, these objects are not 2D manifolds anymore, since the neighborhood of a contact point is nonhomeomorphic to a planar disk. Nevertheless, these complex objects may still be investigated by the usual methods, *e.g.*, by partitioning them into cells and calculating their Euler characteristic. For instance, consider removal of the contact point from the bouquet of k spheres. This operation results in the disjoint set of k+1 components (one point e^0 and k punctured spheres ^1S). Each component has $\chi = 1$, therefore, the initial object has $\chi = k + 1$. Note that the value of χ for any connected and orientable 2D surfaces never exceeds 2 (since $\chi (^LS_C) = 2 - 2C - L$). By contrast, the pseudomanifolds are examples of connected objects with value χ higher than 2.

2.5. Surfaces and Polygons

In some specific cases, a partition of a 2D surface into cells may consist of unit e^2 cell. Thus, a sphere consists of one cell e^2 and one cell e^0. A torus consists of one cell e^2, one cell e^0, and two cells e^1 (crossed meridian and longitude), and. The origin of such an "economical" partition of a torus becomes clear if we cut the torus along its longitude and meridian, geting a rectangle with one e^2 cell, and then, restore the same torus by gluing it from the rectangle. Namely, one should join the opposite sides of a rectangle, obtaining a cylindrical tube, and subsequently paste the holes of resulting tube to get a torus. Mapping of a rectangle to a torus (so that some e^0 and e^1 elements are identified by pasting) is an example of *factorization* of a topological object. However, the manner of gluing is essential: twisting of the same rectangle before gluing results in a Möbius band. Let us assign vectors to the sides of rectangle (collinear if the sides are opposite) and call the gluing to be either of "true type" (if collinear vectors are identified) or of "false type" (if the identified vectors have opposite directions). Then, the cylinder is constructed by the true-type gluing, whereas the Möbius band, by the false type. Closed surfaces may be obtained from rectangle by consecutive *"true + true"*, *"true + false"*, and *"false + false"* types of gluing, and they are the torus, the Klein bottle, and the projective plane, respectively.

Alternatively, various combinations of vectors may be placed on the sides of polygons, and only "true-type" gluing (of collinear vectors) considered (see examples in Figure 7). Generally, the closed and orientable surface S_C may be always obtained from an appropriate polygon, namely, 4C-gon.
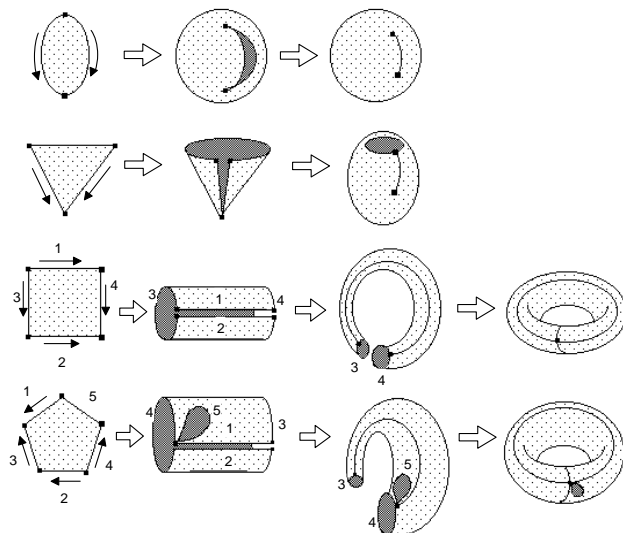

Figure 7. Gluing polygons to orientable surfaces. Numbering and orientations of the polygon sides prompt which sides should be pasted to one another (without twisting). Remaining points and lines on the surface on the right are e^0, and e^1 cells in partition; e^2 cell is shaded).

2.6. Graphs and Surfaces

Usually, the graphs and surfaces are treated as quite different objects since they consist of different e^i elements, and the cycles of a graph are usually not considered as e^2 cells. An important problem is embedding of a graph on a surface: generally, a graph may subdivide a surface into regions, and the number of regions depends on the cyclomatic number of the graph, the genus of the surface, and the manner of embedding. Thus, a monocyclic graph (*e.g.*, a vertex with one loop) may subdivide a torus into two regions or not subdivide it at all. The exact answer exists for the plane: the graph G(V,E) with C cycles and K components divides the plane into r regions so that r = E - V + K + 1 (r = C + 1 for a connected graph). The cycle of a graph is homeomorphic to a closed curve, and the Jordan theorem states that the closed curve (Jordan curve) separates the plane (sphere) into two regions. However, in the general case, the Jordan curve may not subdivide the surface at all as a single meridian (or a single longitude) does not subdivide a torus. The coloring of geographic maps on a surface (*cf.* the famous four-coloring problem for the plane) is another example where the concept of a graph is helpful in the topology of surfaces. Here a *dual* graph is assigned to a map (vertices represent the regions on a map, and the edges are "roads" between regions, crossing the borders).

Hence, the common interrelation between graphs and surfaces is the embedding of a graph on a surface (or simply, it is "a graph *on* a surface"). However, there may be another, somewhat paradoxical, interrelation: "a graph *as* a surface". This interpretation appears if one tries to make a *model* of a topological graph in the *real* 3D world, say by drawing it on paper or joining threads or wires. Indeed, in the real world, where there are no abstract lines (or curves) with zero thickness, a point drawn in ink is a 2D disk (or even flattened 3D ball), and a thread has a 2D surface homeomorphic to a sphere. This sort of *intuitive* mapping is an intriguing mathematical problem, and the bijective (one-to-one) mapping of a graph to a surface with Jordan curves will be discussed in Section 9. (This idea, initially presented by the author in 1986 [52, 53] to an audience of both chemists and mathematicians, has appeared in late 80s in Russian language handbooks on graph-theory [40] and topology [49].) An intuitive mapping of graphs to surfaces is closely related to the principles of modeling in chemistry (see [54-60] and references therein), since any solid model of a molecular graph always has 2D surfaces.

3. Explicit Concepts of Molecular Topology

The above set of visual topology concepts may enable us to check whether the terms "molecular graphs" and "molecular surfaces" are well-defined from the topological viewpoint. What is the precise meaning of a cycle in a molecular graph and of a

hole in a molecular surface? Finally, what is (or what could be) the meaning of the homeomorphism concept for chemical structures?

3.1. Classical Chemical Models

Molecular graph. In a common sense a molecule may be considered as a set of points in the space R^3 (atoms) connected by lines (interatomic bonds). This picture intuitively resembles a graph (in the sense of a graph embedded in R^3). Classical chemical structures drawn on paper or on a computer display may be treated as graphs embedded in plane R^2, although the points are not always visible and are frequently masked (labeled) by symbols of chemical elements. The edges may also be labeled (dashed or bold) to simulate outward appearance of a molecule as the geometrical object in R^3.

This picture is explicit only if an edge represents the localized bond (two-electron and two-centered bond), for instance, in the case of saturated hydrocarbons [61] of general formula C_nH_{2n+x} ($x \leq 2$). Consider the family of acyclic hydrocarbons ($x = 2$, alkanes) and alicyclic hydrocarbons (with ordinary cycles of size 3 and higher). For this class of compounds the concept of connectedness is certain: the connected molecular graph and disconnected set of K components are easily distinguishable, since an edge is assigned to only strong CC or CH intramolecular bonds, and the existence of weak intermolecular bonds may be neglected. Since valencies (for carbon 4 and for hydrogen 1) are not variable, the fundamental formulas (1) and (2) for the cyclomatic number of an abstract graph are equally valid for a molecular graph. The number of vertices $V = N$ (N is the total number of atoms), and the number of edges $E = Z/2$ (Z is the total number of valence electrons), since the electrons are grouped in pairs. Hence, the cyclomatic number for the series C_nH_{2n+x} follows equation (8a) and may be expressed as the balance between the number of localized bonds and number of atoms:

(8a) $C = E - V + 1 = (Z/2) - N + 1$,

For the series C_nH_{2n+x}, we have $Z = 6n + x$, $N = 3n + x$. Therefore

(8b) $C = 1 - x/2$

Hence, the cyclomatic number of a molecular graph is independent of n value, and the value x should be even. It is clear why $x \leq 2$: the case $x = 2$ is the series of alkanes (the graphs are trees, $C = 0$), and the cases $x>2$ correspond to disconnected sets of hydrocarbons. The matching is perfect, and x (the deficiency or excess of hydrogen atoms) is known as the degree of saturation.

Molecular surface. A formal $3D$ body with a well-defined $2D$ boundary may be assigned to a molecule. The $2D$ boundaries appear in various molecular models, say, in the space-filling models, in the van der Waals (frequently abbreviated to VDW) surfaces, and even in the classical ball-and-stick models made of various solid materials (Figure 8).
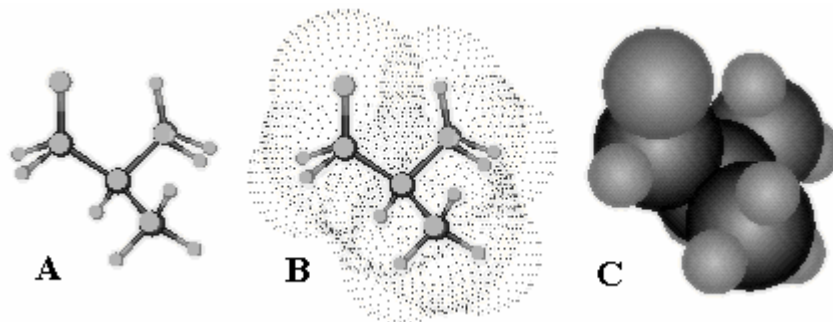

Figure 8. Typical visualization of classical $2D$ molecular models in software programs. Ball-and-stick model (A), Van der Waals $2D$ surface (B) presented by dots, and space-filling model (C) of 2-methylpropane molecule.

Such $2D$ models are widely used in chemical practice, education, and scientific publications, and various tool-kits for molecular modeling are described in literature [54-60] and commercially available (see, e.g., a list of suppliers [61]). It is commonly implied that $2D$ boundary of any solid $3D$ model is a closed and orientable $2D$ surface, that falls into the definition of $2D$ manifold. At the present state of art, $2D$ surfaces may be quickly calculated and visualized on the computer display with the help of various computer software programs.[*)] The shift from a graph to a surface is regarded to be trivial: points should be substituted by overlapping van der Waals spheres of certain diameters, and the external surface around $3D$ body is the desired $2D$ molecular surface. Furthermore, this mapping is also considered reversible and one-to-one. Thus, in many software programs, one may click a mouse in menu option to switch from a graph to an appropriate $2D$ model and reverse.

Therefore, the mapping of a graph to a $2D$ object is usually *not* a problem in molecular $2D$ modeling. Rather, the common problems are related to the manner of visualizing a $2D$ model on the computer display, like seeking better shading algorithms or making a VDW surface smooth [65, 66]. Here, there may be a confusion. Thus, it is convenient to represent the surface of a large biomolecule by the *solvent accessible surface* [67], rigorously defined as a trace of a probe sphere rolling around VDW surface [68, 69]. However, a rolling sphere can mask a cavity (hole) in the initial VDW surface, and the final $2D$ object from topological viewpoint may be *another* $2D$ surface.

Homeomorphism in C_nH_{2n+x} series. Intuitively, any monocyclic hydrocarbon molecule (with ordinary cycle in its molecular graph), presented at the level of $2D$ models, has a surface homeomorphic to a torus. This is not true for the solvent accessible surfaces (the trace of rolling sphere could mask a hole in the VDW surface), however this is correct for the space-filling, VDW, and ball-and-stick models. Therefore, these three types of $2D$ models of polycyclic hydrocarbons C_nH_{2n+x} have more or less pronounced holes, whereas $2D$ surfaces of alkanes have no holes at all. Of course, every hole in $2D$ surfaces appear from a cycle in molecular graphs, namely, a torus appears as a cyclic sequence of overlapping VDW spheres. It is easy to conclude that the genus of the $2D$ surface of the hydrocarbon C_nH_{2n+x} is equal to the cyclomatic number of a parent molecular

graph. This may be proved, considering a mapping between the molecular graph of a hydrocarbon and the 2D surface of its a ball-and-stick model, that is actually a "solid" model of a graph.

The equality of the genus (for a 2D surface) and the cyclomatic number C (for a graph) for the series C_nH_{2n+2} opens the possibility for calculating the Euler characteristic in terms of the balance between electrons and atoms. Let us combine equation (7) for the genus of surfaces S_C and the balance equation (8) for hydrocarbons and arrive at (9a):

(9a) $\quad \chi = 2 - 2C = 2 - 2[(Z/2) - N + 1] = 2N - Z$

By expressing Z and N for series C_nH_{2n+x} with the numbers n and x, we get (9b):

(9b) $\quad \chi = x$

Hence, the index x is nothing else but the Euler characteristic of the 2D surface of hydrocarbons. Thus, the surface of 2D model of any alkane C_nH_{2n+2} is a sphere ($\chi = x = 2$). The surface of any cycloalkane C_nH_{2n} is a torus ($\chi = x = 0$). Generally, the surface of any polycyclic hydrocarbon C_nH_{2n+x} is a sphere with C handles ($\chi = 2 - 2C = x$). For disconnected sets equation (9a) should be rewritten as:

(9c) $\quad \chi = x = 2K - 2C = 2N - Z$

The case x>2 is impossible for a connected surface S_C (for which χ can not exceed 2, see Section 2.4). Thus, for the "hypersaturated" class C_nH_{2n+4} any molecule should immediately fall into disconnected set of two molecules, each with the spherical surface from the C_nH_{2n+2} class (*cf.* equation $C_2H_8 = CH_4 + CH_4$).

[*] An overview of molecular surfaces and software programs for their visualization in now available in the World Wide Web, see the web page [63]. (For citing the electronic information one may refer to the book [64]).

Evidently, when applied to hydrocarbons the homeomorphism concept turns out to be the very old chemical concept of CH_2 homology: within the class of given x, the structures are homeomorphic. Of course, the genus does not distinguish the geometry or the shape of objects. Therefore, any geometrical isomers, stereoisomers, and even branched or linear structures are homeomorphic. The genus is also insensitive to the size (of a chain or a cycle). Therefore, 2D models of methane and polyethylene (saturated on the ends of the chain) are topologically indistinguishable.

A chemist may guess, what the homeomorphism is actually like: it is the order of arranging hydrocarbons in the famous and commonly used Beilstein handbook (which was first published at the end of the last century!) [70]. The statement about homeomorphism is, therefore, an explication of intuitively trivial idea, namely, similarity in homological series. This is a good sign, because it means that there exists a nice reference point to which any uncertain case of homeomorphism in molecular models may be related. Let us keep this result in mind (because it will be useful in further Sections) and express the interrelations of (molecular) graphs and surfaces in visual form (Figure 9).
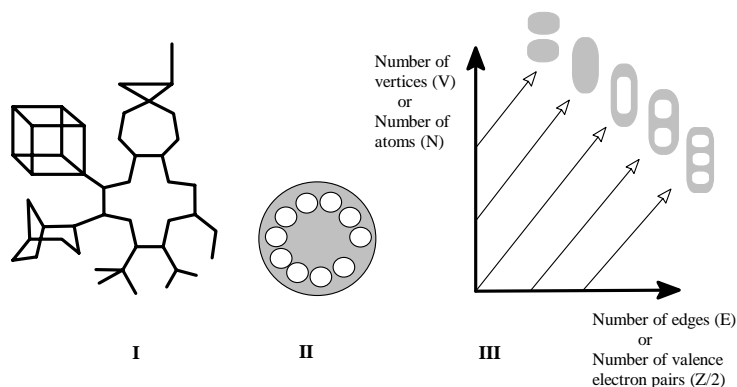

Figure 9.   (I) A molecular graph of a polycyclic hydrocarbon with the cyclomatic number of ten (hydrogen atoms are omitted). (II) 2D surface assigned to this graph is homeomorphic to the surface of a telephone disk with the genus of ten. (III) Graphical visualization of formulas (3), (7), (8a), (9a) as interrelations between indices of abstract graphs (V, E) and surfaces (C, K), and between molecular graphs (Z, N) and surfaces (C, K) for (cyclo)alkanes. Diagonal lines correspond to arrangement of isocyclic (molecular) graphs with homeomorphic (molecular) surfaces.

3.2. Graphs and Surfaces in Physical Models

In contrast to this clear picture of classical chemistry, the pure quantum chemical viewpoint is the opposite: the molecule is neither a graph nor a surface. It has neither a precise 2D boundary, nor definite features to which 1D elements (bonds of a graph) may be assigned. Even the arrangement of the nuclei (the prototypes for vertices of a graph) is uncertain, because they also obey principles of quantum mechanics. Instead of a graph or a surface, a diffuse 3D body with an fuzzy boundary serves as a purely physical image of a molecule. Of course, even very clear topological concepts of connected and disconnected sets look somewhat vague within such a model.

Molecular graphs in physical models.   Nevertheless, it is possible to reconstruct the familiar concepts of a molecular graph and a molecular surface from the quantum-chemical model, although each time we need such a graph or a surface, some calculations should be carried out. According to the approach of Bader [71 -- 73] molecular graphs may be "extracted" from the 3D picture of charge density as follows. The topology of charge density $\rho(\mathbf{r})$ may be characterized by its gradient $\nabla\rho(\mathbf{r})$, which, in turn, allows the discrete combinatorial description. The properties of $\rho(\mathbf{r})$ (which is the scalar field in R^3) are totally determined by the number and nature of its critical points, *i.e.*, the points at which the field vanishes. There are only four types of such critical

points, and they correspond to local maxima, two types of saddle critical points, and local minima (see Figure 10).
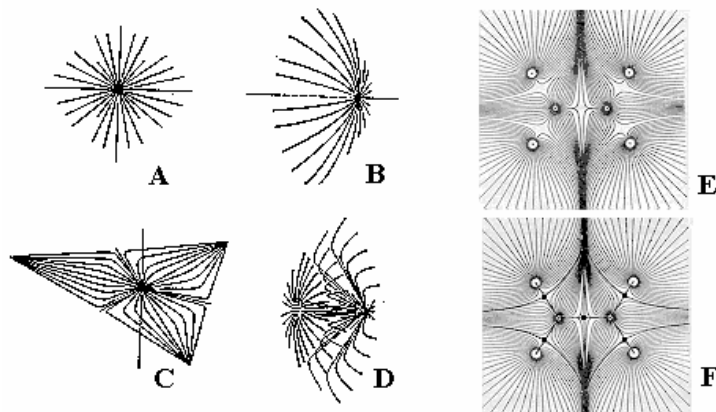

Figure 10.   Visualization of critical points by the pattern of trajectories traced out in their neighborhood by the gradient vectors. A: local maximum (3,-3); B: saddle point (3,-1); C: local minimum (3,+1); D: saddle point (3,+3). The first number in brackets (always 3) is the rank of a critical point (the number of nonzero eigenvalues of the Hessian matrix); the second value is the signature of the critical point, that is, the excess of positive values over negative ones. E: arrangement of trajectories for a molecule. F: design of a bipartite graph from points (3, -3) and (3, -1). Reproduced with kind permission of Professor R. F. W. Bader.

As proven by calculations, local maxima (3,-3) always appear at the position of nuclei. Saddle points (3,-1) are located in the "bond path," a line that connects two local maxima. Therefore, these two types of critical points may correspond to the vertices and edges of a molecular graph. Fortunately, the (3,-1) saddle points are found to appear just at those pairs of atoms that are presumed to be bonded in the chemical sense. In addition, saddle points (3,+1) may be found inside rings (formed by bond paths connected three or more nuclei), and the remaining local minima (3,+3) -- inside cages (formed by four or more nuclei and bounded by at least three cycles). The molecular graphs obtained for molecules with localized bonds (*e.g.* of saturated hydrocarbons C_nH_{2n+x} with large cycles), are usually isomorphic to the conventional graphs. Furthermore, certain graphs may be attributed to molecules with delocalized bonds, for which drawing a graph within classical models is impossible. It is worth noting that Bader's graphs are usually drawn as *bipartite graphs*, because any edge (connecting vertices that are local maxima) is subdivided by a vertex, that is, (3,–1) saddle point.

Molecular 2D surfaces in physical models.   Molecular 2D surfaces (of various types [16, 28, 63, 74, 75]) can also be extracted from physical models of molecular structures. The key idea of most methods is to take a 3D function F(r) and consider the contour surface F′(A) = {r: F(r) = A}, where the function F(r) is equal to some specific parameter value A. For instance, the function F(r) may be the electronic charge density ρ(r). In the general case, the set F'(A) defined in such a manner is a 2D surface (isodensity surface) that surrounds all those points where the electronic charge density is higher than the selected value A. Of course, an accurate choice of the value A may result in the appearance of a closed connected 2D object that resembles familiar molecular surfaces (like VDW surface). In particular, one may visualize the toroidal structure of a monocyclic molecule (say, of cyclohexane) by fixing the scanning parameter of the contour surface (see Figure 11A), whereas in *n*-hexane no such hole can be found at all. The operation seems valid for the general case of the series C_nH_{2n+x} with large cycles.
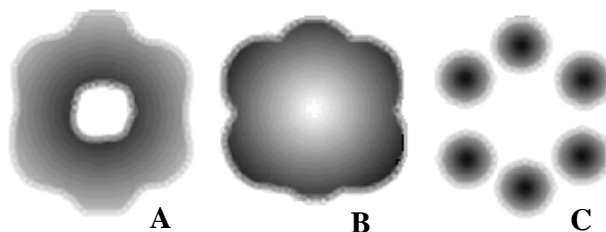

Figure 11.   Schematic representation of a cyclic molecule by a set of nonhomeomorphic contour surfaces with respect to the value of scanning parameter F'(A) = {r: F(r) = A}. For a monocyclic molecule, a toroidal surface (A) may collapse to a sphere (B) or *vice versa*, diverge into a disconnected set of spheres (C).

The obvious difference of this quantitative approach from classical qualitative 2D models is that the genus (and even connectedness) of molecular 2D surface thus obtained is a relative rather than absolute property. For small values of A (deficiency of electron density) the isodensity surface becomes a loose, essentially spherical balloon surrounding all nuclei (Figure 11B). Therefore, the topological difference between cyclic and acyclic molecules (that are intuitively not homeomorphic) disappears. For large values of A (excess of electron density) the contour surface is represented by a disconnected set of several essentially spherical surfaces, each surrounding one nucleus (Figure 11C). Similar results may be obtained if the function F(r) is the molecular electrostatic potential [28, 63]. Here, the parameter A may have both positive and negative values. Therefore, in some cases the surface may not be closed and/or only portions of molecular entity are displayed by contour surfaces. An important aspect of utilizing contour surfaces is the study of the arrangement of convex and concave domains with the tools of algebraic topology [28]. This problem is important and relevant to molecular recognition.

The representation of a molecule by a *set* of contour 2D surfaces *instead of one* surface is an interesting concept of chemical topology; one may study the abrupt changes in molecular topology varying continuously the scanning parameter A. However, the dependence of the fundamental topological properties - - like connectedness and cyclicity -- on some artificial

empirical parameter A (used to obtain the contour surfaces) seems to be distant from the problems where the homeomorphism concept may be fruitful.

A specific sort of 2*D* models appears in molecular orbital (MO) theory [76, 77]. The electron wave function (and signs assigned to its parts) has only indirect physical meaning, nevertheless a contour 2*D* surface may be defined in a usual manner (for a fixed value of a parameter A) for any molecular orbital. Although 2*D* contour surface of a separate MO does not represent the entire molecular surface, some important MOs (like frontier orbitals essential from chemical viewpoint) may be homeomorphic for different molecules. The topic is extensively reviewed [17, 18, 75 -- 79] but will be outside of the scope of this article because of the following reason. The picture of essentially delocalized MOs is poorly compatible with the classical picture of localized bonds (which forms the background of the molecular graph concept). A graph may serve as an input for calculating the properties and topology of MOs (say in the Huckel method [80, 81] or in the model of localized orbitals [82 -- 85]). However, only an indirect image of a graph can be reconstructed from an orbital (or from the complete set of MOs). The cyclomatic number of molecular graph, therefore, is *not* a concept of MO theory.

4. Intuitive Chemical Concepts Related to Topology

Intuitive cut-and-paste. Consider the relation between a chain and a cycle, *e.g.*, between *n*-hexane C_6H_{14}, which does not have cycles, and the closest family of monocyclic isomers C_6H_{12} having a cycle with three to six carbon atoms. A chain in an abstract graph (drawn on paper) is easily converted to a cycle by simply adding a new edge somewhere in a tree (Figure 12A). However, it is impossible to create the molecular graph of cyclohexane by adding a new edge to the molecular graph of hexane. This would violate vertices' degrees, which are constant according to the context of our consideration. Instead, it is necessary to remove two hydrogen atoms first, and then join the emerging "free valencies" to a cycle (Figure 12B). Free valences have direct experimental evidence [86]: these are free radical centers.

The closure of a cycle by stepwise removal of hydrogen atoms and formation of a bond is an intuitive topological process. The operation resembles cut-and-paste procedure in the topology of surfaces. The removal of two hydrogen atoms is cutting (making two holes), and formation of the C–C bond is gluing the holes. Generally, the choice of the pairs of hydrogen atoms to be cut from the *n*-hexane chain may be random, and the mental pasting should, indeed, result in 5-, 4-, and 3-membered cycles, all isomeric to cyclohexane. An example of such "cut-and-paste" from hexane C_6H_{14} to propylcyclopropane C_6H_{12} is shown in Figure 12C, F.
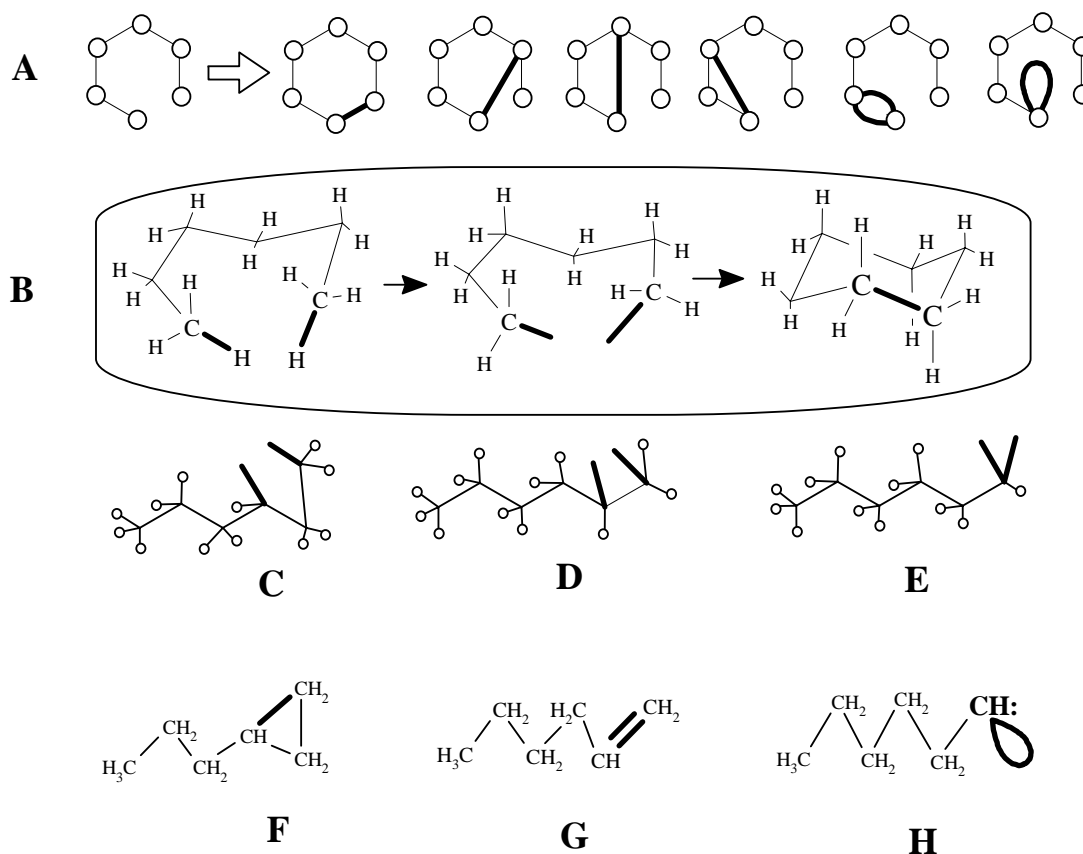

Figure 12. (A) Conversion of a chain into a cycle in an abstract graph by drawing a new edge. (B) The same process shown as a "cut-and-paste" operation in molecular graphs; free valencies are shown in bold. (C), (D), (E) Random choice of two hydrogen atoms for cut in the structure of hexane. A monocyclic molecular graph (F), a multigraph (G), and a pseudograph (H) (represented by common structures) obtained after pasting of free valencies in diagrams (C), (D), and (E).

One may easily imagine the cut of two hydrogen atoms adjacent to a neighboring carbon atoms (as in Figure 12D). In this case the mental cut-and-paste results in the formation of a double bond, familiar to chemists [87], and the structures are isomeric *hexenes* C_6H_{12} (e.g., Figure 12G). Finally, the pair of removed hydrogen atoms may even be incident to the same atom (Figure 12H). Here, the mental cut-and-paste should result in the appearance of an edge incident to the same vertex, that is, in a loop (Figure 12D). Although this situation is less trivial, such a class exists and is familiar to an organic chemist. These are *carbenes* [88] where the "free valencies" are joined together into a lone pair. Random cut-and-paste in *n*-hexane molecule results in

three isomeric carbenes of the C_6H_{12} formula.

The mental picture discussed above is related to the *intuitive chemical topology*: a double bond and a loop of carbenes (the lone pair) are intuitively indistinguishable from larger cycles, at least in their origin (*cf.* all diagrams in Figure 12). However, the concepts of a lone pair and a multiple bond are in conflict with physical models. Furthermore, although a lone pair is an important chemical concept used for decades, it is still ill-defined even in terms of graphs or surfaces. The same is true for the modeling of free radicals. The situation appears somewhat paradoxical: lone pairs, free radicals, and multiple bonds are responsible for essential changes in molecular topology (like interconversions of chains to cycles and disconnected sets to connected ones), and chemists yet have a poor idea of how to express them in graphs or surfaces. Let us overview some aspects.

Double bond. The concept of multiple bonds (double or triple) appeared during the last century. The goal of this concept was to preserve the valence of a carbon atom in an unsaturated compound, and now the multiple bond notation is beyond any question in the chemical literature [87]. The multiple edge naturally falls into the definition of a molecular multigraph with a "two-membered" cycle, because its appearance (as the appearance of any larger cycle) increases the cyclomatic number of a multigraph by one, and the subsequent removal of a double bond (like the destruction of a cycle) produces a tree. In early ball-and-stick models, the double bond was presented by two bent cylindrical tubes, and the $2D$ surface of such a solid $3D$ model is, of course, homeomorphic to a torus. The intuitive argument, approving these models of the double bond, is clearly related to the homeomorphism concept. If any member of the family of cycloalkanes C_nH_{2n} (no matter the size of a cycle) matches topology of the torus ($x = \chi = 0$), then it is natural to consider C_2H_4 (n = 2) as being a specific case within this series.

In the space-filling and VDW models, the atoms forming a bond are considered to be spherical domains. Here, the model of a cyclic molecule C_nH_{2n} has a toroidal surface formed by overlapping spheres; even three spheres may be adjacent in such a way to leave a hole. However, in the case of double bond, it is impossible to imagine a hole between two adjacent spheres; the multiple contact A=B is reduced to a single contact. Therefore, the decrease in the cycle size (say, from 3 to 2) within the series C_nH_{2n} results in the shift of the toroidal feature to the spherical one, in contrast to the homeomorphic shrinking of a large cycle to a bent bond in the ball-and-stick models. Such a pronounced conflict in the topology of two traditional models of a double bond is a serious problem in chemical education. The author remember a handbook for secondary school students that recommended: "to make a double bond, one should take a solid ball and put two matches (or sticks) inside". Also, in some modern computer programs the choice of the "ball-and-stick" option in the menu results only in *one* stick for C=C bond.

The elegant idea of the "banana-like" double bond [89, 90] in the valence bond theory [91] perfectly matches the classical bent bonds. Also, in MO theory the principle of *localized* orbitals may be used to visualize double bond in somewhat similar manner [85]. Two pairs of localized orbitals doubly overlap resembling a bent multiple bond. However, this does not mean that the *toroidal* feature of a bond is reflected in molecular orbitals. First, orbitals have nodes at atoms. Second, the equivalent picture of a C=C bond (one σ- and one π-bond) corresponds to at least triple overlap of *p*-orbitals in different regions (one contact in the plane of a C_2H_4 molecule and two contacts higher and lower the plane), as if it would be the topology of a pretzel.

The concept of bent "banana-bond" contradicts some other physical models. Thus, the isodensity contour surface for ethylene provides no evidence for the expected "emptiness" between bent bonds (which is observed for larger cycles). On the contrary, there is an excessive charge density for the double bonds. Also, there is no appropriate "cycle-like" critical point for the C=C bond in the gradient of the electron density $\nabla\rho(\mathbf{r})$, and the Figure 10F (just the case of ethylene) displays the absence of a feature that may resemble larger cycles. Therefore, the extracted bipartite graph of an alkene C_nH_{2n} in the Bader's model [71--73] is a tree rather than a multigraph. As a compensation, the concept of ellipticity of bonds is used to describe the difference between single and multiple bonds. Hence, the supply of topological objects in physical models of a double bond is diverse (sphere, torus, pretzel, etc.), and the models themselves are frequently revisited.

Free radicals and open-shell molecules. The thermal or photochemical decomposition of saturated hydrocarbons results in highly reactive short-living species, free radicals [86]. Although the precursors have well-defined molecular graphs and $2D$ surfaces, the products have not. Radicals have unpaired electrons, and there may be several unpaired electrons as in a biradical molecule (like O_2). It is still unclear how to combine these "free valences" with the molecular graph concept. In the Lewis dot formulas [92, 93], the radical center is a single dot near an atomic symbol. In the Linnet double-quartet theory [94], an odd number of dots may appear between a pair of atoms. Because free electron has a spin, an oriented arrow is frequently assigned to the free radical center to indicate direction (the sign) of the spin. In triplet states, the arrows are collinear (Hund's rule), whereas the recombination of free radicals requires opposite (antiparallel) spins. Drawing of energy levels (with directed arrows) frequently substitutes drawing the structures of radicals. In physical models of radicals, the concept of spin density distribution is used. Although it is possible to draw an isodensity $2D$ surface of such a $3D$ body, it is unclear how a graph-like object can be reconstructed from it.

The above-mentioned mental pasting of "free valencies" (Figure 12) corresponds to a real process. Two disjoint radicals may recombine to a connected molecule, and a single biradical may actually (not only imaginary) recombine forming a molecule with a cycle, a double bond, or a lone pair. The processes are treated as the conversion of excited triplet states of molecules to the singlet states. Thus, trimethylene biradical forms cyclopropane, triplet ethylene is converted to the "usual" ethylene (having a double bond), and triplet methylene is changed to singlet methylene with a lone pair.

Lone pairs and vacancies. A lone pair is another example of a concept which carries much information for a chemist, but has no exact physical meaning. This concept has been first introduced by Lewis and formed the basis for later electronic theories of chemical bonding. Lone pairs are used to describe the formation of donor–acceptor bonds; another application of lone pairs is prediction of molecular geometry. Traditional representation of a lone pair by Lewis and Langmuir [93, 95] involved a pair of dotes located near an atom symbol, although from the topological viewpoint, this is a rather poor image. There is still no general convention how lone pairs may be   expressed in classical $2D$ models, therefore their presence

is always ignored. Only in the Gillespie–Nyholm approach to molecular geometry [96 -- 98] is the lone pair (a nonbonding domain) considered as an object equivalent to a bonding domain with respect to arrangement of both domain types around an atom. In the pictorial form this arrangement is expressed as a cluster of touching $3D$ spheres or even as a set of $1D$ circles on a $2D$ sphere.

In physical models some excess of the electron density function (and some convex domains in contour surfaces) may be assigned to lone pairs. In the Bader model, lone pairs appear as definitive critical points in the Laplacian of charge density $\nabla^2\rho$, but not in the $\nabla\rho$ analysis (that allows one to extract a graph) [73]. Nevertheless, it may be visualized at least as $2D$ image, either in the perspective drawing of a contour map [73], or as $2D$ isosurfaces in R^3 (see an excellent pictorial presentation on WWW pages [99, 100]). Hence, it is still an open question how to "extract" the lone pair to molecular graphs. Furthermore, there is no physical evidence for the existence of a lone pair, since there are no reasons why two electrons should occupy the same region.

The concept of a lone pair plays a fundamental role in the description of heterolytic cleavage and formation of chemical bonds, as reflected in the concept of Lewis acids and bases [101]. A Lewis base (*e.g.*, NH_3) has a lone pair, and a Lewis acid (*e.g.*, BH_3) has a vacancy (the lack of electron pairs to form the stable octet configuration of a noble gas). The vacancy thus defined is also hardly representable in molecular graphs or surfaces, although it is related to depletion of the charge density. Sharing of a lone pair (donated from the base to the acid) results in the formation of a donor–acceptor (coordination) bond ($BH_3 + NH_3 = NH_3BH_3$). Reactions of this sort, which are familiar even to undergraduates, incorporate the same logical "modeling paradox" as do the recombination of two free radicals: a molecule with a well-defined graph and well-defined $2D$ surface is formed from ill-defined model structures.

The center of Lewis acidity or basicity may be located in the carbon skeleton with localized bonds. Examples are carbanions (CH_3^- with a lone pair) and carbocations (CH_3^+ with a vacancy). In molecular graphs, these centers may be visualized considering the sign of a charge as a vertex label. Complementary centers may recombine to an ordinary covalent C–C bond (*e.g.*, $CH_3^+ + CH_3^- = CH_3$–CH_3) resembling recombination of radicals (Figure 13A).

Let us proceed from this analogy and consider the formation of a cycle (Figure 13B). A long chain between dual centers (a zwitter-ion) may be closed to a large cycle. The shortest chain (*i.e.*, bond) between cation and anion (CH_2^+–CH_2^-) may also be "closed" to a small cycle, that is the double bond CH_2=CH_2. (Indeed, this zwitter-ion is known as a polar resonance form of a double bond.) Therefore, a double bond appears in the same manner as any other cycle from an acyclic zwitter-ion. Finally, there is intriguing possibility to place the dual centers (cationic and anionic) as close as possible, to the single atom. Such coalescence of CH_3^+ and CH_3^- in the single carbon atom is the case of methylene CH_2 (in the singlet state), which is not charged. Methylene is the ambivalent species, having both a lone pair and a vacancy and acting as both a Lewis acid and a base.
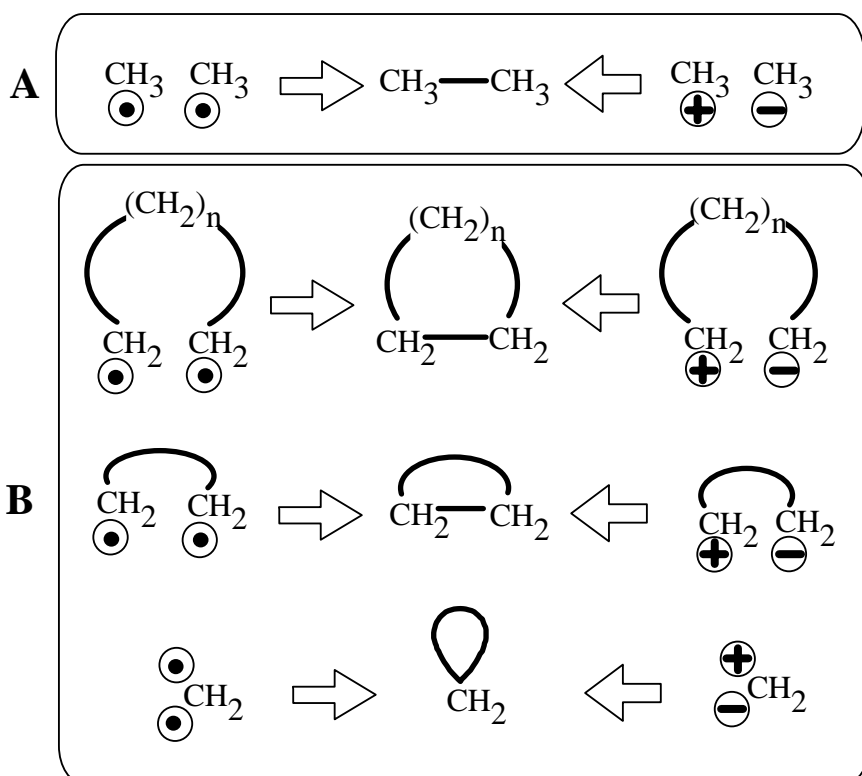

Figure 13.　　　(A) Two possibilities to obtain a molecule with a well-defined molecular graph from two molecules (with ill-defined molecular graphs), either from radicals (left) or from ions (right). In both cases a disconnected set is recombined to a connected molecule. (B) Intuitive topological equivalence of a large cycle, double bond, and lone pair (middle column) in respect to formation of a cycle from biradicals (left column) or dipolar chain (right column). Radical centers are labeled by dots.

Hence, "obtaining" the lone pair of methylene from either a biradical or by coalescence of dual centers confirms its direct relation to the large cycle and to the double bond. In addition, let us remember that CH_2 is the smallest possible homologue of the C_nH_{2n} family (n = 1), which has the unit cyclomatic number for any member. The analogy of the lone pair to a loop (as a smallest cycle in a graph) and to the topology of torus (x = χ = 0) is pronounced, although this is a somewhat strange image: an extremely bent bond that connects an atom to itself. The model is not completely new. Rather, it is century-old. It was

suggested by Nef in 1896 for CH_2 in his "methylene theory" [102].

The examples discussed above illustrate deep relationships between fundamental chemical concepts, surface topology, and homeomorphism. However, these concepts, especially lone pairs and free radicals, are still ill-defined in terms of common graphs and $2D$ models. It seems that accurate mathematical redefinition of these concepts may lead to a picture, which is self-consistent at least *chemically*. Why not use the homeomorphism concept to approach better harmony in commonly used classical models? Let us explore this possibility.

5. Topology of a Lewis Formula: Pseudograph, Graphoid, and Topoid

5.1. Molecular Pseudograph

The apparently clear term *molecular graph*, discussed in Section 3.1, is actually ill-defined: chemists commonly use various sorts of molecular graphs [1, 3, 9]. For instance, it is frequently useful to assign vertices and edges of a graph only to *some* "important" atoms and/or bonds. One may consider only "heavy" atoms (as in the so-called hydrogen-suppressed graphs) or the bonds representing only σ-frameworks (graphs for π-systems). A single vertex may also represent a functional group. These graphs (and even molecular multigraphs with multiple edges) are "incomplete" in the sense of original Lewis dot formula that consists of *all* atoms and *all* valence electrons (represented by dots). Perhaps, the best image of a Lewis formula is the *molecular pseudograph*, a multigraph with loops representing lone pairs. Only this graph represents *all* valence electron pairs by edges (including nonbonding lone pairs) and *all* atoms. As we mentioned, Nef pioneered the use of loops 20 years before Lewis' suggestion of pairs of dots, and this intuitive graph-theoretical idea was overlooked.

A clear model of molecular pseudographs appeared only in 1970s after the papers of Ugi *et al.* [103, 104]. Ugi used the representation of a molecule by a connection table (BE-matrix) that resembles adjacency matrices for multigraphs but with number of valence electrons for each atom (z_i) on the main diagonal. (For atoms from Main groups of the Periodic system $z_i < 8$.) The loop appears automatically when reconstructing a graph from the matrix, because entries of the main diagonal denote the numbers of valence electrons, necessary for correct count of vertex degrees in a molecular pseudograph. Sometimes, molecular pseudographs appeared in different fields of mathematical chemistry (*e.g.*, [32, 105, 106]). However, they are rarely used. Probably one of the reasons is that chemists frequently draw "lobes" of *p*-orbitals near the atoms in molecular graphs, and the loops may be confused with *p*-orbitals. Because nobody has popularized the model, let us discuss whether a pseudograph has any advantages.

(i) *Cycles and electron count*. Equations (1) to (3) are equally valid for an ordinary graph or a pseudograph. Because vertex degree in molecular pseudograph is deg $v_i = z_i$, we may write Σ deg $v_i = E = \Sigma z_i = Z/2$ and transform the equations (1)--(3) to equation (8a) for molecular pseudographs. Above, we used equation (8a) to count ordinary cycles in the hydrocarbons from balance of N and Z. Therefore, a lone pair and a double bond belong to the same sort of cycles, as does any large cycle, not because of arbitrary definition, but because of the correct electron count.

(ii) *Invariance of valency.* The value deg v_i is a *local* property of a point, indicating how many e^1 elements appear in the neighborhood of a point e^0. If deg v_i is fixed, then it is unimportant for a point what happens to the second "end" of an incident edge: this "end" may be closed to a loop, attached to an incident vertex, or to several vertices. Because an atom contributes to a molecule fixed value z_i and z_i = deg v_i, the value z_i should also be locally constant and independent of any environment around an atom. For instance, the neutral carbon atom may be oxidized, reduced, have any number of neighbors of any nature, and the terms "oxidation state", "coordination number", and "valence" may not coincide in the series like CO_2, CO, CH_4, and CH_2. Nevertheless, the vertex degree of every pseudograph is locally preserved, because equation deg $v_i = z_i = 4$ means that a carbon atom belongs to the 4th main group in the Periodic Table of Elements. Recall that in pseudographs of CO and CH_2, a loop formally adds two valencies to a vertex.) For a nitrogen atom, deg $v_i = 5$ should be assigned in either of these cases: HNO_3, HNO_2, NH_2OH, or NH_3. This property is unique for the molecular pseudograph [31, 32] and is violated in any other "molecular graphs" with heteroatoms as labels.

(iii) *Isomorphism and similarity*. The number of valence electrons z_i is *not* the charge of a nucleus of element, and value z_i may be the same for isovalent atom(s) and ion(s). The same is true for the vertex degree. Therefore, unique pseudograph may represent several isovalent species, that have the same Lewis dot formulas (cf. series CH_4, NH_4^+, BH_4^-, and BeH_4^{2-} or NO_3^-, CO_3^{2-}, and BO_3^{2-}). More explicitly, within such series the molecules have isomorphic pseudographs. This is convenient, because the isoelectronic series are usually isostructural [29, 95, 107, 108], and therefore, the *geometrical similarity* may be expressed in terms of *isomorphism of molecular graphs*. Thus, isomorphic pseudographs of isoelectronic series NH_3, PH_3, and CH_3^- (with total of 4 edges and the pyramidal shape) are *not* isomorphic to pseudographs of another isoelectronic series BH_3, AlH_3, and CH_3^+ (with total of 3 edges and the planar configuration). This helps one to avoid uncertainties like drawing the same graph to apparently isostructural BH_3 and NH_3 (which, in fact, are not), as in many graph-theoretical approaches and computer software.

(iv) *Octet rule and resonance.* Old, but still useful, octet rule [95] is translated as the preference of four edges incident to a vertex. Of course, a loop is only one edge (although with two ends). In pseudograph of NH_3, despite local deg v_i is 5, there are only four edges (of which one is a loop) and the octet configuration is valid. For the case where the structure violates the octet rule (like HNO_3 or N_2O) the charges may be redistributed until the octet structure is achieved. This procedure causes a transformation of a graph to another one. In terms of pseudographs, a set of nonisomorphic graphs (resonance forms) is assigned to the same molecule (see Figure 14). On the other hand, different molecules may have the same (isomorphic) pseudograph (*cf.* zwitter-ion NH_3BH_3 with the covalent structure CH_3CH_3 and other examples in Figure 14).
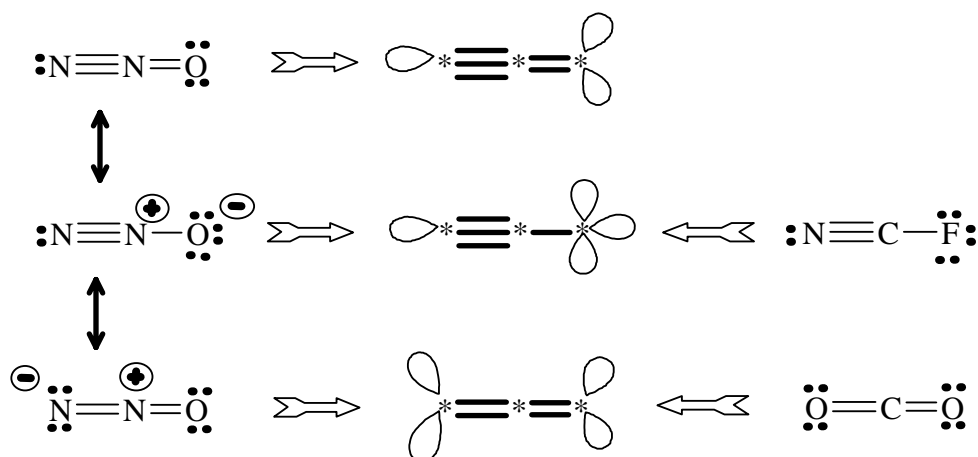
Figure 14.   Relationship between resonance structures expressed by means of isomorphism of pseudographs. On the left: design of resonance structures for N_2O to obtain the octet configuration. In the middle: pseudographs corresponding to the resonance structures. On the right: octet molecules with pseudographs isomorphic to pseudographs of resonance structures.

We may conclude that some chemical terms and concepts (that may have imprecise definition in *classical* molecular models) become clearer after being translated into the language of pseudographs, because the pseudographs seem to coincide with Lewis formulas. Furthermore, every *abstract* pseudograph corresponds (if at all) to only a finite set of *specific molecular pseudographs* (see previous paragraphs).

It is clear why a tree (Figure 10F) cannot represent *chemical structure* of ethylene. Topology of a tree contradicts to equation (8a) and chemical formula C_2H_4. The place for this tree (with deg $v_i = 3$ and deg $v_i = 1$) is not vacant; such a graph may be isomorphic to $H_2B–BH_2$, $H_2B–CH_2^+$, at least to the dication of ethylene, but not to the ethylene with value C = 1 deduced from electron count. Therefore, bipartite graphs extracted from $\nabla\rho(\mathbf{r})$ analysis, only in partial cases (namely, for saturated hydrocarbons) are isomorphic to chemical graphs. The intrinsic topology of Lewis formulas is different from the topology of critical points, and it is still not clarified in the mathematical sense.

5.2. Molecular Graphoid

Although the molecular pseudograph perfectly matches the initial Lewis concept, free radicals are still not covered by this model. The mapping, valid for electron pairs to edges only, severely restricts the extension of the graph-theoretical concept to molecules with unpaired electrons. In ordinary graph theory, an edge is supposed to have two ends, which are adjacent either to a pair of vertices, or to the same vertex). However, graphs are merely the sets of e^0 and e^1 elements with informal requirement that sets are closed and compact (so that every e^1 element has exactly two e^0 boundaries). Then, one may figure that some e^0 elements may be removed.

To design the topology of free radicals, it seems necessary to introduce a nonclosed topological object related to a graph but somewhat different [31]. Consider a connected pseudograph with several terminal vertices. Let us delete L of its terminal vertices, preserving the incident edges. As a result, a novel mathematical object will appear that still will consist of e^0 and e^1 elements but is not closed. Let us call it *graphoid*. Evidently, graphoid has two topologically distinct sorts of edges. There are usual edges, homeomorphic to a closed interval [a,b], and unusual L "semi-edges" (each with "punctured end"), that are homeomorphic to half-open interval [a,b).

A graphoid may be alternatively treated as the simplest case of a *pseudo-hypergraph* (see Section 2.2), because a semi-edge here is *not a pair* of vertices, but an independent element incident to a vertex (terminal hyperedge). In contrast, the loop is a usual edge in the sense that it is the *pair* of vertices, although this is a very strange pair: the same vertex is taken two times. Expanding the standard notation (2c,2e) for two-centered two-electron bond, one may treat the lone pair and free radical as a sort of (1c,2e) and (1c,1e) "bonds". The planar representation of a graphoid (Figure 15A) as a pseudo-hypergraph containing $2D$ disks instead of e^1 elements is shown in Figure 15C. Here three elements adjacent to vertices [(2c,2e), (1c,1e), and (1c,2e) "bonds"] are topologically distinct. The König graph of this object is a bipartite graph with some unique terminal vertices that are images of semi-edges (Figure 15D).
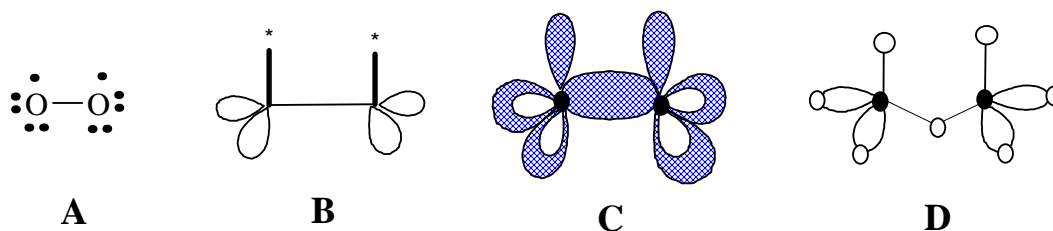

A   **B**   **C**   **D**

Figure 15.   Different models for the biradical molecule O_2. (A) Lewis dot formula. (B) Graphoid (semi-edges are in boldface, pricked vertices are starred). (C) The same graphoid treated as the pseudo-hypergraph with usual and terminal hyperedges and hyperloops. (D) The König graph of the previous pseudo-hypergraph.

Molecular graphoid can be assigned to any open-shell molecule by simple mapping of the unpaired electrons to the semi-edges. The degree of a vertex in molecular graphoid may be defined as the number of e^1 elements incident to this vertex. Hence, deg v_i is equal to z_i. A molecular graphoid may be connected or not (consists of K components), and we may even continue considering it as a usual labeled graph with the goal to calculate its cyclomatic number C. Indeed, because neither punctured vertices no semi-edges participate in cycles, the value C may be calculated from the number of normal vertices and bound edges from the equations (2) and (3). The C number is the sum of all (independent) cycles, multiple bonds, and lone pairs of a molecule.

Consider a molecule with N atoms and Z valence electrons of which L are unpaired. If bonds are localized, the molecular graphoid has N vertices and 1/2 (Z - L) usual edges. Since formula (3) is valid for molecular graphoid, let us express the balance of components and cycles in terms of electron count by equation (10):

(10a) $N - 1/2 (Z - L) + C = K$

Let us rearrange the parts and rewrite it as equation (10b):

(10b) $2N - Z = 2K - 2C - L$

5.3. Concept of Molecular Topoid

Equation (10a) expresses topological features of free radicals (K and C in graphoids) in terms of counting the electrons and atoms. Let us note, that formula (10b) resembles (9a) for the Euler characteristic of hydrocarbon surfaces, although there is another parameter L. Furthermore, formula (10b) for molecular graphoids looks suspiciously similar to the formula (7) -- the Euler characteristic of an orientable 2D surfaces $\{^L S_C\}_K$ with L punctures (see Section 2.4). The result is fascinating, because no hypothesis about 2D surfaces has been used in our definition of molecular graphoid: this was nonclosed set of only 0D and 1D elements. Therefore, the existence of equation (10b) itself poses a natural question of mapping the graphoid to an orientable 2D surface.

How to define such a mapping? As it was mentioned in Section 2.6, intuitive mapping "graph as surface" is widely used in chemistry (*cf.* graphs and surfaces for the C_nH_{2n+x} series). The principle of mapping is old and related to early attempts of molecular modeling. Trying pass from the structures on a plane to spatial models, chemists of the last century have constructed molecular models making them not only of various solid materials, but also of empty tubes. The presentation of a bond (bounded e^1 cell in a graph) by a 2D cylinder (empty inside) prompts how the desired leap in dimensions may be achieved for a graphoid. Semi-edge may be a cylinder with punctured vertex corresponding to a puncture on the 2D surface.

Consider a graphoid with the cyclomatic number C and L punctured vertices in the real 3D space. Replace the edges by empty rubber tubes attached to small rubber spheres (vertices). Some cylindrical tubes are closed (by spheres of usual terminal vertices) and some tubes are open (semi-edges). The 2D surface thus appeared may be deformed (*e.g.*, inflated) to the standard form of a sphere with C handles (cyclomatic number of a graphoid) and L punctures. This orientable surface $^L S_c$ is just the required 2D image of a graphoid [31, 52]. For the particular case L = 0 (ordinary pseudograph) the surface is closed, and the set of K disconnected graphoids corresponds to an ensemble of K disjoint surfaces. When, turning from an abstract graphoid to the molecular graphoid we may inflate any image of a Lewis formula, as in the example presented in Figure 16. Let us call the resulting 2D boundary a *molecular topoid*.

For the case K = 1 we therefore, state that:

For any molecule with N atoms, Z valence electrons (L of which are unpaired), and C independent cycles (the total of lone pairs, multiple bonds, and cycles), there exists a unique orientable surface called a molecular topoid with C handles, L punctures, and the Euler characteristics defined by equation (11a).

(11a) $\chi = 2 - 2C - L = 2N - Z$

In the general case of molecular ensemble consisting of K components,

(11b) $\chi = 2K - 2C - L = 2N - Z$

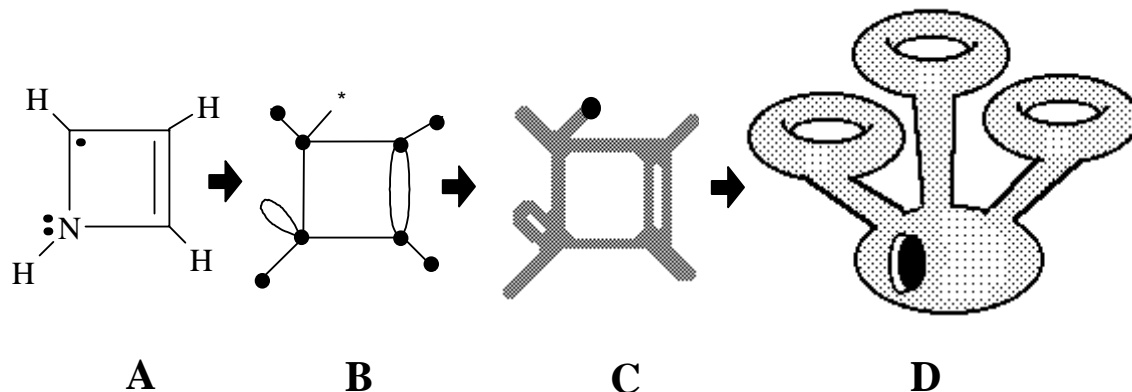

A   **B**   **C**   **D**

Figure 16.   Mapping of a Lewis formula (A) to molecular topoid (D). Intermediate steps: molecular graphoid (B) and its 2D presentation (C). Free radical center is a dot in Lewis formula and pricked vertex (labeled by white color) in graphoid.

6. Some Properties of Molecular Topoids

Topoids are just the desired combinatorial $2D$ images of molecules where only the concept of homeomorphism is essential and may be easily visualized.

6.1. *Overview and Manipulations with Topoids*

Molecular topoid is a combinatorial $2D$ object. It is not a conventional molecular $2D$ surface, although it coincides with space-filling $2D$ models for the specific case of saturated hydrocarbons (acyclic or alicyclic with large cycles). By contrast to space-filling models, it is possible to assign some $2D$ image (topoid) to molecules with free radical centers. Equation (9b) $x = \chi$ (defined above only for the even values of x) remains valid for any family C_nH_{2n+x} with odd value of x, opening possibility to calculate the Euler characteristic of the surfaces of free radicals. Thus, methyl radical from the C_nH_{2n+1} family has $x = \chi = 1$, and the corresponding topoid is a punctured sphere. Topoids of simplest biradicals from the family C_nH_{2n} (x = 0), like triplet methylene, ethylene, and polymethylenes are homeomorphic to the cylinder ($\chi = 0$). The value x for this family is the same as for the series of cycloalkanes, singlet alkenes, and singlet homologs of methylene. Of course, cylindrical topoids of biradicals C_nH_{2n} are not homeomorphic to singlet molecules C_nH_{2n} with toroidal topoids. A cylinder (^2S) and a torus (S_1) are not homeomorphic (differing in number and nature of holes), however their Euler characteristic χ is the same (see Section 2.3).

There is no uncertainty in distinguishing carbanions (like those from the $C_nH_{2n+1}^-$ family) from carbocations (from $C_nH_{2n+1}^+$ family) by the genus of the corresponding topoids. Each member of the first class, like CH_3^- anion, has a lone pair (a loop in the molecular pseudograph) represented by a handle on the $2D$ surface of the topoid. The second class, the acyclic saturated carbocations (like CH_3^+ and its homologs), has no this feature, and topoid is represented by a sphere. Similarly, the presence of heteroatoms (centers of Lewis basicity and acidity) causes a change in the genus of topoids. Thus, the dual molecules NH_3 and BH_3 are represented by torus and sphere, respectively. Any molecule, to which it is possible to assign the Lewis formula, has certain graphoid and topoid, and resonance forms, of course, have homeomorphic topoids.

The topoid model resembles the ball-and-stick representation (at least in the possibility of making bent multiple bonds), although with essential modification. The difference is that for topoids, we still need the *balls* (spheres) for atoms, but there is no necessity in *sticks* (or even tubes) for bonds. More strictly, imaginary "kit for molecular topology modeling" by topoids consists of only punctured spheres made of an ideal elastic rubber. The "sticks" appear automatically from the deformation of punctures to round holes and further stretching to the desired tubes. Pasting $1D$ boundaries of the tubes produces the bond image.

Accurate definition of the initial kit is simple. Consider any atom (for simplicity, from Main Groups of the Periodic Table) with z_i unpaired valence electrons as a graphoid with only one vertex surrounded by z_i semi-edges. At the $2D$ level it is a rubber sphere with z_i punctures. The addition of an electron is equivalent to making a new puncture, whereas removal of an electron is pasting a puncture by a point (as if a point e^0 would be a positron). Hence, to cover all nontransition elements with maximum $z_i = 8$, we need only eight spheres with the number of punctures from 1 to 8. (This number may be expanded to include transition metals by additional punctures for d-electrons.) Eight punctured spheres represent arrangement of elements in columns of the Periodic Table: isovalent atoms-analogs are homeomorphic, as are the isovalent ions. Let us assume that the specific sphere *without* punctures represents a proton H^+ (or an alkaline metal cation), whereas the hydride anion H^- and He atom (with lone pair) correspond to a torus.

The rules of making complex topoids from rubber spheres are evident: it is possible not only to mutually join few holes from different spheres (making bent double and triple bonds), but also to paste the holes from the same ball (making lone pairs), and even leave some free holes (for radicals). The neon atom (with four lone pairs) is the sphere with four handles (obtained by pasting of eight punctures in pairs). Care should be taken with the manner of pasting the holes one to another. False pasting (see Section 2.4) may result in nonorientable surfaces (like a Klein bottle). Before considering the problem in more detail (*vide infra*), let us be restricted to considering at this point the simplest orientable $2D$ models.

6.2. *The Cut-and-Paste Procedure*

Homeomorphism of abstract surfaces is a sort of equivalence. Hence, homeomorphism of a lone pair, a double bond, and a usual cycle at the level of topoids should be also regarded to as a sort of equivalence. What could be the meaning of this equivalence? First type of equivalence is manifested in respect to the isomerism phenomenon. All these structural features are cycles in molecular pseudographs; let us designate a cycle of size i as c_i, a lone pair as c_1, and a double bond as c_2. If one enumerate *all isomers* of a structure with given chemical formula, the equivalence of cycles c_i is significant, since the structures with degenerate cycles (multiple bonds and lone pairs) are isomeric to structures with ordinary cycles. Thus, there are four isomers with the formula C_3H_6: cyclopropane (with cycle c_3), propene (with cycle c_2), and two isomeric carbenes (each with cycle c_1), see also Figure 12.

Second, there are some chemical arguments that cycles c_1, c_2, and c_3 are similar in their electronic effects if one consider them functional groups. Thus, cyclopropyl fragment c_3 strongly stabilizes an adjacent carbocation center (*cf.* abnormal stability of tricyclopropylmethyl cation [109]). The same effect is known for lone pairs c_1 (in immonium, amidinium, and guanidinium salts) and for double bonds c_2 (in allyl cation and relevant vinylogs). This effect, appeared for the cycles adjacent to any vacancy, indicates the presence of a Lewis basicity (evident or hidden) in cycles c_1, c_2, and c_3. However, this property is not intrinsic for larger cycles c_i.

Let us seek for the prompt of the equivalence of cycles within topology concepts. To build a connected graph with V vertices, it is necessary to have *at least* (V – 1) edges, and acyclic graph is a tree. The addition of any extra edge to a tree (leading to a graph with V vertices and V edges) causes excessive connectedness manifested itself in the appearance of a cycle. At the $2D$ level the analogous trend reveals itself in passing from an abstract sphere (inflated tree) to an abstract torus (inflated monocyclic pseudograph). Excessive connectedness may be deteriorated: cut a cyclic edge (in a graph) or a handle (in a surface) and obtain a still connected topological object. There is another operation frequently used instead of simple cutting in the topology

of surfaces: the *cut-and-paste* procedure. The procedure is the following: cut across a handle and paste some round caps (lids) to the borders of the resulting holes. The Euler characteristic of the initial surface is increased by two. A finite sequence of such cut-and-paste procedures should completely destroy all handles, and this is a method for proving that two geometrically distinct $2D$ objects are topologically equivalent.

To built a connected acyclic molecule from N atoms, it is necessary to have at least $(N-1)$ electron pairs arranged in localized bonds (of course, considering only molecules with localized 2-centered 2-electron bonds). The addition of an extra electron pair to the connected molecule (leading to a molecule with N atoms and N electron pairs so that $N = Z/2$) should cause an *excessive* molecular connectedness in the topological sense manifested itself in appearance of cycles c_i. At the $2D$ level, the spherical topoid (*e.g.*, for the family of alkanes) is changed to a toroidal topoid (cycloalkanes, alkenes, and carbenes). Therefore, cutting a cyclic edge belonging to *any* cycle c_i (in a molecular graph) or of a handle (in a molecular topoid) should result in a still connected topological model.

Hence, the topological equivalence of cycles c_i of any size in molecular pseudographs and topoids should manifest itself upon their destruction. In chemistry, such destruction is not a trick, but real thing: what in topology is mental, in chemical topology may be experimental. The role of a knife for cutting a bond is played by a photon: irradiation frequently results in the homolytic cleavage of localized bonds. Photochemical cleavage of a saturated cycle, ethylene, or singlet methylene results in the corresponding biradical. All these processes are topologically indistinguishable: a cut across a torus leads to a cylinder, even for cycles c_2 and c_1 (excitation of a double bond or a lone pair to the triplet states), so the intuitive similarity is perfectly visualized. Photochemical excitation of more complex molecules (with cycles of various size at the same structure) may result in higher (than triplet) excited states, corresponding to several cuts of various handles.

An analogy with the cut-and-paste procedure is less evident, although equivalents to "scissors and glue" (*e.g.*, for a transformation of a torus into a sphere) are invisibly presented in many chemical handbooks (e.g., [110]). These are extremely reactive chemical species, namely atomic hydrogen, elementary halogens, and hydrogen halides, and the reactions are shown in Figure 17. Hydrogenation of methylene, ethylene, and cyclopropane (with cycles c_1, c_2, and c_3) results in methane, ethane, and propane, respectively. Here, the handle in the topoid is cut, and the appeared holes are pasted by hydrogen atoms (as lids). The lone pair c_1 in carbene is not an exception. Protonation of the same species CH_2, C_2H_4, and C_3H_6 by hydrogen halides HX to alkyl halides readily occurs. (One would say these hydrocarbons "neutralize" the acid.) Reaction mechanism involves intermediate formation of methyl, ethyl, and isopropyl cations [109 -- 111], all having topoids homeomorphic to a sphere. Here, the visual ring cleavage of cyclopropane is topologically indistinguishable from the destruction of a double bond and a lone pair by the action of a Brønsted acid. The same change from torus to sphere manifests itself in the protonation of ammonia to ammonium salt. Finally, the chlorination reaction of carbenes, alkenes, and small alicyclic molecules readily occurs, and the formula is changed from C_nH_n to dichlorides $C_nH_nCl_2$ with the disappearance of initial handle or a cycle c_1, c_2, c_3 and even c_4. Pasted fragments are evidently chlorine atoms (with new c_1 cycles).

Fluorination reaction [112] provides probably the best visualization of the cut-and-paste procedure: the reaction readily occurs with the cleavage of cyclic σ-bonds (for large cycles), with the destruction of multiple bonds (between any pair of heteroatoms) and even with further cut-and-paste of several lone pairs. Thus, the fluorination of carbon monosulfide :C=:S: (with four initial handles) may result in the complete destruction of all handles and the formation of CF_3–SF_5. Even atomic xenon with four lone pairs may be transformed into XeF_6. Figure 17 shows the examples for the case when a handle is adjacent to a blackbox with hidden content (a chain, a bond, or a single atom): if there is any handle, the reagents destroy it.
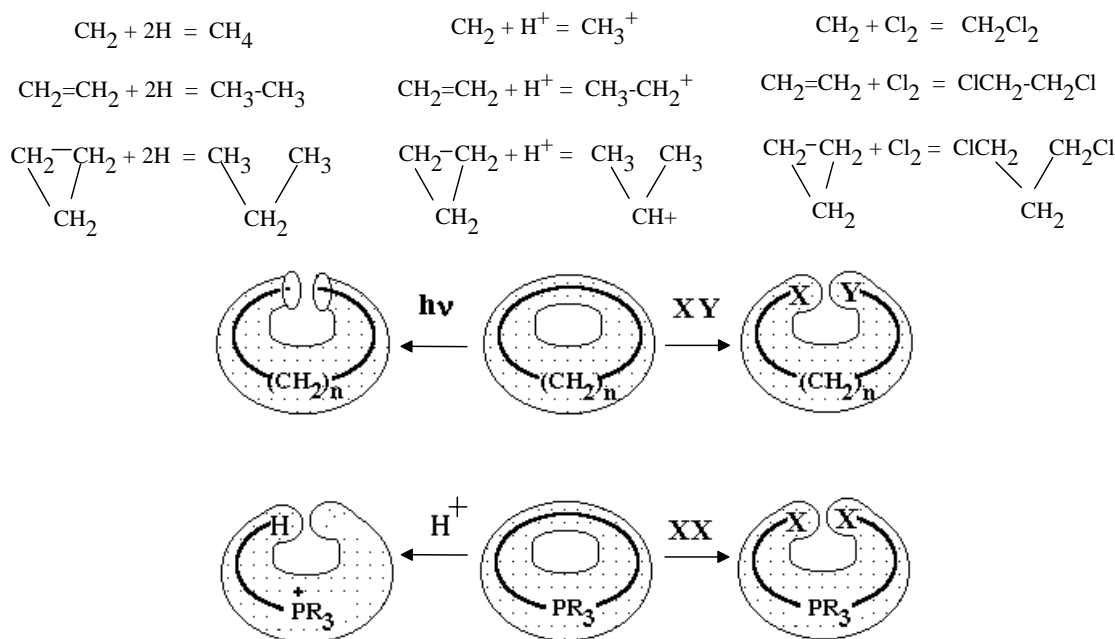
$$CH_2 + 2H = CH_4 \qquad\qquad CH_2 + H^+ = CH_3^+ \qquad\qquad CH_2 + Cl_2 = CH_2Cl_2$$

$$CH_2{=}CH_2 + 2H = CH_3\text{-}CH_3 \qquad CH_2{=}CH_2 + H^+ = CH_3\text{-}CH_2^+ \qquad CH_2{=}CH_2 + Cl_2 = ClCH_2\text{-}CH_2Cl$$

Figure 17.   Some cut-and-paste processes with destruction of a handle, where the cycles, double bonds, and lone pairs behave similarly. XY may be HH, HHal, Hal_2 (Hal is a halogen); XX may be Hal_2.

Of course, there may be (and there are) exceptions where some reactions occur with difficulty. Say, hydro- or halogenation of higher cycloalkanes (in contrast to small cycles and alkenes) requires rather drastic conditions. By contrast to the lowest homologues, the cyclohexane is even insoluble in hydrochloric or sulfuric acid. Nevertheless, the acidic ring

cleavage of a saturated macrocycles is possible [111] in the media of super strong "magic acid", like HSO_3CF_3 or $HSbF_6$, that have no selectivity to the size of a cycle. First-row elements have lower coordination number than their higher analogs, therefore, the possibility of higher fluorides (*cf.* SF_6 but OF_2, PF_5 but NF_3) is totally excluded by octet rule. Lower (in contrast to fluorine) electronegativity of hydrogen atom prevents exhaustive "hydrogenation of lone pairs", *cf.* formation of higher fluorides (PF_3 and PF_5) by contrast hydrides (PH_3 but not PH_5). Finally, protonation of lone pairs usually occurs only once, perhaps by electrostatic reasons (H_3O^+ and H_2F^+ but not H_4O^{2+} or H_3F^{2+}). Existence of such counterexamples, however, only proves that the reality is more complex than an ideal cut-and-paste procedure of transforming a torus to a sphere. Nevertheless, the fact of existence of real images to the initially pure topological abstraction is fascinating.

6.3. Virtual Handle and Self-crossing in 2D Surfaces

Another paradox, seeming to contradict the common sense, is that the cycles c_1 and c_2, indistinguishable from larger cycles at 2D level, intuitively should have a sort of toroidal emptiness (cavity). Emptiness in the center of a large saturated cycle is clear, being parallel to real depletion of electron charge density. However, for a double bond and a lone pair, many calculations indicate an opposite effect, local excess of electron density. Therefore, the homeomorphism looks unacceptable: continuous decrease of the volume of cavity (from larger cycles to smaller ones) should necessarily cause a catastrophic collapse of a hole to nothing (*e.g.*, in the case of ethylene or carbene). How to reconcile the existence of toroidal feature with its disappearance? Is there any better topological image to avoid this paradox other than "placing matches to a ball"?

Let us turn to the mathematical definition of a torus, that is formally the surface of rotation of a circumference around an axis. Of course, the axis and circumference are not crossed. Consider a shift of the axis and circumference towards each another (Figure 18), continuing the rotation, until the cross-section at one point appears. The hole of the torus seems to collapse to a point. Then, let us continue shift of an axis with (still rotated) circumference. The toroidal surface becomes self-crossed. (The same result may be achieved if one would continuously increase the diameter of rotated circumference.) However, this self-crossing *does not mean gluing*. There is reverse homeomorphism, a continuous deformation, that may allow one to restore a hole in the torus. The idea is that homeomorphism ignores the space in which objects are initially embedded, so it can be completed in a higher dimensional space.

Imagine a 2D creature (from *Flatland*) that followed the rotation process from the plane: from its viewpoint two disjoint circumferences make a connected object because the internal part is invisible (Figure 18A). Spectator from the 3D world may
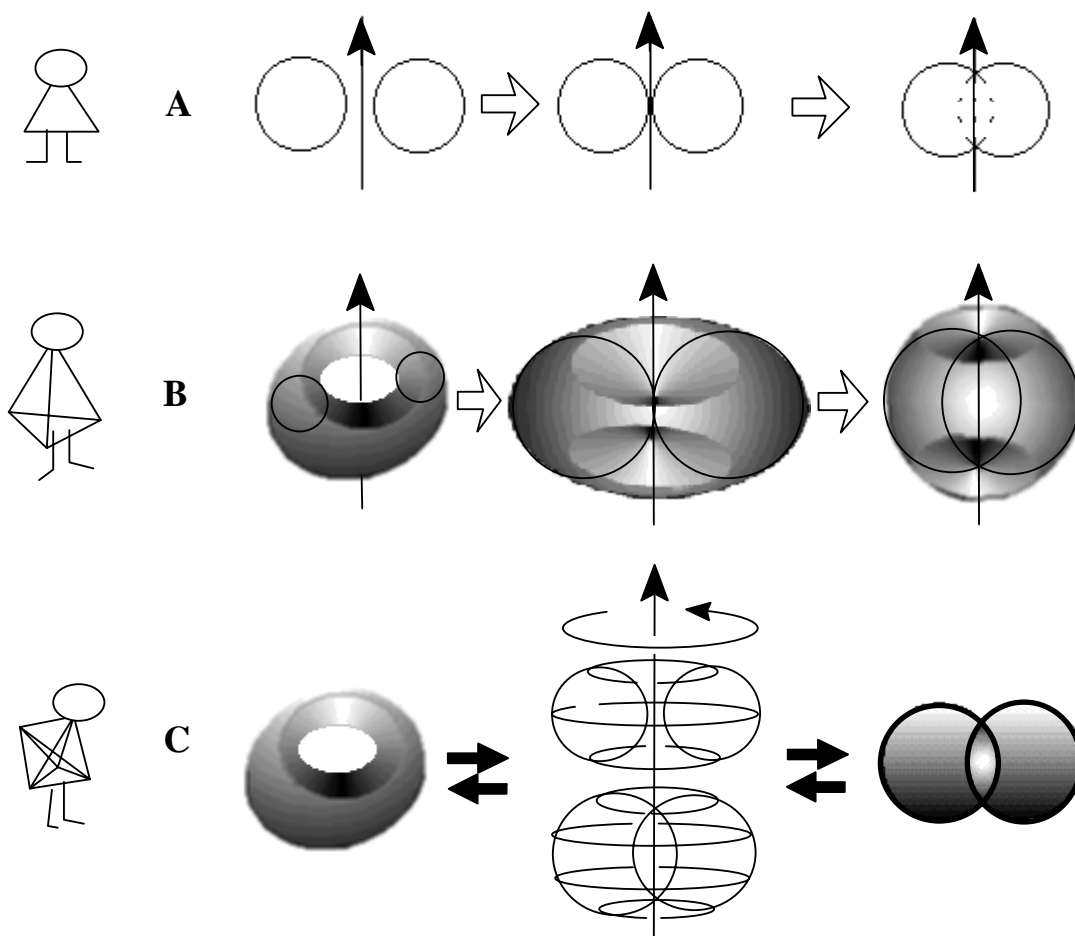

Figure 18. Torus as the surface of rotation of a circumference around an axis. Shift of rotated circumference to the axis causes self-crossing of toroidal surface, that looks differently R^n in spaces. (A) 2D world: collapse of disjoint objects to connected one. (B) 3D world: disappearance of a hole. Self-crossing manifests itself in the appearance of concave domains around points on the external 2D surface. (C) 4D world: self-crossing of a torus as an inessential reversible deformation in R^4 space. A spindle-like 2D region of self-crossing is equally visible from outside and from inside the toroidal surface.

continuously disconnect the collapsed circumferences on the plane by *homeomorphic* shift. In turn, a 3D creature has a problem with a self-crossed torus, because one can see only the external part of the surface (that looks like a fruit, apple or peach), and

can not see the hidden internal part (that resembles a stone of peach or a spindle) (see Figure 18B). Nevertheless, even in 3D world the object is not homeomorphic to a sphere: the cut around two points (visible in the external region) should result in two disjoint cylinders, one inside another. (Dissection by a plane may also help to view the internal self-crossing region.) However, a 4D creature will not notice something mysterious at all (Figure 18C). Both internal and external parts of a torus will remain visible in R^4, and the elliptical "spindle" may be continuously changed to a hole of a torus after inessential homeomorphic distortion. This deformation in R^4 is just the desired homeomorphism between the torus with a hole and the self-crossed torus. Furthermore, the presence of a hole in a 2D surface is not only a geometrical property (visible or not). This is *the group-theoretical feature* of an object, manifested in its fundamental group [46 -- 49]. Either ordinary torus or its self-crossed image have the same (isomorphic) fundamental group.

As it was mentioned above (see Section 3.2) the isodensity 2D surface of a cyclic molecule *may* have a toroidal hole (at some parameter value), although this hole can paradoxically disappear with a decrease in the scanning parameter. The isodensity surface, a 2D surface embedded in R^3, is regarded to display exclusively the external part [16]. However, in the appropriate model it would be possible to assume the possibility of self-crossing. Take a toroidal isodensity surface of a large cycle (at some value A) and continuously decrease the scanning parameter A until, at some instant, the external torus undergoes apparent leap to a spherical (apple-like) surface. The process is similar to the rotation of a circumference with continuously increased diameter. The surface of rotation is self-crossed, and the elliptical domain inside is invisible. Of course, an excess of density inside the isodensity surface *always* exists by definition (otherwise the hole should remain). Therefore, a part of it may be safely attributed to the contribution of the self-crossing.

The concept of self-crossed topoid may be useful to clarify the old discussion of the nature of a double bond. The logical paradox between *spherical* space-filling model (that violates the common valency of carbon atom) and *toroidal* ball-and-stick model (that preserves valency but has a hole) is reconciled in the model of extremely strained and strongly self-crossed torus. Such a model is quite certain topological object: two tubes crossed in 3D world perfectly satisfy both classical models. There is no necessity in "matches in a ball": a hole exists, but it is invisible from outside. Furthermore, the electron density at the self-crossing elliptical domain, with evidence, *must be excessive*, as it is proved by calculations. One should also remember that in the Bader's approach [72] a double bond has only one critical point, typical for a single bond. However, this may be result of a coalescence of two other critical points (one for the second bond and another for a cycle). At least, the remaining unique critical point has pronounced *ellipticity* along the bond path.

The same concept may be useful for the 2D model of a lone pair, if we consider as self-crossed torus, even more strained than the double bond. From the standpoint of the VSEPR theory (abbreviation for valence shell electron pairs repulsion [96 -- 98]), the best 2D image for both a lone pair and a multiple bond is a spherical domain that exceeds in size the domain of a single bond. Why not to consider this domain an external surface of self-crossed torus? Of course, two bent tubes (cylinders) crossed in 3D world, or even the single but self-crossed tube, have larger size than the diameter of a single noncrossed tube.

Note, the reversible deformation (homeomorphism) of self-crossed torus to its usual image with a hole, trivial for a 4D spectator, may not be achieved at all in 3D world, as it was with two circumferences in Flatland. (Similar picture exists for knots: a knot, homeomorphic to a torus, can be unbound in R^4, but not in R^3.) Nevertheless, the hidden toroidal nature of a double bond or a lone pair (as intrinsic cycles of a pseudograph) is clearly manifested in any process that may destroy the masked handle, like photolysis or the action of Brønsted or Lewis acids (see examples above).

7. Invariance of the Euler Characteristics in Chemical Reactions

A chemist clearly distinguishes a chain from an ordinary cycle in respect to their interconversion in the chemical reaction. Thus, a cyclization is opposite to a ring cleavage reaction, and a recyclization (changing a cycle to another cycle) is intuitively different from a formation or destruction of a cycle. Similarly, a reaction with the change in the number of components (like an addition or elemination) is clearly different from a process with the preservation of the number of components (like a substitution or isomerization). Therefore, in the common sense, the cyclicty and connectedness are variable parameters in chemistry, that may freely appear or disappear upon a reaction. The precursors of the same molecule may be topologically different, cyclic or not, connected or disconnected. No restrictions are evident to the interconversion of components and cycles: a cycle may be formed from a connected molecule (another cycle, chain, or even polycycle) or from several disjoint molecules (chains and/or cycles).

By contrast, in the model of molecular topoids, every change in the cyclicity and connectedness is strictly predetermined by equations (11). Consider a chemical equation of any reaction as the interconversion of one set of molecular topoids to another one. Assume that the bonds in the initial and final ensembles are the localized (2c,2e) bonds, the sets may be disconnected, and some electrons may be unpaired. Let Z and N be the total number of valence electrons and atoms in the initial ensemble. A reaction is a rearrangement of electrons between atoms within the initial ensemble, leading to the final ensemble. According to the common material balance equation of a reaction, the values Z and N should remain the same in the final ensemble. Any ensemble follows equation (11) $\chi = 2N -- Z$. If there are no changes in Z and N upon a reaction ($\Delta Z = \Delta N = 0$), then, there are also no changes in the Euler characteristic and $\Delta \chi = 0$. In other words, within the model of molecular topoids, the *Euler characteristic should be invariant in a chemical reaction.*

The structural changes via reactions from the topological viewpoint are the interchanges of C handles (ordinary cycles, multiple bonds, lone pairs), L unpaired electrons, and K components. The equation (11) implies that $\chi = 2K -- 2C -- L$. Therefore, any rearrangement of electrons and bonds should follow the same topological balance equation (12):

(12) $\Delta \chi = 2\Delta K -- 2\Delta C -- \Delta L = 0$

Clearly, the components, handles (lone pairs, double bonds, and cycles) and unpaired electrons can not spontaneously appear or disappear without leaving a trace (in contrast to conventional models). Any change in C, L, K is strictly predetermined

by the conservation law (12). Let us consider some examples (Figure 19).
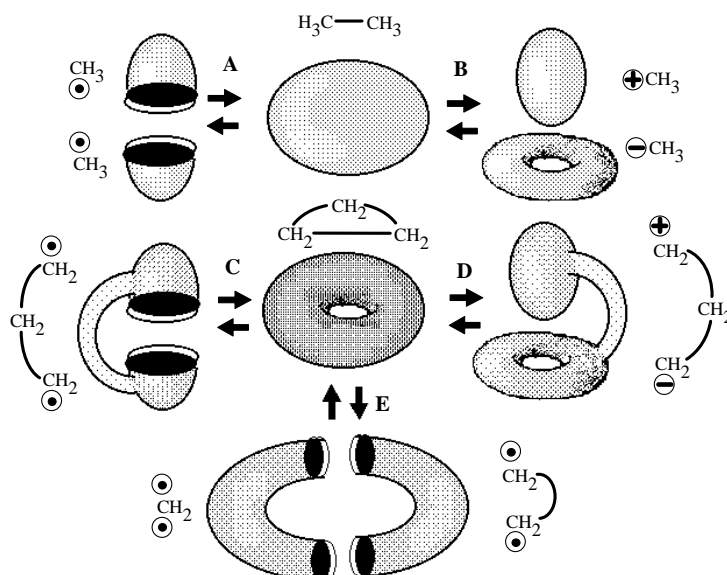

Figure 19.   Examples of five possible types of interconversion of handles, holes, and components in molecular topoids with preservation of the Euler characteristic as illustrations of equations (12a)--(12e).

Loss of connectedness (case of boa and elephant). By definition, a localized bond is the (2c,2e) bond. In the classical Lewis concept, a bond can be formed either by recombining two radicals, or by donating an electron pair from a Lewis base to an acid. Within the model of molecular topoids, the homolytic formation (from radicals) resembles gluing of a globe from two hemispheres that are pasted to each other by $1D$ boundaries around the holes (Figure 19 A). Heterolytic bond formation (BH_3 + $NH_3 = BH_3NH_3$ or a methyl cation and anion forming ethane) is equivalent to the combination "sphere + torus = new sphere" (Figure 19 B). The visual image of the process may resemble nut-and-bolt manipulations (with the disappearance of a hole in a nut), however the difference is that cylindrical walls around the area of contact are supposed to "dissolve" inside the newly formed sphere. An interesting and more pronounced visualization may be found in *The Little Prince* by Antoine de Saint-Exupéry: "a boa constrictor digesting an elephant" looks like a hat (Figure 20).
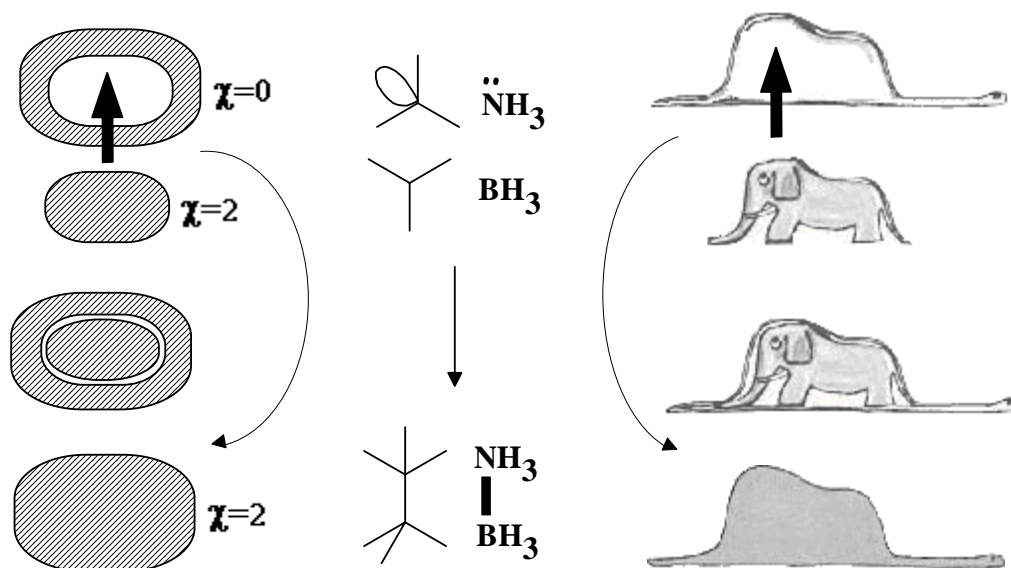

Figure 20.   The surface of sphere pasted to the hole of a toroidal surface results in a new spherical surface with preservation of the Euler characteristic. The process is shown for different cases, which are topologically indistinguishable.

In both cases, of homolytic or polar formation of a bond (Figures 19 A, B), the value $\Delta\chi = 0$, because for topoids of reagents and a product $\chi(\{^1S,^1S\}) = \chi (\{S_0,S_1\}) = \chi (S_0) = 2$. In both cases the initial number of components decreases ($\Delta K = 1$). However, this decrease is compensated by immediate disappearance of holes. These are either two holes of the hemispheres (and the balance equation is reduced to $2\Delta K = \Delta L = 2$) or one hole -- a handle -- of a torus (then the equation is $\Delta K = \Delta C = 1$). Hence, the equation (12) is valid for both cases. Therefore, in chemistry the *connectedness cannot appear from a disconnectedness* in a simple way (like A + B = C): the price to be paid is the destruction of holes. Of course, the same balance equation describes the reverse processes of homolytic or heterolytic bond cleavage.

Formation of cycle (Uroboros paradox). The appearance of cycles may be simply reduced to the previous cases by connecting two free radical centers (or two dual polar centers) by a chain. An analogy with taking a connected sum of surfaces is evident. The connected sum of two hemispheres ($^1S \# ^1S \sim {}^2S$) is a cylinder (Figure 19 C). The connected sum of sphere and torus ($S_1 \# S_0 \sim S_1$) is again a torus (although it may be distorted as shown in Figure 19 D). Now, paste the ends of a chain as

described above and obtain a cycle (torus) in both cases. Evidently, $\Delta\chi = 0$. In the first case the balance equation is $2\Delta C = -\Delta L$, and the appearance of one toroidal hole (birth of molecular cyclicity) is compensated by destruction of two other holes of a cylinder. The second case corresponds to the balance equation $\Delta C = 0$ (because there are no changes in K or L) and is curious. Trying to destroy the initial hole (by locating a stretched fragment of a torus in its own cavity) we create a new hole! (Figure 21 A). By other words, a hole is preserved upon gluing, and hence, *a cycle cannot be created or destructed in the intramolecular hetorolytic reactions* (where $\Delta K = \Delta L = 0$), it may only change the size.

The last statement seems contradicting to the chemical intuition: what about common cyclizations, where a cycle is formed from a chain? Let us call this case the *Uroborus paradox*. The Uroborus -- a serpent devouring its tail (Figure 21 B, C) is an archetypal alchemical symbol, famous in the story of Kekule's dream. At first glance, the process on Figure 21 D serves as an image of forming a cycle from an acyclic structure (*cf.* the ring closure processes in Figure 21 E, F, G). However, if one consider all cycles in the molecular pseudographs (handles in topoids), this analogy is false: reactions 20 E -- G are examples of *cycle preservation* (although the size of a cycle is changed). Furthermore, the intuitive analogy to Uroborus fails by another reason. From the standpoint of topology, any serpent has a tunnel inside it, and the total 2D surface of its 3D body is homeomorphic to a torus. (By the same reason the boa in Figure 20 is not homeomorphic to a hat.) This fact, evident in biology long ago [113], is important in the modern topological classifications of biological species [114]. Therefore, all cases D -- G in Figure 21 (either chemical or biological) are better represented as gluing to itself of a deformed and stretched torus (Figure 21 A).
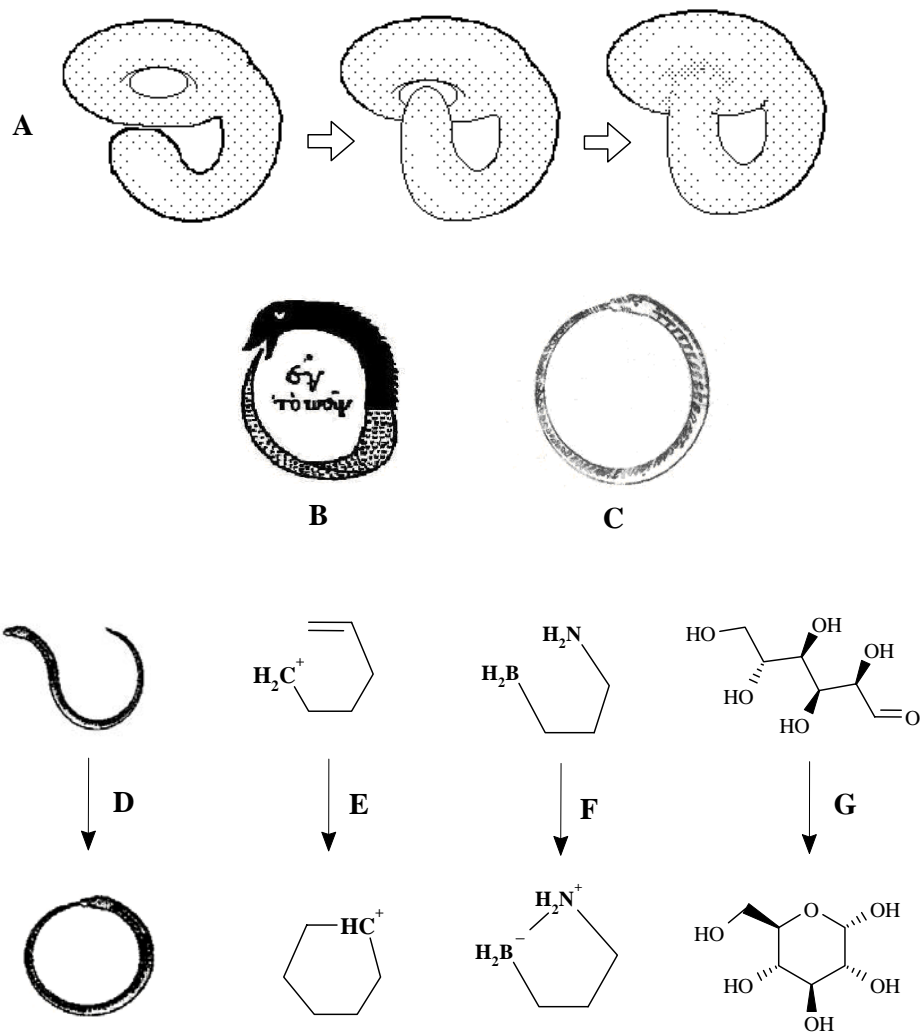

Figure 21. (A) The preservation of a hole via an attempt of pasting a fragment of the same surface into the toroidal cavity and the "Uroboros paradox" (see text). The image of Uroborus in pre-Christian alchemical tradition (B) and in Medieval-Christian mysticism (C). The paradox is manifested in the preservation of a handle (in the topoid) or the cyclomatic number (in the molecular pseudograph) in apparent "cyclizations": (D) an inessential deformation of the initially toroidal 2D surface of a biological object, (E) the intramolecular electrophilic addition to a double bond (cycle c_2 is changed to c_6), (F) the intramolecular interaction of a Lewis base and acid (cycle c_1 is changed to c_5), (G) the cycle-chain tautomerism of glucose (the same conversion of cycles as in the case E).

Topological balance equations. The existence of the same "topological balance" for reversed processes (homolytic or heterolytic cleavage of a cycle) is evident. We may prove [31] that the four examples above and the last one in Figure 19 E completely exhaust all types of interconversion of invariants K, C, L. Indeed, if one of values (K, C, or L) is not changed, we may equalize it to zero in equation (12) and consider the remaining pair of invariants to be interconverted:

(12a) $2\Delta K = \Delta L$ (Figure 19 A)

(12a) $\Delta C = \Delta K$ (Figure 19 B)

(12b) $2\Delta C = -- \Delta L$ (Figure 19 C)

We may also consider that nothing is changed (just the above example of the serpent),

(12d) $2\Delta C = 2\Delta K = \Delta L = 0$,   (Figure 19 D)

and finally, that everything may be interchanged, so that

(12e) $2\Delta K -- 2\Delta C -- \Delta L = 0$.   (Figure 19 E)

No other possibility is permitted, and spontaneous "birth or death" of only one invariant is prohibited. Lest there be any doubt, a few examples of balance for some specific cases are presented in Figure 22. These structural equations, which look like *ring closure* and *ring opening* reactions, in fact are *ring preservations* from topological viewpoint and should be referred to as *recyclizations* (expanding the author's early classification of heterocyclic ring transformations [115]).
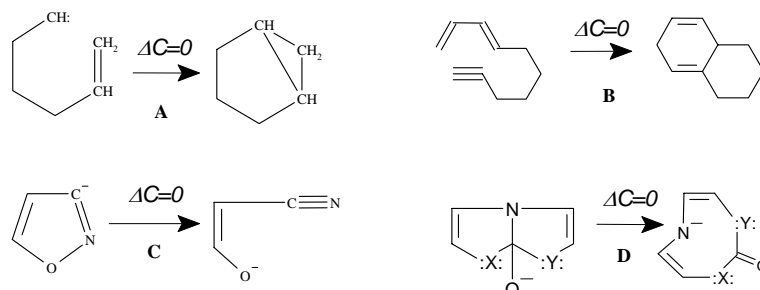

Figure 22. Some reactions related to the "Uroborus paradox" treated as a conservation of the handles (in topoids) or of the cyclomatic number (in molecular pseudographs) in the intramolecular reactions ($\Delta K = 0$). In none of the reactions ("bicyclizations" A, B or "ring-opening" reactions C, D) is the number of cycles changed ($\Delta C = 0$).

8. Homeomorphism of Topoids

A topologist, who does not make a difference between the doughnut and the coffee-cup, will never mix them up during a breakfast. Although the objects are homeomorphic, they are functionally not interchangeable, differing in shape and constitution. On the contrary, the homeomorphism of chemical models provides many examples where the homeomorphic objects are, indeed, functionally interchangeable in practice.

Let us look at the homeomorphism of topoids as a continuous mapping of one certain $2D$ model to another. Topoids are assigned to real molecules with the discrete number of atoms and electron pairs. Therefore, the reverse side of any homeomorphism is discrete (not continuous!) and certain (not arbitrary) leap in the number of atoms and electrons. Equations (11a,b) state that $\chi = 2 N -- Z$. Let us fix $K = 1$ and $L = 0$. Then, the homeomorphism of molecular topoids (the invariance of χ) should follow only from the balance of N and Z. The homeomorphism is expected relating somehow to a chemical similarity. Are there any known types of similarity if only atoms and electrons are counted? An intuitive answer is "Yes": a knowledgeable chemist may easily recall a few famous electron-count concepts, like the Langmuir isosterism, the Hückel rule for aromatic polygons, or the Wade rules for cage boron hydrides.

In the simplest case, the values N and Z may be fixed; then, the homeomorphism ($\chi = const$) is expected for isovalent molecules with the same number of atoms. This case corresponds just to the similarity type known as isosterism. Isosteric molecules (like CO and N_2, benzene and borazene, $POCl_3$ and $SiCl_4$, etc.) have surprisingly close geometry, spectra, and (quite frequently) physical properties (see reviews [29, 107, 108]).

Moreover, consequent insertion of only certain fragments should preserve the value χ. But this is possible only if the inserted fragment has $\chi = 2 N -- Z = 0$. Therefore, a topoid of inserted group should be homeomorphic to a torus or cylinder (to which $\chi = 0$), and the electron count for this group ($2 N = Z$) may be written as the ratio $Z/N = 2$. Consider a set of groups with such a ratio, with small N (from 1 to 4), and with the possibility to insert such a group more than once.

CH$_2$ group. This group (with $Z/N = 2$ and $N = 3$) is famous, being responsible for the phenomenon of already mentioned CH_2 homology. (The term *homology* is used here in the chemical sense [116], not in topological [41]; furthermore, chemical homology is an elder concept). Although the principle is very old, it has strong influence on the modern molecular similarity concepts [117], being a sort of reference point to answer the question "What chemical similarity may be at all". Homologues display monotonicity and additivity in physical properties and pronounced similarity in chemical behavior. Sometimes homologues display sort of a periodicity in their properties, that is, superposition of two monotonous functions for the odd and even members. The isosteric combinations $-BH_2^-$, $-NH_2^+$, $-BH_2NH_2-$ may be used to replace $-CH_2CH_2-$ fragments, but the chains formed are less stable [118].

Homeomorphism in C_nH_{2n+x} series (see Sections 3.1 and 6.1) resembles the definition of homeomorphic graphs. Expanding the scope on homological relationship, one may insert the CH_2 group into any cycle c_i, even if a cycle be the lone pair c_1. In pseudographs, it looks like the subdivision of a loop. Thus, taking as a precursor a Lewis base (like NR_3, PR_3, SR_2) one may obtain the "homological" structure of a dipolar *ylide* (like CH_2NR_3, CH_2PR_3, CH_2SR_2) without violation of the genus of a topoid. The ylides are important reagents for organic synthesis [119, 120], used, for instance, in the famous Wittig reaction. The ylides are strong Lewis bases (as are their homeomorphic precursors), although with lone pairs located on the carbon atoms (Figure 23, II). The resonance structures of ylides are frequently drawn as neutral ones with the double bond instead of a lone pair (a sort of intuitive equivalence between the cycles c_1 and c_2). It is difficult to insert several CH_2-groups into the lone pair of NR_3 (or

into the double bond $CH_2=NR_3$), since the pentacoordination is impossible for the nitrogen atom. However, it is do possible for the case of phosphorus, and the $-PR_3-$ fragment may belong to a large cycle, resembling CR_2 group (R is any alkyl group).

Some cases of CH_2 homology, treated as homeomorphism, are featured. The family C_nH_{2n} is homeomorphic to the inserted group. Consequently, for the pairs $[CH_2, CH_2]$, $[CH_2, CH_2=CH_2]$, and $[CH_2=CH_2, CH_2=CH_2]$ there is no evidence which group is inserted, and which cycle c_i is taken for insertion. The *object* and the *operation* with the object become identical. The formation of ylide is also symmetrical: one may treat it as the insertion of $-NR_3-$ into methylene's lone pair, or *vice versa*; the $-PR_3-$ group may be "inserted" into a C-C bond of a large cycle. Furthermore, perhaps in chemistry only, the homeomorphism may be equally "mental and experimental", having parallel to really observed reaction. The abstract insertion of methylene to ethylene corresponds to the high yield reaction, that is, formation of cyclopropanes from carbenes and alkenes. The homology of ammonia and ethylamine (which differ by ethylene) corresponds to Michael addition of amines to alkenes. In any Diels-Alder reaction involving the ethylene and a diene, the resulting cycloadduct is homeomorphic to the initial diene. Even the saturation of ethylene by hydrogen is a specific homological operation (the "insertion" of a CH_2CH_2 group into an H-H bond). Of course, H_2 (a spherical topoid) is the parent for C_nH_{2n+2} series if n = 0. Hence, the chains and cycles may be expanded or shrunk, remaining homeomorphic. Less trivial examples of homological series with delocalized bonds will be discussed in Section 11.

CH^+ group. This fragment (with Z/N = 2 and N = 2) is responsible for the similarity in π-isoelectronic chains and cycles. The insertion of CH^+ group makes planar delocalized π-systems longer (ethylene to allyl cation or allyl anion to butadiene) without violation of initial planarity and number of π-electrons. This is essential for delocalized cycles. One may easily recall, that 5-, 6-, and 7-membered aromatic rings (cyclopentadienyl anion $C_5H_5^-$, benzene C_6H_6, and tropylium cation $C_7H_7^+$) differ from one another just by a CH^+ group [121, 122]. Hence, these "homological" aromatic structures have homeomorphic topoids in quite the same sense as usual CH_2 homologs are. Furthermore, the insertion of a CH_2 group may also preserve aromaticity, and this phenomenon is known as homoaromaticity [122]. The homological fragment CH^+ may be substituted by isosteric groups BH and NH^{++}, the insertion of which into the cycle $C_5H_5^-$ result in the pyridinium cation $C_5NH_6^+$ and borabenzene anion $C_5BH_6^-$, both being aromatic and isostructural to benzene. Molecular topoids for aromatic pyrrole and benzene are also homeomorphic (the double bond is substituted by a homeomorphic lone pair), and homeomorphic insertions of BH, CH^+, or NH^{++} groups into the pyrrole ring result in (neutral or charged) heteroaromatic hexagonal structures (see examples in Figure 23, III). Although CH^+ cannot form long chains, within the class of fused benzenoid hydrocarbons it may be inserted and removed mutually, resulting in *nonbenzenoid* arenes. Homeomorphism equally preserves aromatic and antiaromatic types, and the insertion of CH^+ (and its isosters) into the antiaromatic rings causes the inheritance of antiaromaticity.

BH group. The fragment BH is essential: it has two vacancies (unlike the methylene group) and the capacity of forming the multicentered bonds with three neighbors (see Section 11). This group, therefore, may serve as a vertex of a polyhedron. Indeed, BH is a well-known homological difference in the families of boron hydrides B_nH_{n+x} [123]. Such hydrides form two neutral homological series with x = 4, 6, (*nido-*, and *arachno-*boranes, from the Greek for "nest-like", and "web-like", respectively) and one family of dianions $[B_nH_n]^{2-}$ known as *closo-*boranes (from the Greek for "closed").

Conventional structures assigned to these three classes with delocalized bonds are remarkable (see Figure 23, IV suggested by Rudolf [124]). The *closo-*class is represented by "deltahedral" boranes clusters with a skeletal pattern resembling triangulation of the sphere, whereas the *nido-*, and *arachno-*classes may be obtained by removal of a cluster vertex in an appropriate *closo-*polyhedron (deltahedron) [124 -- 127]. An attempt to calculate their Euler characteristic using formula (11) results in x = χ (just as it was for the C_nH_{2n+x} family). The values for B_nH_{n+4} (χ = 4) and B_nH_{n+4} (χ = 6) clearly indicate that the genus exceeds the value allowed to the closed orientable 2D manifolds (maximum χ = 2 for sphere), and the nature of their topoids will be discussed in Section 12.

Already mentioned CH^+ group may be also inserted into the *closo-*polyhedron as another homological fragment, resulting in the stable carborane families $[CB_nH_{2n}]^-$ and $C_2B_nH_{2n}$ [111] with preservation of the *closo-*structure. Of course, the Euler characteristic χ = --2 is the same for every class. Hence, the topoid should be a pretzel, and the graph should be bicyclic. However, only the first member of the neutral carboranes matches such a structure (three BH fragments inserted into the bonds of acetylene pretzel result just in $C_2B_3H_6$), whereas higher homologs are delocalized. Other examples of CH^+-homology in delocalized clusters are represented by the polyhedrons $C_5H_5^+$ and $C_6H_6^{2+}$. Hence, we may conclude that insertion and removal of the homological BH and CH^+ groups in such clusters is equivalent to an inessential perturbation of a structural pattern around the cage.

NH_3 group. Unlike other above-mentioned homological groups, the group NH_3 (with Z/N = 2 and N = 4) cannot subdivide chains, cycles, or clusters. This group, however, is able to make a shell around a point-like cation. Indeed, ammonia is a common ligand in coordination chemistry, capable of multiple coordinating to either a transition metal cation or even to a main-group cation (like in complexes $M(NH_3)_n^{m+}$ in liquid ammonia [128]). One would say that such a coordination of several ligands to a Lewis acid makes no essential change to the initial cation (Figure 23, I). Perhaps, only the total size and shape are increased upon the coordination. The size and shape, however, are geometrical properties, not topological, and the coordination resembles a remarkable homeomorphism from a sphere to the 2D surface of a hedgehog.

The same homeomorphism (with more pronounced enlarging of the spherical shape) is typical for ligands with longer chains, the homologs of ammonia (like mono-, di-, and trialkylamines). The formed external shell becomes hydrophobic. The higher hydrophobicity (and higher stability) of such complexes may be achieved by the addition of novel handles to the spherical surface. Thus, the use of cyclic polydentate ligands (like kryptands and aza-analogs of crown ethers) results in so stable hydrophobic cations, that the initial mineral salt may be easily dissolved even in a nonpolar solvent. The topology of such complexes, described in terms of graphs (trees and polycycles) or surfaces (sphere with pasted handles) is completely parallel to the picture of saturated hydrocarbons C_nH_{2n+x}. The molecules PR_3 (isovalent and homeomorphic to NH_3) represent another class of suitable ligands, as well as the homeomorphic carbenes CR_2, which may form complexes with transition metals. Topological shrinking of ligands (removal of NH_2^+ group from NH_3 or CH^+ group from CH_2) results in the hydride anion H^-, which is

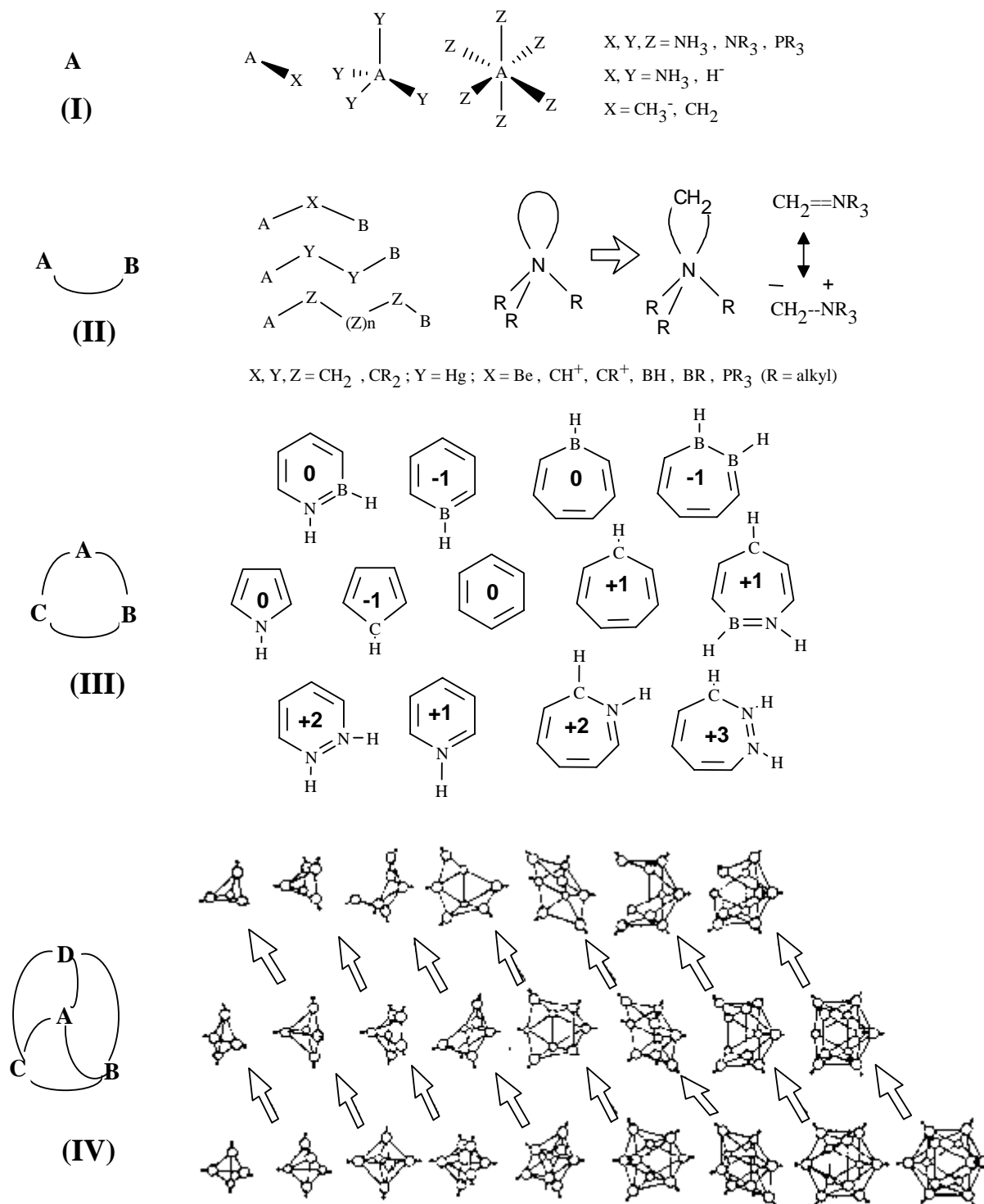another common ligand capable for coordination.

Figure 23. Design of molecular structures by the insertion of certain groups with $\chi = 0$ (see the text). (I) The use of ligands in coordination chemistry (A is a center with vacancies). (II) Examples of groups that may be inserted into a bond A–B without changes of the genus. (III) Insertion of groups BH, CH$^+$, NH^{2+} into the planar aromatic rings with preservation of aromaticity (the number within the ring is the charge of molecule). (IV) Insertion of groups BH and CH$^+$ within the series of boron hydrides and carboranes with preservation of structural pattern (isostructural families are in horizontal rows). Arrows indicate the relationship between *arachno-* (top row), *nido-* (middle row) and *closo-* (bottom row) structures.

A special case, that (with some care) may be treated as a sort of homeomorphism, is the insertion of metals from the second column of the Periodic Table with Z/N = 2 (Mg, Zn, Hg, and Cd) into some bonds (*e.g.*, C–Hal or Hal–Hal), although only a Hg atom may form short chains. These reactions are extremely useful in organometallic chemistry (*e.g.*, the Grignard reaction), and homeomorphic structures are formally enlarged without change in their topology. Here the simplest "homologs" (with pronounced ionicity of bonds) dramatically differ from the parent members (with covalent bonds), however, there are still not enough data to conclude about the similarity types within longer homological series (with several metal-metal bonds).

Let us emphasize that the concept of homeomorphism of topoids, being applied to the inserted fragments, brings together many previously disjoint chemical similarity types in a unique manner. Although the enlarging or diminishing of an

object (a geometrical change) appears in homeomorphic series, the initial topological pattern is conserved. Furthermore, we may even classify the initial patterns (and their homeomorphisms) in terms of usual topological cells:

e^0 cell (a point-like cation) homeomorphism around the point (Figure 23, I);

e^1 cell: (a linear bond) homeomorphism along the line (Figure 23, II);

e^2 cell: (a fragment of planar cycle) homeomorphism around the plane (Figure 23, III);

e^3 cell: (a spatial cavity in deltahedrons) homeomorphism around the space (Figure 23, IV).

The inserted groups only slightly overlap, each being responsible for its own cell and dimension. The evident homeomorphism *between* groups indicates that homeomorphism in chemistry is just a concept independent of dimensions.

Aromaticity and homeomorphism. Note that the total number of handles is not responsible for aromaticity or antiaromaticity, expressed by the Hückel rule ($4n$ and $4n+2$ π-electrons). The presence of cycles c_i ($i>2$) and their planarity is essential, because isolated handle (a multiple bond or a lone pair) outside the delocalized perimeter brings nothing to the π-electron count. However, the possibility to count π electrons appears only because there are small cycles c_1 and c_2 within the perimeter of a cycle c_i. Therefore, for the case of usual polycyclic conjugated hydrocarbons with total C' large cycles c_i ($i>2$) and total C handles in topoids (C' plus double bonds) the difference between "large and small" handles C-C' corresponds just to the Hückel rule: it is odd for the aromatic case and even for antiaromatic. Of course, the groups BH, CH^+, and NH^+ may be freely inserted or removed without changing the C-C' value. This rule is also not violated if the cycles c_1 of NH groups are counted as handles. Moreover, since the fragments NH, CH^-, BH^{2-}, $CH=NH^+$, and $CH=CHCH^+$ have the same topology of a pretzel (intact or bitten) and bring two π-electrons, they may be freely interchanged without loss of aromaticity (or antiaromaticity). This adds real "flexibility" to the common (hetero)aromatic structures, because one may topologically shrink larger fragments to smaller ones (see examples in Figure 24).
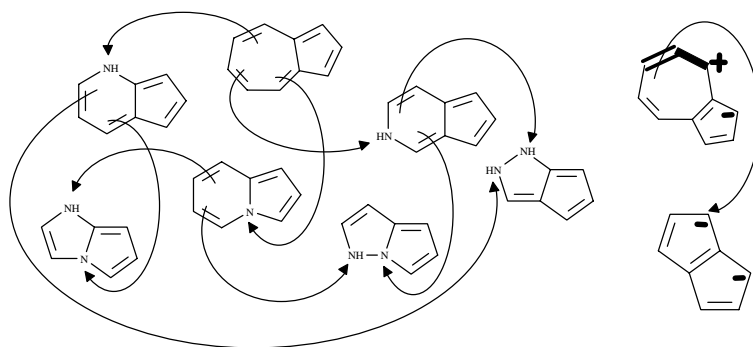

Figure 24. Topological shrinking and preservation of aromaticity. On the left: Design of heteroaromatic pseudoazulenes from azulene structure as a shrinking of double bond(s) to lone pair(s). On the right: Shrinking of azulene (shown as resonance form) to dianion of pentalene as homeomorphism of allyl cation (bold fragment) to π-isoelectronic CH_3-anion.

9. Surfaces with Jordan Curves as Exact Images of Graphs

9.1. Idea and Algorithm of Representing Graph by Labeled Surface

A molecular topoid is a 2D surface with only three invariants (K, L, and C), and from the combinatorial viewpoint, it looks poorer than a molecular graph (graphoid) from which the topoid is obtained. Molecular graph carries a lot of combinatorial information about a molecular structure (connection pattern, isomorphism, size of cycles, branching), whereas in molecular topoids all these features are totally lost. Can this information be reflected in topoids? The question may be reformulated as a quite general and purely mathematical: how to display the adjacency of e^0 and e^1 elements of a graph (manifested for instance in the incidence matrix of a graph) by any manner on (in) a 2D surface?

As we mentioned above (see Section 2.6) this question is rarely (if ever) appeared in topology. Instead, only the inverse problem ("graph-on-surface") is usually considered, that is, how to assign a graph (*e.g.,* a dual graph) to a *labeled* surface (*e.g.,* a colored map). Of course, we may place any sort of labels on a 2D surface in order to represent adjacency of vertices of a graph, however it is required that two nonisomorphic graphs have differently labeled surfaces. What might play the role of these labels? As we repeatedly mentioned, an intuitive *one-to-one correspondence* between graphs and surfaces ("graph-as-surface") is implied in chemical modeling. Thus, in the classical solid space-filling models every atom is represented by a *colored* solid ball (which is an image of a vertex in a graph), and the bond (image of an edge of a graph) is visualized on a 2D surface as a *circumference*, which is an area of contact of two colored balls. Therefore, circumferences on a 2D surface are suitable labels for edges of a graph, and any abstract graph (with the cyclomatic number C) intuitively is a set of circumferences drawn on the surface S_c. Each circumference (Jordan curve) is the image of an edge, and the appeared 2D regions symbolize the vertices.

Let us define more precisely how to represent a *pseudograph* G by a surface labeled by Jordan curves. Let G be a pseudograph with E edges and cyclomatic number C. Create a tubular neighborhood N(G) of G by an adding a ball around every vertex and a solid cylinder around every edge. (The balls and cylinders we add should be "small enough" to preserve all cycles of G from occasional disappearance.) Let S_C denote the boundary of N(G). Then, S_C is a closed orientable surface of genus C. Now, in each of the solid cylinders in N(G), choose a meridional disk, and let J denote the set of all of the boundaries of these meridional disks. Thus, J is a collection of circles in S_C. Let $S^i_c = (S_C, J)$, which is the surface S_C *together* with the collection of circles J. Since every meridional disk matches exactly one edge and $_{25}J = E$, the above procedure unequivocally assigns unique

labeling of a surface $S_c^i = (S_C,J)$ to the graph G. Lest there be any doubt on where to locate a meridional disk, put it "in the middle" of an edge, or subdivide every edge by a new vertex (to get a bipartite graph) and build the disks at the places of new points. The overall procedure is visualized in Figure 25. Let us write $H(G) = S_C^i$, if the labeled surface is assigned to a graph by the just discussed algorithm H, that we shall call the *canonical algorithm*.

It should be underlined, that the canonical algorithm H is equally applicable for mapping a graphoid (with some e^0 elements absent) to an open orientable surface $(^LS_C, J)$ labeled by Jordan curves. The difference is trivial: holes should be regarded as specific 2D regions, hence the borders between a surface and the holes are some special sort of Jordan curves. (For assignment of a surface ^LS_C to a graphoid see Section 5.2.)

9.2. Dual Graphs for Labeled Surface

Consider a labeled surface S_C^i and put a question inversed to just discussed. How to assign a graph dual to this surface, requiring that Jordan curves are prototypes of edges? There may be two types of dual graphs.
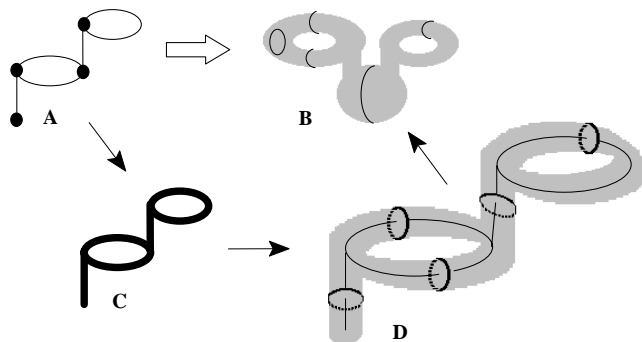

Figure 25. Canonical algorithm of mapping a pseudograph (A) to a surface labeled by Jordan curves (B). Intermediate steps: tubular 3D neighborhood of a graph (C) and addition of meridional disks (D) as the images of edges.

The first graph G_{ext} (*externally dual graph*) is defined as follows: put one vertex in each 2D region of S_C^i and connect vertices only if a path from one vertex to another crosses a 1D Jordan curve between the regions. The reconstruction (restoring) of the edge from a torus with meridian gives a loop. The total procedure (shown in Figure 26, top) will be written as $F_{ext}(S_C^i) = G_{ext}$, and it resembles drawing of dual graphs for (geographical) maps.
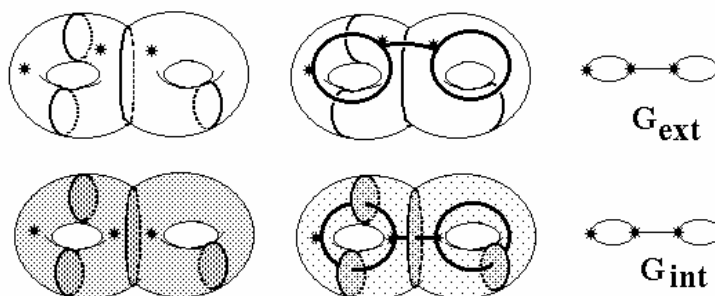

Figure 26. Visualization of two types of dual graphs that can be assigned to a labeled surface. *Top*: externally dual graph (on the surface). *Bottom*: internally dual graph (inside the surface).

Another dual graph G_{int} (*internally dual graph*) is defined by the reversal of the above canonical algorithm in Figure 25. Namely, for each 1D circle on the surface S_C^i, we should add (if possible) a meridional 2D disk so that the circle becomes the boundary of this disk. (This is not always possible, *e.g.*, in the case of a torus we may place a 2D disk to any meridian, but not to a longitude.) The appearance of disks results in a set of e^3 cells bordered by e^2 cells (either initial S_C or new 2D disks). Now, locate a point (vertex of the G_{int} graph) inside each e^3 cell, and draw an edge only if there is a path from one point to another that crosses the 2D disk. (Whenever the two sides of a nonseparating Jordan curve are the part of the same region, we will create a loop in the graph) The procedure (shown in Figure 26, bottom) will be denoted as $F_{int}(S_C^i) = G_{int}$. The definition of G_{int} may illustrate how chemists "see" a molecular graph (atoms connected by bonds) hidden *inside* the molecular space-filling models.

Above we suggested a method (canonical mapping H) of obtaining a labeled surface from a graph. Now let us check whether *the same graph* (or a graph isomorphic to the initial one) will be returned back from the labeled surface by the operations F_{int} and F_{ext}. Evidently, if S_C^i is obtained from the graph G by the canonical algorithm $H(G)$, the internally dual graph is the same graph G:

(13) $F_{int} [H(G)] \sim G$

Here "~" means "isomorphic to", and brackets indicate subsequent action of operations. Hence, the operation F_{int} restores the same graph.

Less trivial is relation (14):

(14) $F_{ext} [H(G_i)] \sim G_i$

Nevertheless, it is true, since the canonical algorithm H is so "good" labeling of S_C^i, that G_{int} can be continuously deformed to G_{ext} giving the isomorphic graph (see Figure 26).

9.3. Labeled Sphere and Trees

Several circles may be arranged on the surface in either equivalent or nonequivalent manner. Let S denote any surface containing a collection of disjoint circles J_1 and another collection of disjoint circles J_2, where the sets J_1 and J_2 may intersect. We define (S,J_1) to be equivalent to (S,J_2) if there is a homeomorphism h from S to itself such that $h(J_1) = J_2$.

Now let $S_c^i = (S_0,J)$ be the sphere labeled (partitioned) by any number of circles in any manner. Then, it is true that:

(15) $F_{ext}(S_0,J) \sim F_{int}(S_0,J)$,

(16) $H [F_{ext}(S_0,J)] = H [F_{int}(S_0,J)] = (S_0,J)$,

Hence, for *any* labeling of the sphere both types of dual graphs always coincide (expression (15)). Of course, the dual graph here is always a tree. Furthermore, the application of the canonical mapping H to this dual tree restores just the initial arrangement of labels (expression (16)).

THEOREM 1:   *The number of nonequivalent labeling (partitions) of the sphere by E Jordan*

curves is equal to the number of nonisomorphic (and nonrooted) trees with E edges.

The proof elementary follows from expressions (13) -- (16) and the equality J = E.

9.4. Labeled Torus and Monocycles

The case of a sphere is unique because any labeling by circles is in the one-to-one correspondence to a certain tree. Generally, a labeled surface may not have a dual graph at all, or the internal dual graph may be absent. This is evident from the cycles **a**, **b**, **c**, and **d** (Figure 27) drawn on the toroidal surface.
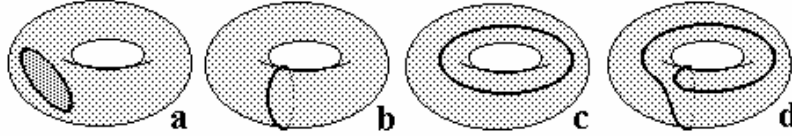

Figure 27. Various possibilities of arrangement (embedding) a closed Jordan curve on the torus (see the text).

Case **a** is the worst: no dual graph can be assigned to this labeled surface, and this arrangement of a circle on a torus cannot be an image of any graph. Case **b** is the best: both dual graphs exist and are isomorphic. Cases **c**, **d** are intermediate: graph G_{ext} exists but G_{int} not. Cases **b**, **c**, **d** may be generalized: any closed spiral line on the torus is representable as a "sum" of few longitudes and few meridians n**b** + m**c** (n and m are natural numbers showing how many times the fragment of spiral "resembles" meridian **b** and longitude **c**). Then **b** = 1**b** + 0**c**, **c** = 0**b** + 1**c**, **d** = 1**b** + 1**c**.

Let us say the labeling of a torus is *perfect* if at least one closed cycle is different from the cycle **a**. Let us say, the labeling of the torus belongs to the same (n,m) class if it is perfect and if at least one circle used for labeling is of n**b**+m**c** type, where **b** is a meridian and **c** is a longitude. Let us write this labeling as $(T^{n,m},J)$, where J is a set of closed curves. Then, for any $(T^{1,0},J)$ labeling of the torus by any number and any arrangement of circles it is evident that:

(17) $F_{ext}(T^{1,0}, J) \sim F_{int}(T^{1,0}, J)$,

(18) $H [F_{ext}(T^{1,0},J)] = H [F_{int}(T^{1,0},J)] = (T^{1,0}, J)$

Hence, for any (0,1) class of labeling of the torus (perfect and by at least one meridian) both dual graphs, external and internal, coincide (expression (17)). Of course, such dual graph is always a monocyclic graph (maybe with a loop or a multiple edge). Furthermore, the application of the canonical procedure H to this dual graph restores just the initial arrangement of labels $(T^{1,0}, J)$ (expression (18)).

We may conclude that the (0,1) class of labeling of the torus is the best, because it is the same as for the sphere, and therefore, within this class we may freely switch from graphs to surfaces (operation H) and back (using either of two operation, F_{ext} or F_{int}). This seems impossible for other (m,n) classes, where the operation F_{ext} is defined but F_{int} is not. Nevertheless, there are some homeomorphisms on the torus that take any n**b**+m**c** curve to the meridian 1**b**+0**c**, or, in other words, any "bad" (m,n) class of labeling to a "good" (1,0) class. For instance, we may always *invert* a torus with longitude(s) to a torus with meridian(s), changing a labeling from (0,1) to (1,0) class (Figure 28).

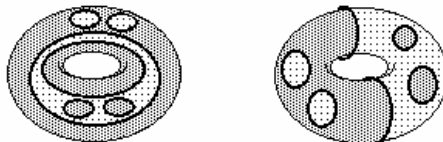Figure 28. Labeling of a torus from the (0,1) class (left) and from the (1,0) class (right). A homeomorphism $h(T^{0,1},J) = (T^{1,0},J)$ that transforms the left object to the right one is the *inversion* of a torus with Jordan curves.

By other words, there is a homeomorphism h: $h(T^{0,1},J) = (T^{1,0}, K) = (T^{1,0}, J)$. The operation h opens the possibility of extracting the G_{ext} graphs (which are isomorphic to the initial graph G) "indirectly" from the class where they are impossible. Such a homeomorphism (although less visual) of a torus to itself is possible for any $T^{m,n}$, and let us state that $h(T^{m,n},J) = (T^{1,0}, K) = (T^{1,0}, J)$. Therefore:

(19) $\quad F_{ext} (T^{m,n},J) \sim F_{int} (T^{1,0},J)$

(20) $\quad H [F_{ext}(T^{m,n})] = H [F_{int}(T^{1,0})] = T^{1,0}$

THEOREM 2: *The number of nonequivalent labeling (partitions) of the torus by E Jordan curves within each $T^{m,n}$ class is equal to the number of nonisomorphic monocyclic pseudographs with E edges.*

The proof is evident, because for the good class ($T^{1,0}$) each pseudograph is in the one-to-one correspondence to a certain labeled torus, and any labeling ($T^{m,n}$,J) from "bad" class may be reduced to a good class by a homeomorphism h.

The question arises, whether the relationships similar to the just discussed exist for the surfaces with more than one handle? Even for the case of pretzel the picture is unclear, and the author offers this problem for professional topologists.*) Anyway, expressions (13) and (14) are true for C > 1.

10. Chemical Applications of Surfaces with Embedded Jordan Curves

The theorems proved in the previous section may be useful in the general methodology of molecular 2D modeling. First, the chemical problems related to the isomorphism of graphs (*e.g.*, the chemical isomerism) may be translated to the language of equivalent and nonequivalent embedding the Jordan curves on a 2D surface. Second, the problem of 2D visualization of a lone pair and multiple bond (still poorly or even contradictorily resolved in common models) may get an explicit mathematical answer. Third, an intriguing expansion of the common principles of 2D molecular modelling may be suggested for the cyclic molecules with the delocalized bonds.

10.1. Chemical Isomerism and Homology: a Novel Viewpoint

A unique parallelism between trees and a labeled sphere (Theorem 1) relates the fundamental problem of chemical isomerism in saturated hydrocarbons (usually treated *only* at the level of graphs) to the problem of nonequivalent arrangements of Jordan curves on a sphere. To make this statement clear, consider *hydrogen-suppressed* graphs of alkanes. Let us represent the family of these graphs by the set of labeled spheres. Let us draw an arrow between two labeled spheres only if an addition of one Jordan curve to a labeling $(S_0,J)_m$ results in a labeling $(S_0,J+1)_n$ (see Figure 29 A). Because each labeling $(S_0,J)_n$ corresponds to a unique tree, let us shift from the set of surfaces to the set of trees, keeping the set of arrows the same (Figure 29 B). Now a novel relationship (manifested by the set of arrows) appears between the trees with V vertices and V+1 vertices. From the chemical viewpoint, Figure 29 B represents a combinatorial relationship between the structures of alkanes, namely, between their higher and lower homologues (graphs joined by an arrow) and isomers (graphs on the same level of the diagram). However, this relationship follows *only* from the topologyof surfaces, and it *does not* follow from the graph theory.

The old problem of chemical enumeration (*e.g.*, of isomers and CH_2 homologues) frequently implies the application of the orbits of a graph automorphism group [1, 2, 8, 130] (defined on the permutation of vertices *or* edges). A labeled surface is *another* combinatorial object with another type of the "automorphism group". The further discussion is beyond the scope of this paper, and our goal is only to underline the existence (and importance) of this problem. In Figure 29 C -- E the same -- *novel* -- type of relationship (consequence from Theorem 2) is shown for the families of 2D objects (from $T^{1,0}$ and $T^{0,1}$ classes) and the corresponding monocyclic pseudographs. If the labeled surfaces represent usual molecular pseudographs (not only hydrogen-suppressed graphs), then nonequivalent arrangements of J curves equally cover isomers, ylides, betaines, or resonance structures with heteroatoms. Therefore, isomerism and isosterism become indistinguishable from the combinatorial viewpoint.

----

*) Very recently E. Flapan (Los Angeles) stated [129] that the following theorem is true:

Let C be any fixed positive integer. For a given surface S of genus C, let Q_i denote any finite set of disjoint simple closed curves contained in S which has the property that if we cut S open along all of the curves in the set Q_i, then we will obtain a collection of planar surfaces. We will say two such collections Q_i and Q_j are equivalent if there is a homeomorphism h from S to itself such that $h(Q_i) = Q_j$. Let Q denote the set of all equivalence classes of such collections of curves. Let P denote the set of all pseudographs with cyclomatic number C. Then there is a bijection between Q and P.
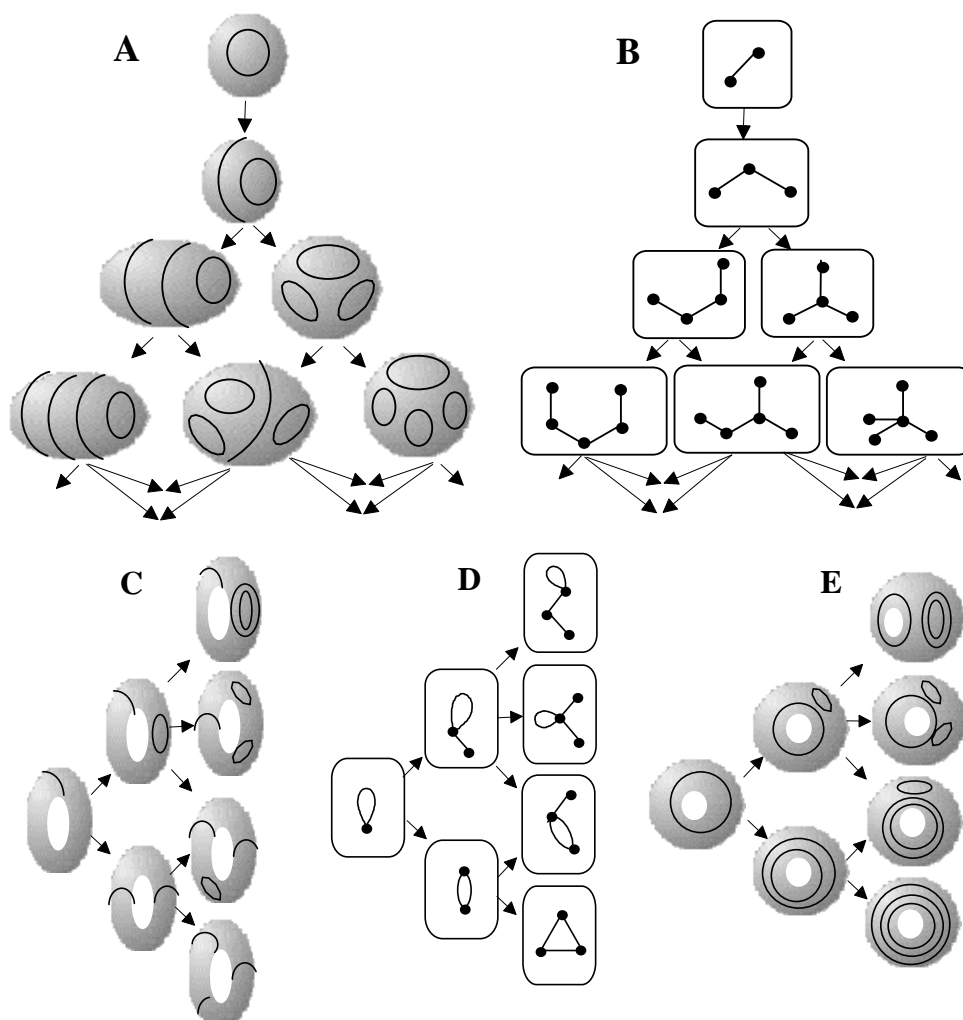
Figure 29. An illustration of one-by-one addition of circles (Jordan curves) to a sphere (A) and a torus (C and E). An arrow shows the possibility to obtain a novel labeling of a surface by placing a circle to the previous labeling. The same type of relationship is shown for the the dual graphs of labeled surfaces, trees (B) and monocyclic pseudographs (D).

10.2. Homeomorphism and Isotopy: Lone Pair and Double Bond

As mentioned in Section 3, the relationship between structural formulas drawn on paper and some classical 2D models is usually considered as a simple one-to-one correspondence. Upon careful inspection, this relationship appears not so simple (Sections 5 -- 8), and the correspondence, from the topological viewpoint, may not be one-to-one (see Section 9). Fortunately, the manner in which chemists construct various 2D models (*e.g.*, space-filling and ball-and-stick models) from structural formulas resembles canonical mapping H. Indeed, in most 2D models of cyclic molecules (say, of saturated hydrocarbons C_nH_{2n+x}) it is always possible to place a *meridional disk* between the positions of two atoms, former vertices of a graph. There may be a disk between adjacent balls in the space-filling 2D models, or a disk across a "stick" in the ball-and-stick models. Therefore, an intuitive one-to-one correspondence (molecular graphs -- classical molecular 2D surfaces) may be explicitly confirmed. The expanded one-to-one correspondence between molecular graphoids and molecular topoids (involving free radicals, multiple bonds, and lone pairs) is, of course, also possible. Equations (13) – (18) prove this, and the structural formula (molecular graph, multigraph, pseudograph, or graphoid) represented as a 2D model may be unequivocally reconstructed (returned back unchanged) as a dual graph of any type, either external or internal.

Nevertheless, the canonical mapping of a molecular graph to a labeled surface does not exhaust all strategies of topological design at 2D level of molecular modeling. Equations (19), (20) indicate that for *cyclic* molecules, it is possible to assign *more than one* 2D model, which will be in the one-to-one correspondence one to another and to the parent molecular graph. For instance, the toroidal 2D model of a monocyclic molecule may have the arrangement of Jordan curves from any (m,n) class. Let us apply this idea to represent a double bond and a lone pair, the simplest cycles in molecular pseudographs, and the worst cases of molecular 2D modeling (see Section 4). Both features are frequently represented by a *single circle* (Jordan curve) on a *spherical* surface (see Figure 30 A, B). In the case of ammonia (Figure 30A), such a circle helps to represent the most compact arrangement of bonding and nonbonding electron pairs (as a set of circles on a sphere) in order to predict molecular geometry [97, 98]. In the case of ethylene (Figure 30 B), a circle represents a single interaction of two VDW spheres along the C=C bond.
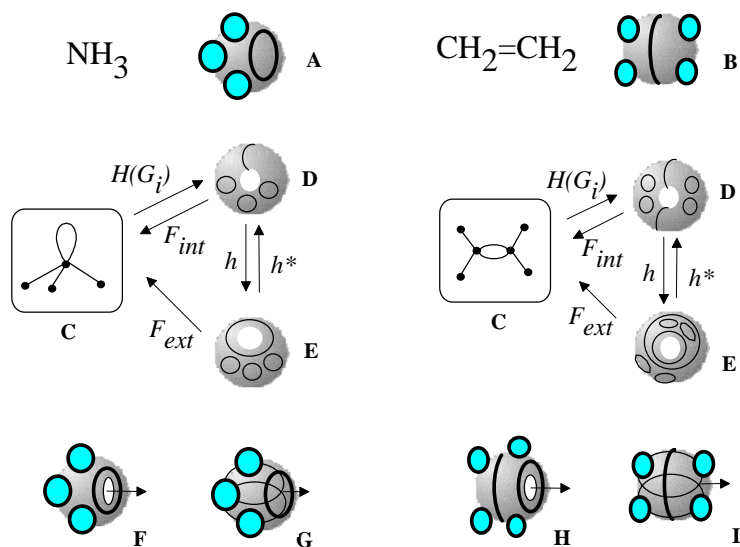
Figure 30. Various *2D* models of NH_3 (left) and C_2H_4 (right); Jordan curves on surfaces represent electron pairs. Standard *2D* model of NH_3 (A) and C_2H_4 (B) with a single Jordan curve on a sphere. Molecular pseudographs (C) and their toroidal topoids with meridians (D) and longitudes (E) representing the edges of the parent graphs. The surfaces with longitudes and visible holes (F,H) may be self-crossed (G, I).

Within the model of labeled topoids this picture is changed. Of course, the surfaces of NH_3 and C_2H_4 are toroidal with one circle for a lone pair and two circles for a double bond. For each case, the corresponding molecular pseudograph G_i (Figure 30 C) may be transformed either to a surface with meridian(s) (Figure 30 D) or to a surface with longitude(s) (Figure 30 E) by applying the canonical mapping $H(G_i) = (T^{1,0}, J)$ and the homeomorphism $h(T^{1,0}, J) = (T^{0,1}, J)$. For each molecule, the models D and E (Figure 30) are homeomorphic, but *not isotopic*. The initial monocyclic graph G_i may be unequivocally restored from these *2D* models by different ways (see Section 9), directly (D to C or E to C) or indirectly (considering the homeomorphisms h and h* between D and E).

As mentioned above (Section 6.3), the most logical *2D* image of a lone pair (and of a double bond) is a "pseudo-spherical" surface with the masked hole (self-crossed torus). The self-crossed surfaces with longitudes (G and I) have some advantages over the models with meridians. Only the longitudes (not the meridians) are equally visible in both self-crossed and normal toroidal surfaces (*cf.* cases F and G or H and I in Figure 30). The self-crossed model of ammonia with a longitude (Figure 30 G), resembling the common model (Figure 30 A), allows a symmetrical arrangement of the circles (electron pairs) around the surface and may, therefore, predict the same geometry type of NH_3 as does the VSEPR model. Furthermore, in the model G (Figure 30), the longitude may be continuously shifted throughout the invisible self-crossed part, illustrating well-known phenomenon of the pyramidal ammonia inversion. Similarly, the model of C_2H_4 with two longitudes (E) is more preferable than the model with meridians (D). The first one (model H in Figure 30), being changed to the self-crossed image (Figure 30 I), has only one longitude on the external surface (and one more inside). The model in Figure 30 I resembles the standard space-filling model of C_2H_4 (Figure 30 B). Furthermore, the elliptical self-crossed region inside the double bond (the trace of a hole) is located along the axis C-C in complete agreement with the model of Bader. Finally, any difference in the isotopy of the discussed 2D models in R^3 (presence of usual or masked hole, drawing a circle as a meridian or as a longitude) is compensated by their topological indistinguishability (at least, in space R^4). Therefore, an inessential difference may be removed by an appropriate homeomorphism.

10.3. Isotopy and Delocalization in Cycles

The substitution of one $T^{m,n}$ class by another, possible for cyclic molecules, may be interesting for the case of *conjugated* chains and cycles. An alternating sequence of single and double bonds (along a chain or around a planar cycle) results in essential delocalization of double bonds. Expression of this phenomenon is impossible in terms of common molecular models. In a molecular graph, the position of a single or a multiple edge is strictly fixed. Similarly, in conventional *2D* models the position of a single meridional Jordan curve (or two curves) is localized in the specific *2D* region. However, a homeomorphic change of a labeled *2D* model (from $T^{1,0}$ to $T^{0,1}$ class) may help to resolve this old paradox of chemical modeling.

A topoid of a conjugated molecule may have several handles, and each handle has various number of Jordan curves. Consider the simplest example of the delocalized cyclic molecule, the cyclopropenilium cation (Figure 31), that consists of cycles c_2 and c_3. We may represent the double bond by a toroidal fragment with two meridians (Figure 31 A) or with two longitudes (Figure 31 B). However, the cyclic cation has localized and delocalized bonds, so we may relate the manner of embedding a Jordan curve with the localization of a bond. Let a meridional Jordan curve represents a *localized* bond. Indeed, one may always add a disk (wall) to such a curve and locate the disk in a certain position bounding the nuclei inside the surface. Now assume that the Jordan curve homeomorphic to a longitude of a torus represents a *delocalized* bond. This also makes sense: a longitude (image of a bond) rounds the *2D* toroidal surface with nuclei inside. Hence, for the cyclopropenilium cation we may draw three longitudes rounding the "large" hole (cycle c_3) and one meridian across the additional "small" hole (Figure 31 C). This picture is parallel to the concept of σ-delocalization in the aromatic systems, recently discussed in quantum-chemistry [131, 132].
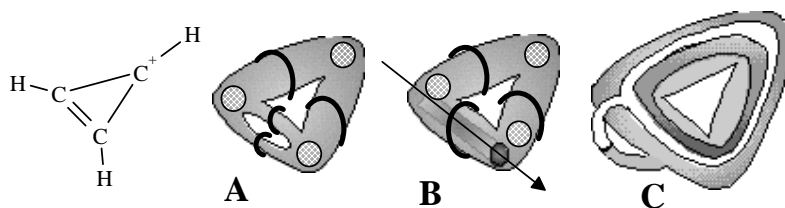
Figure 31. Various arrangement of Jordan curves on the surface of pretzel representing C-C bonds in 2D models of the cyclopropenilium cation. (A) Four meridians. (B) Two meridians and two longitudes; an arrow indicates the arrangement of the second hole with one more longitude inside. (C) Three longitudes and one meridian (circles for the hydrogen atoms are not shown).

In general case, the topoid of a conjugated molecule with several handles may have various types of Jordan curves: some of them are "meridian-like" and other may be "longitude-like". The benzene molecule may be represented as a topoid with six longitudes and three meridians (or vice versa). Clearly, a graph G_i that may be reconstructed from these 2D models (directly by the operation F_{ext} or indirectly by the combination of operation F_{int} with the homeomorphism h*), is the parent molecular graph G_i (like a single Kekule formula of benzene).

11. Delocalized Bonds and Hypertopoids

There are a lot of molecules to which it is impossible to assign certain molecular structure with localized two-centered and two-electron (2c,2e) bonds and, hence, to draw a certain molecular graph. The reasons may be different. For example, there may be violation of habitual valency of an atom (e.g., of the hydrogen atom in the hydrogen bonds X-H-X or of the carbon atom in transition states X-CR$_3$-Y of S_N2 reactions). Another reason is the delocalization of free electrons, lone pairs, and double bonds, manifested for instance, in the appearance of unexpectedly higher symmetry of a molecule (benzene, charged or radical allyl system, nonclassical cations) or in an abnormal length of single and double bonds (conjugated dyes). Finally, there may be a deficiency of edges (2c,2e-bonds) necessary for forming a connected graph (like in H_3^+, CH_5^+, boron hydrides), so that the structures should be discussed only in terms of three-centered and two-electron (3c,2e) bonds. Perhaps, the worst cases for molecular modeling are the cation radicals (like H_2^+ and CH_4^+) where it may be necessary to assume the existence of two-centered one-electron (2c,1e) bonds.

For these uncertain cases, the conventional structural formulas are frequently drawn with dashed lines, where the concepts of cyclomatic number, connectedness, and homeomorphism become unclear. Any discussion of topology for these cases seems possible only in terms of molecular orbitals or at least the graphs extracted from $\nabla\rho$ analysis of the electron density. Nevertheless, the necessity of storing the structural information about molecules in computer databases, independently on the type of intra- and intermolecular bonds, stimulates attempts to describe delocalized structures in terms of graphs and matrices. [133 -- 135].

11.1. Attempts to Use Molecular Graphs and Hypergraphs

In parallel to the MO pictures (poorly compatible with the traditional concept of bonds) chemists continue developing the combinatorial models related to the molecular graph concept even for the uncertain cases discussed above. The first (and the eldest) model, pioneered by Lapworth, Robinson, and Ingold [136], is the use of curved arrows that complement molecular graphs (Figure 32 A -- C). The arrows indicate a topological feature (free radical, lone pair, or a single/multiple bond) to be selected and rearranged in the molecular graph. Evidently, this approach is combinatorial because the entities and their number are exactly indicated, and the "fortune" of each entity is predetermined by an arrow. Finally, an uncertain delocalized structure is assumed to lie in-between certain graphs (resonance forms) with exact cyclomatic numbers and connectedness. The resonance forms may be isomorphic (as in examples on Scheme 32 A, B), nonisomorphic (as in conjugated cyanine dyes), or even disconnected graph (like in the boundary structure in Figure 32 C for the hyperconjugation of a CH$_3$ group). The qualitative combinatorial picture of a molecule as a set of resonance structures becomes quantitative in the formalism of valence bonds theory [91].
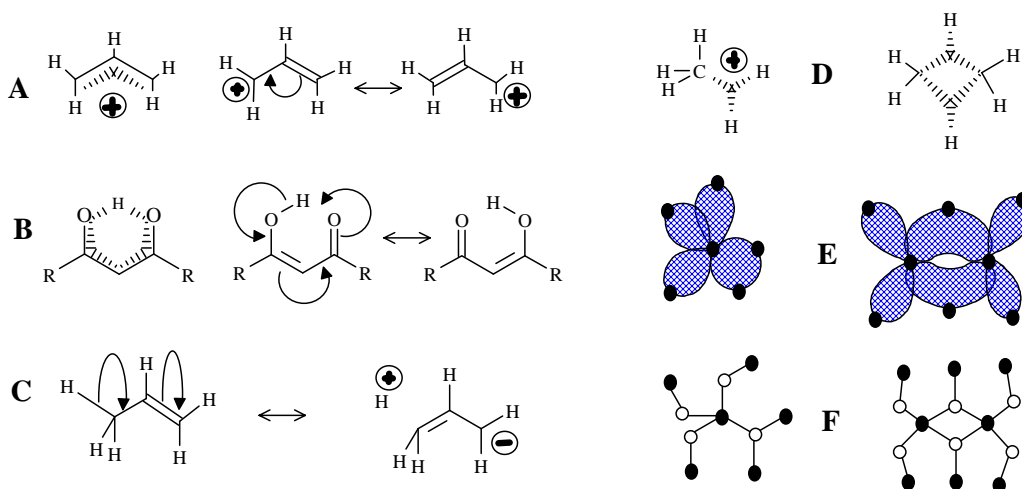

Figure 32. Various topological representation of molecules with delocalized bonds. (A) Delocalization in the allyl cation. (B) An example of the intramolecular hydrogen bond. (C) The hyperconjugation in propene illustrated by the disconnected resonance formula. (D) The standard representation of molecules CH_5^+ and B_2H_6 with (3c,2e) bonds; (E) the same structures represented by hypergraphs (with bonds as planar 2D disks) and corresponding König graphs (F).

Another concept, also related to graph theory, is the formalism of depicting (3c,2e) bond by adding specific subgraphs adjacent to the localized (2c,2e) skeletal framework. Thus, the (3c,2e) bond may be regarded to as a specific vertex of degree 3 (the image of a bond, not of an atom) connected by dashed edges to three atoms participating in the multicentered bonding (Figure 32 D). The models originate from the so called *styx-formulas* suggested by Lipscomb for the structures of boron hydrides [123]. (The letters *s*, *t*, *y*, *x* initially denoted different types of (2c,2e) and (3c,2e) bonds in boranes.) The *styx*-formulas were generalized [137], reviewed [111], and extensively used by Olah and others to describe the topology of hypervalent electron-deficient molecules and clusters. In such "molecular graphs", vertices have two types of labels (one for atoms and another for (3c,2e) bonds) and two types of labeled edges, usual (for (2c,2e) bonds) and dashed (joining differently labeled vertices). We may conclude that the *styx*-formula is an intuitive application of the *hypergraph* concept for molecular modeling (see Figure 32 E). Indeed, the common *styx*-formulas with (3c,2e) bonds (like in Figure 32 D) resemble an *incomplete* König representation for hypergraphs (Figure 32 F), because usual (2c,2e) bonds are still drawn as edges, not vertices. Understanding of this fact [32] was fruitful and led to the development of topological indices of molecular hypergraphs and algorithms for storing the data on delocalized structures in computer databases [138].

Both concepts discussed above are ill-defined on the level of 2D models. The topological invariants of hypergraphs with (3c,2e) bonds are uncertain at the 2D level. Of course, the König graphs (with definitive cyclomatic number) may be helpful for the development of certain 2D images for molecules with (3c,2e) bonds. However, it is still unclear what type of topological objects should be assigned to the radical cations with (2c,1e) bond (like H_2^+ and CH_4^+). Such species and their fragmentation form the central subject of the mass-spectroscopy, where the lack of good structural models is pronounced [139]. Let us prove that the concept of topoids may serve for the rigorous description of (3c,2e) and (2c,1e) bonds as fundamental topological invariants, and the curved arrows of chemists relate to specific topological transformations.

11.2. Pseudomanifolds and Their Euler Characteristic

As we mentioned in Section 8, an attempt to calculate the Euler characteristic for topoids of boron hydrides starting from the electron count ($2N -- Z = \chi$) leads to $\chi = 4$ (nido-class) and $\chi = 6$ (arachno-class). Similar calculation for a cation CH_5^+ (with the 3c,2e-bond) lead to $\chi = 4$, and the cation-radical CH_4^+ (with 2c,1e-bond) has $\chi = 3$. These χ values are impossible for the closed 2D manifold. Nevertheless, there are a lot of triangulable 2D objects with $\chi > 2$ that consists of usual topological cells e^i. These objects, however, are *not* the 2D manifolds. They are the *pseudomanifolds* (see Section 2.4 and Figure 6). The simplest pseudomanifolds are the bouquets of spheres. Let us examine, how these simplest models may relate to molecular topoids, and how one may calculate their Euler characteristic without partition into cells.

A bouquet of spheres (unlike a usual sphere) has a specific point with a neighborhood of this point not homeomorphic to a planar 2D disk. Consider a bouquet of m_i+1 spheres (designated as $W^{m_i+1}(S_0)$) attached to the same point. Let us call this point *a base point of index* m_i. The index of a base point (that is, m_i) should not be confused with the number of spheres around this point (that is, m_i+1); a single sphere S_0 (a "bouquet of one sphere" $W^1(S_0)$) has index $m_i = 0$ for any point on its surface.

Consider a set of k disjoint bouquets $\{W^{m_i+1}(S_0)\}_k$ each with the single base point of index m_i. Let M be equal to Σm_i. The Euler characteristic χ for a single bouquet of spheres $W^{m_i+1}(S_0)$ and for the disconnected set of k bouquets follows equations (21a) and (21b), respectively.

(21a) $\chi[W^{m_i+1}(S_0)] = 2 + m_i$

(21b) $\chi[\{W^{m_i+1}(S_0)\}_k] = 2K + M,$

Let us construct more complex objects from a bouquet of spheres. Consider a finite number k of such bouquets and allow making of any number of punctures or holes (except puncturing the base points) and any gluing of the holes together
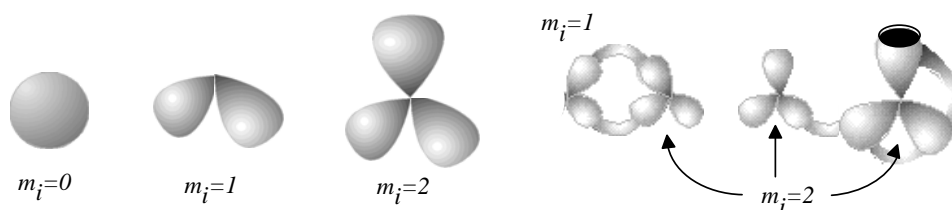

Figure 33.   Indices of the base points in various pseudomanigolds derived from the bouquets of spheres. All diagrams together form a single disconnected pseudomanifold W having K = 5, L = 1, C = 3, M = 10, and $\chi(W) = 13$.

(with a restriction to preserve the orientability). Some punctures may be preserved upon the gluing. The result will be the appearance of handles and a change in the number of components k. Of course, the pasting preserves any index m_i and the total value M. The resulting object is a (disconnected) pseudomanifold W (see Figure 33). To calculate the Euler characteristic $\chi(W)$, consider a mapping $f(W) = \{{}^L S_C\}_K$, that takes a pseudomanifold to a usual orientable (may be disconnected) 2D surface $\{{}^L S_C\}_K$. The mapping requires the substitution of "abnormal" k base points by "normal" 2D-fragments. For instance, remove a base point and paste the appeared m_i+1 holes by a sphere ${}^{m_i+1}S$ (sphere with m_i+1 punctures). The resulting object is the set of orientable surfaces $\{{}^L S_C\}_K$, and let it be exactly K components, C handles, and L punctures. Then the Euler characteristic of the initial pseudomanifold should be (22):

(22a) $\chi(W) = 2K -- 2C -- L + M$

The proof is obvious: reverse the mapping f(W) to return back k   "abnormal" base points and apply the formula (21b).

11.3. Molecular Hypertopoids and their Homeomorphism

The pseudomanifolds derived from the bouquets of spheres may be helpful as exact topological images of molecules with multicentered bonds. Let us assume that for such $2D$ models the Euler characteristic satisfies equation $\chi = 2N - Z$ (as it was for localized case) and write:

(22b) $\chi(W) = 2K - 2C - L + M = 2N - Z$

This hypothesis is very strong: we may have no an *a priori* knowledge about the mapping of a molecule to a pseudomanifold, however, the electron count is always exact. Therefore, for any uncertain type of chemical bond we may use equation (22b) to "extract" the set of topological invariants (K, C, L, and M) and the $2D$ model itself! Let us assume that the index of a base point reflects the type of bonding. Thus, for a molecule with usual localized (2c,2e) bonds the value M is equal to zero (because any point on usual $2D$ surface has index $m_i = 0$). Of course, for this case of bonding, a pseudomanifold is reduced to usual $2D$ manifold (topoid), and equation (22b) is changed to equation (11b). Let us examine how to extract possible $2D$ images (pseudomanifolds) for the simplest (3c,2e) and (2c,1e) bonds.

For the simplest molecule H_3^+ with one multicentered (3c,2e) bond, we have $\chi = 2N - Z = 6 - 2 = 4$. If the molecule is considered to be connected (K = 1) and has neither cycles nor unpaired electrons (C = L = 0), then M = 2 (M = $\chi - 2K = 4 - 2 = 2$). The $2D$ model is assumed to be a pseudomanifold, and $M = \Sigma m_i$ implies that there may be k base points. Consider k = 1, then the presence of unit base point of index $m_i = 2$ corresponds to the bouquet of *three* spheres. The resulting mathematical image perfectly matches the known structure of H_3^+: $2D$ regions are atoms, and (3c,2e) bond is the base point to which the spheres are attached.

For the simplest cation-radical molecule H_2^+ we have $\chi = 2N - Z = 4 - 1 = 3$. Assume, that the molecule has *no free radical centers* (unlike usual free radicals H or CH_3), because here the unpaired electron forms a specific (2c,1e) bond. Therefore, L = 0. If the molecule is again considered connected (K = 1) and without cycles (C = 0), then M = 1 (M = $\chi - 2K = 3 - 2 = 1$) and the $2D$ model uniquely corresponds to the bouquet of *two* spheres. Of course, such topological $2D$ image of the (2c,1e) bond (two spheres pasted by a point) differs from that of (2c,2e) bond (a tube) and (3c,2e) bonds (three spheres pasted to a point).

Let us call these prototype models *molecular hypertopoids*. In the previous sections we proved the usefulness of the homeomorphism principle for usual topoids. Let us apply it to hypertopoids. By taking a bouquet of 2 or 3 spheres as the models of H_2^+ and H_3^+, we may label the spheres (any one or every one), drawing new Jordan curves on them. A suitable combination of curves may be related to the homeomorphic insertion of specific groups (like CH_2, BH or other fragments) without violating the value χ. The stepwise addition of Jordan curves symbolizes homological series. The possibility of arranging the same number of curves by various ways is the isomerism. Such a labeling (homeomorphic insertion of CH_2 groups) in H_3^+ cation leads to the homological family of protonated alkanes $C_nH_{2n+3}^+$. The parent cation CH_5^+ (with hypercoordinated carbon atom) and its homologues have the same topological pattern as in the initial molecule H_3^+ (see Figure 34 A). Homological series of H_2^+, of course, is the family of radical cations of alkanes $C_nH_{2n+2}^+$, (like CH_4^+). For this series the $2D$ surface is not smooth; it has a node representing (2c,1e) bond.

Another familiar topological operation, that may be applied to hypertopoids, is the connected sum. As usual, this operation requires the removal of terminal hydrogen atoms and pasting the appearing pair of holes with a suitable tube (a fragment homeomorphic to cylinder). The connected sum of two hypertopoids H_3^+ (Figure 34 C), using as a simplest tube the group CH_2 or BH_2^- results in the dications (1) and (2). Both dications CH_6^{2+} (doubly protonated methane) and BH_6^+ (doubly protonated BH_4^- anion) are still unknown. However, the second pasting of a tube BH_2^- instead of other pair of hydrogen atoms (Figure 34 D) leads to the familiar diborane (3) with two (3c,2e) BHB bonds and one cycle (handle in the pseudomanifold). The third addition of BH_2^- anion to diborane (now as a homeomorphic insertion, labeling of bridging hydrogen atom) results in the known *arachno*-type anion $B_3H_8^-$ (4) with a BBB three-centered bond. Further $2D$ design of higher boron hydrides seems trivial, resembling the *styx*-description [111, 123].

New families of hypertopoids may be designed by pasting additional tubes to different spheres of the same hypertopoid H_3^+. The resulting families should differ in the number of handles, although within every family the homeomorphism should be manifested. Example of a long tube to be pasted is the $(CH_2)_n$ chain that should appear instead of pair(s) of terminal hydrogen atoms. The addition of one, two, and three tubes is shown in Figure 34 E, F, G. The obtained structures (5), (6), (10), (11), (15), and (16) are well-known [109 -- 111]. These are famous families of *nonclassical* carbocations (like the norbornyl cation) either registered by spectral methods or unequivocally postulated as intermediates in carbocyclic and Meerwein-like rearrangements. (Most of the discussed cations with few exceptions, are short-living species for which it would be better to refer to as the intermediates.) Consider the homeomorphic shrinking of a chain to a single bond. This operation establishes homeomorphic relationship of three families of nonclassical carbocations to three cations: aromatic cyclopropenyl (17), delocalized allyl (12), and cation $C_2H_5^+$ (7), that is, the protonated double bond of ethylene. This last step of shrinking is completely parallel to the homeomorphisms of larger cycles to the double bonds (although one edge is now a "hyperedge", that is, (3c,2e)-bond). However, the possibility of shrinking is still not exhausted.

The final step of homeomorphism in molecular pseudographs of localized structures was the topological shrinking of a multiple edge to a loop. This was "inessential" shrinking of the double bond in C_2H_4 to the lone pair in CH_2 preserving the genus of a topoid. Now, the shrinking of a protonated double bond to the protonated lone pair may be also treated in terms of inessential homeomorphism of hypertopoids. Of course, the protonated ethylene (7) with (3c,2e) bond is an intermediate to form ethyl cation. Therefore, let us consider the protonated methylene (8) (with the formal (3c,2e) bond) also as an intermediate to form methyl cation. The difference is only that the "hyperedge" (that should be incident to 3 different vertices) is actually incident only to 2 vertices, although twice to one of them. Hence, it combines features of a loop and a normal edge resembling hyperloops in the pseudo-hypergraphs (see Section 2.2 and Figure 2).
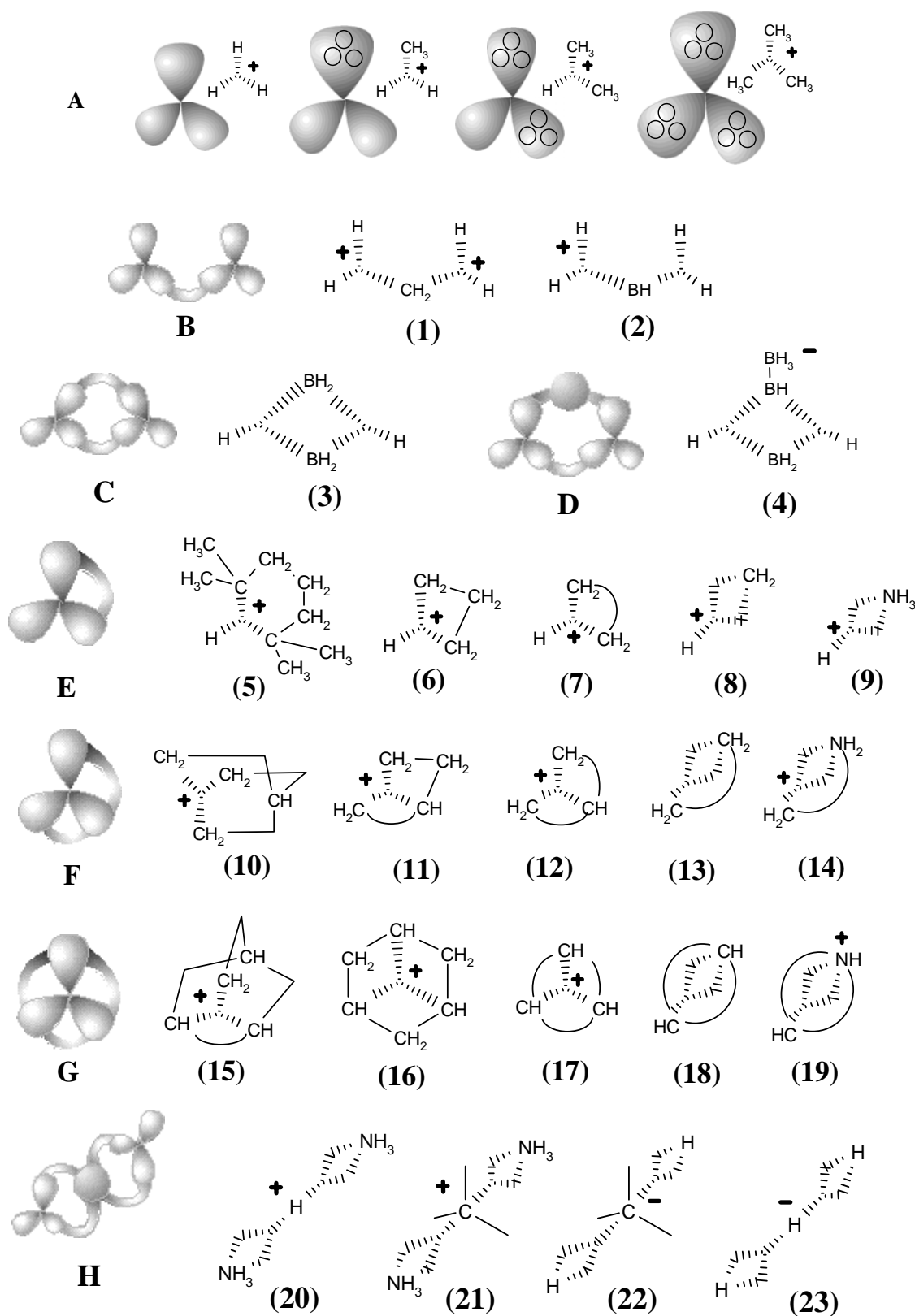
Figure 34. Homeomorphism in hypertopoids (see the text). Standard representation of molecules with multicentered bonds by *styx*-formulas may be expanded if three ends of (3c,2e) bond (shown by dashed line) are incident to two atoms (as in diagrams (8), (9), (13), (14), (18) -- (23)).

Such an assumption opens the possibility of visualizing the intermediate step of interaction between any Lewis acid and Lewis base centers. In particular, we may add one more Jordan curve to the hypertopoid of protonated methylene **(8)** and obtain the homeomorphic image **(9)**, that is the intermediate for ammonia protonation related to the simplest hydrogen bond. Further additions of Jordan curves to the 2*D* image of structure **(9)** (insertion of CH_2 or BH_2^-) symbolize intermediate states of bonding in BH_3NH_3 and quaternary ammonium salts $CR_3-NR_3^+$. Now, we may shrink edges in the allyl and cyclopropenyl cations **(12)** and **(17)**, making parallel to the interaction of a lone pair with carbocation in the immonium cation **(14)** and protonated cyanic acid **(19)**. The diagrams of ethylene **(13)** and acetylene **(18)** (isoelectronic to the cations **(14)** and **(19)** and differed by the homological CH^+ fragment from

the cations (12) and (17)) may illustrate the intermediate step of heterolysis (polar resonance) of the multiple bonds.

The above homeomorphisms allow us to suggest how two lone pairs may be involved in multicentered bonding. Consider two cationic intermediates H_3N^+-H and H-NH_3^+ (each represented by formula (9) and hypertopoid in Figure 34 E) and make their connected sum (Figure 34 H) using the anion CH_3^- as a sort of a tube. The result is the delocalized cation (21), that is an intermediate for degenerated S_N2 reactions. A homeomorphic shrinking of CH_3^- to H$^-$ (or, simply, homeomorphic removal of CH_2) leads to the formula (20), the simplest example of hydrogen bond $[NH_3$-H-$NH_3]^+$. The diagram (20) is also an intermediate step of the proton exchange between a conjugated acid (NH_4^+) and base (NH_3). Shrinking of both terminal NH_3 groups in the previous examples to H$^-$ results in the model systems [H-CH_3-H]$^-$ (22) and [H-H-H]$^-$ (23) two "delocalized" lone pairs (cf. the topology of these anions H_3^- and CH_5^- with that of cations H_3^+ and CH_5^+).

One may conclude that the homeomorphism in topoids and hypertopoids has the same nature. In both cases the homeomorphism, that is, the preservation of the Euler characteristic, follows from the electron count. Therefore, the procedures of homological shrinking and expansion are heuristic tools in the establishing of novel similarity relationships for complicated cases of chemical bonding. In turn, a hyperloop may be recommended for use together with common styx-formulas.

11.4. Interconversion of Molecular Hypertopoids

Intuitively, any change of index m_i of the base point requires a "touch" (that is, pasting) of $2D$ surfaces: otherwise, how would we make a bouquet without a touching? However, any such "touching" means either a decrease in the number of components or the appearance of a cycle (self-touching). Hence, the change of m_i (and of the total M value) requires appropriate changes of the other invariants K, C, L for abstract pseudomanifolds.

The same is true for molecular topoids and hypertopoids. The bonds of various nature (two- or three-centered, one- or two-electron bonds) may be interconverted, and the processes may be described in terms of joining and disjoining of appropriate (pseudo)manifolds with changes in the values m_i and M. The question is how the topological invariants K, C, L, M of molecular hypertopoids are interchanged in real reactions. In the preceding section, the invariance of $\chi(W)$ within the homeomorphic series turns out useful to compare and classify the structures. We may suppose, that the principle of preservation of the Euler characteristic of hypertopoids in chemical reactions may be important to compare and classify the reactions. The assumption that $\Delta\chi(W) = 0$ immediately leads to (23):

(23) $\Delta\chi(W) = 2\Delta K -- 2\Delta C -- \Delta L + \Delta M = 0,$

which is the topological balance equation. If some parameters are not changed via a reaction, equation (23) is reduced. Thus, equations (12a) -- (12e) discussed in Section 7 for interchanges of the systems with localized bonds (M = 0), are still valid and meet the particular case $\Delta M = 0$. For the cases where the index M is changed to other parameters ($\Delta M =/= 0$) the following set of equations appears:

(24) $\Delta M = -- 2\Delta K$

(25) $\Delta M = 2\Delta C$

(26) $\Delta M = 2\Delta C -- 2\Delta K$

(27) $2\Delta K -- \Delta L + \Delta M = 0$

(28) $2\Delta C -- \Delta L + \Delta M = 0$

(29) $\Delta M = \Delta L$

Let us retrieve the examples and inspect them with the goal to visualize the features of each interconversion (Figure 35).

Heterolytic processes. First three equations (24) -- (26) correspond to polar processes (value L is preserved). Inspection of the right-hand parts of these equations shows that the change of index ΔM here is even, e.g., this may be a change from M = 0 to M = 2 or reverse. The simplest illustration of balance (24) is the change of a (2c,2e) bond (M = 0) to a (3c,2e) bond, like a protonation (or electrophilic alkylation) of a hydrogen molecule or alkane resulting in the series $C_nH_{2n+2}^+$ (n may be zero).

The formation of the bouquet of three spheres $W^3(S_0)$ from only two disjoint spheres is shown in Figure 35A. A sphere of an electron deficient species (H$^+$ or CR_3^+) is moved closer to another sphere, that is the source of (2c,2e) bond. The localized bond represented as a Jordan loop (closed curve with a point) may be C-C, C-H or H-H bond. At the instant of touch the loop is "pinched" (as a sort of girdle tightening a sphere into two ones) and finally shrunk to a point to which three spheres become attached. Of course, the χ value is preserved. Let us call the operation μ_2 (polar joining).

The formation of a (3c,2e)-bond is reversible (Figure 35A). Let us also reverse the operation μ_2 and disjoin the bouquet of spheres so that two usual spheres appear and call the operation μ_2^* (polar disjoining). For instance, the hypertopoid H_3^+ may be disjoint to two spherical topoids H$^+$ and H_2. If the spheres would be labeled (say, by isotopes H, D, and T for the case H_3^+ or there may be different alkyl groups joint by the (3c,2e) bond) the disjoining μ_2^* may occur in any of three directions. Indeed, the isotopic exchange (like $H_2 + D^+ = H_2D^+ = HD + H^+$) and the interchange of alkyl groups in hypercarbon intermediates are well-known.

Topological operation μ_2 represents the first step of any polar interactions X + Y = Z, where X is an electron deficient species (Lewis acid) and Y is a Lewis base (real or masked) before the usual bond is formed. Hence, the formation of cationic intermediates (6) -- (9) (Figure 34) via the protonation of a cycle (in ammonia, carbene, ethylene, or cyclopropane) without destruction of the handle in a topoid is indistinguishable from the protonation of H_2 and alkanes. These reactions belong to the same μ_2 type and follow the same balance equation (24).

The case corresponding to equation (25) appears if the connected sum of spheres is taken for the operation μ_2, say, if

two complementary centers (Lewis base and acid) are at the ends of the same chain. Particular cases are the formation of the norbornyl cation, the processes of hydride migrations in alkyl cations, and resonance in allyl or cyclopropenyl cations. The reversed operation μ_2^* corresponds to the "ring opening" of the protonated cyclopropane, ethylene, and ammonia (Figure 35B).

Equation (26) corresponds to the collapse of at least two components to a cycle with the appearance of multicentered bonds. Example is the dimerization reaction $2BH_3 = B_2H_6$ (Figure 35C).

Homolytic processes. The next three cases (27) -- (29) relate free electrons to multicentered bonding; here the changes in L (appearance or disappearance of holes) cause changes in M value. Evidently, these processes are important for structural modeling in the mass-spectrometry, where the bonding types are interchanged in ionized species.

The simplest case (27) is the gluing of a punctured sphere to a point on usual sphere making a bouquet; the topological change may be denoted as $^1S + S_0 = W^2(S_0)$. This may be formation of the radical cation H_2^+ from the radical H and cation H^+ (or any homeomorphic case). Analogously, the radical addition to the (2c,1e) bond may cause formation of the (3c,2e) bond (Figure 35D). Let us call the operation μ_1 (homolytic joining) and consider the reversal operation μ_1^* (homolytic disjoining), when a bouquet is destroyed so that any resulting surface may hang a puncture. Such homolytic disjoining is possible for the cation H_3^+, where the bouquet $W^3(S_0)$ may be homolytically destroyed to another bouquet $W^2(S_0)$ and a punctured sphere $^1S_0$. The chemical image of the sequense μ_1 and μ_1^* (shown in Figure 35D) may correspond to the isotopic exchange $H_2^+ + D = H_2D^+ = HD^+ + H$.

Equation (28) appears for the case of "pinched torus" (an object obtained if a tube connects different spheres in the bouquet $W^2(S_0)$), and it helps to illustrate the cleavage of an ionized cycle to a chain (Figure 35E). The pinched torus of a cyclic radical cation after the cleavage μ_1^* of the cyclic (2c,1e) bond is destroyed to a stretched punctured sphere, and the appeared free radical and cationic centers are on the opposite ends of the chain.
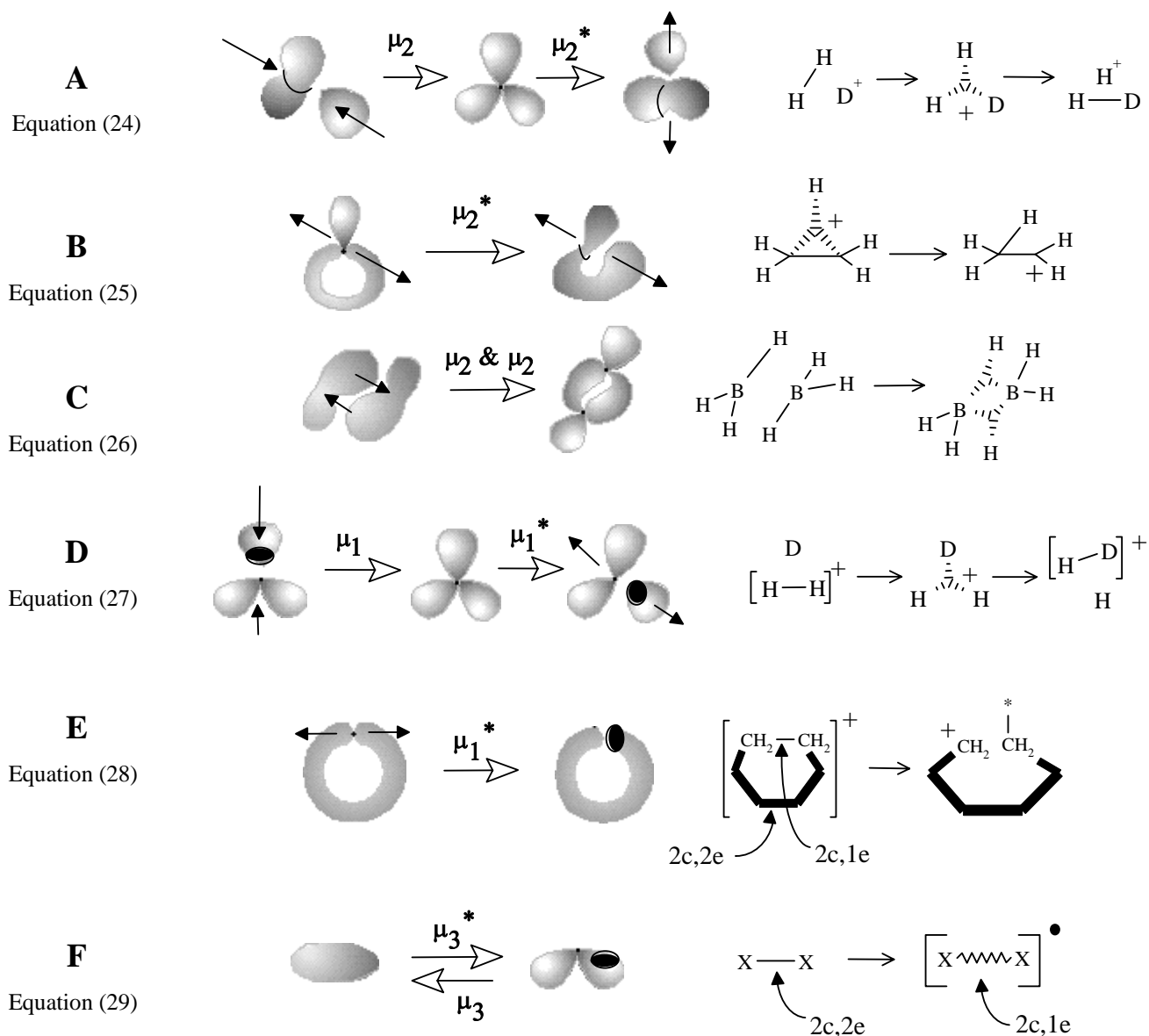

Figure 35. Illustration of equations (24) -- (29) by various types of joining and disjoining of 2*D* objects. An example of the chemical equation is shown for every case (see the text). The black arrows indicate a direction of joining/disjoining.

The last equation (29) is essential. Expression $\Delta M = \Delta L$ is   the case when everything else (namely, C and K) is fixed.

Then, one puncture (free electron) may appear only if it is compensated by the increase of M by one. This may be possible for an intermediate step of conversion of the "non bonding" free radical center to a bond; let us denote this operation μ_3. The reverse process (operation μ_3*) may be an intermediate step of homolysis of a bond. We can not refer to the operations m3 and m3* as *polar* or *radical*, they are independent on the type of formed or broken bond. Rather, these processes should be related to the topological change of a molecule via a photochemical excitation and mass-spectral rearrangement. If an electron leaves the region of the usual bond (single or multiple) with $m_i = 0$, the residual domain should acquire the properties of a (2c,1e)-bond with $m_i = 1$ (Figure 35F). Analogously, a puncture may "appear" from the region of a (2c,1e) bond ($m_i = 1$), and the remaining region should acquire the properties of the base point with $m_i = 2$, *i.e.*, the novel (3c,2e) bond should appear. Finally, we may consider an analogous shift of a puncture from the area of the (3c,2e) bond, that requires a decrease of M (or m_i) from 2 to 3. This is possible for $W^4(S_0)$, bouquet of four spheres. Therefore, one may imagine a weak (3c, 1e) bond (for instance, in the hypothetical dication H_3^{2+}) as the bouquet $W^4(S_0)$.

   Topological design of reaction mechanisms.   The mechanism of a reaction may be complex, involving various intermediates and transition states to which it is difficult or impossible to assign a certain topological object. The model of hypertopoids may be helpful for distinguishing intermediate species (in respect of their topology) and reaction mechanisms themselves. Consider the simplest heterolytic formation of a covalent bond (step A to C in Figure 36). In Section 7 this process was regarded to as a pasting of a sphere to the cavity of a torus (the case "boa and elephant"). However, this representation follows only from the "*brutto*" balance equation (12b), and the mechanism was neglected. Taking into account the operations μ_2 and μ_2* (that follow balance equations (25) and (26)) it is possible to draw the process as the stepwise conversion A → B → C understanding the manner of the hole disappearance. Moreover, the topology of the intermediate particle B helps to clarify that the mechanism of formation of the covalent bond from pure ionic precursors may involve single electron transfer (B → D → C). Furthermore, the intermediate structures B and D may illustrate that the homolytical formation of a covalent bond may have a complex mechanism (involving steps E → D → C or E → D → B →C). Finally, conversion of two radicals to a ionic bond (*e.g.*, in the common reaction Na + Cl = Na$^+$ + Cl$^-$) can be clearly described by sequence E → D → B → A.
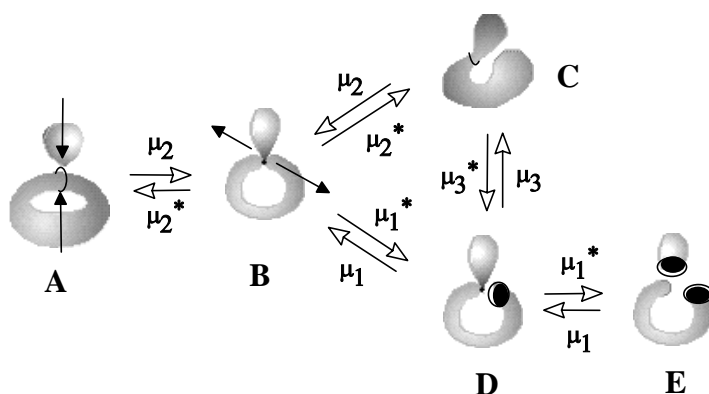

Figure 36. Visualization of the topology of intermediates via common chemical reactions. A formation/cleavage of a single covalent bond (C) from/to a disjoint pair of Lewis acid and base (A) or two radicals (E) via intermediates (B) and (D).

   Curved arrows, resonance, and topology. A parallel for the model of curved arrows (still popular in many handbooks) may be suggested on the level of pseudomanifolds. A delocalized structure (a pseudomanifold) lies between boundary resonance structures (usual manifolds). A curved arrow usually indicates how to transform one resonance structure to another displaying the rearrangement of electrons (an electron pair or a single electron) along the molecular framework. Let us assign a certain topological operation (μ_1, μ_1*, μ_2, μ_2*, μ_3, or μ_3*) to the "action" of any curved arrow. One simple example is shown in Figure 37 for resonance structures of a typical delocalized dye. Here only two operations (μ_2 and μ_2*) are required to transform one resonance structure to another involving the delocalized structure as the natural intermediate step. The curved arrows, therefore, should be regarded as explicit topological operations.
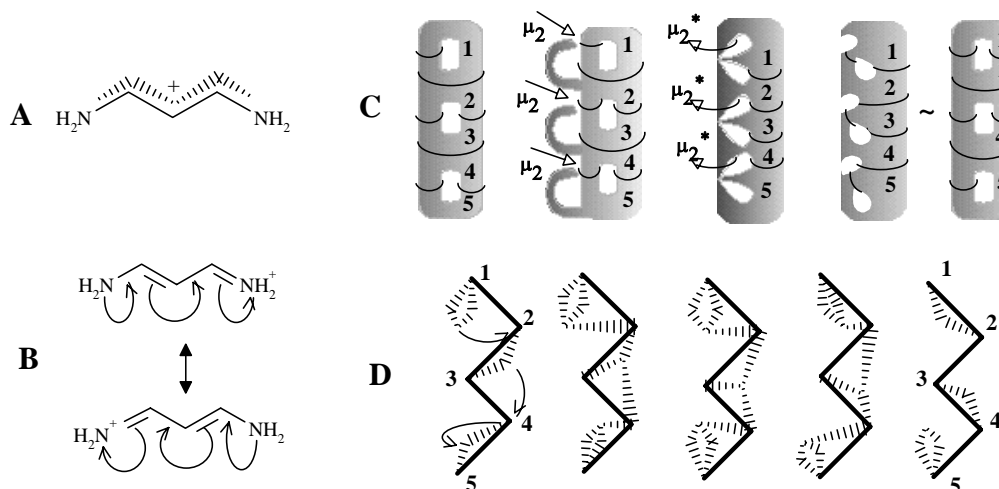

Figure 37. The visualization of topology of a delocalized molecule. A delocalized cation (A), two resonanse formulas (B), the

stepwise representation of the structure by topoids and hypertopoids (C) and by generalized *styx*-formulas with hyperloops (D).

Expanded 2D images of delocalized molecules. The last remark on the model of hypertopoids concerns their outward appearance. Of course, the discussed above $2D$ surfaces of pseudomanifold with base points are not smooth. However, the electron density around (3c,2e) bond usually resembles smooth spherical domains around (2c,2e) bonds. Is it possible to imagine other types of smooth $2D$ models with topological invariants parallel to the discussed above?

The supply of $2D$ objects with $\chi = 3$ and $\chi = 4$ can be expanded, and some examples are shown in Figure 38.. Some of these objects (that are also pseudomanifolds) allow the representation with external smooth spherical surface. Thus, image of (2c,1e) bond may be changed from the bouquet $W^2(S_0)$ we used above to a smooth spherical object -- a sphere with $2D$ disk pasted inside the surface. Similarly, we may change the image of (3c,2e) bond from the bouquet $W^3(S_0)$ to another pseudomanifold -- a single sphere with three $2D$ disks inside each being adjacent to a line. (Both images strongly resemble the architecture of soap bubbles.) Most intriguing is that this visual change of the models has no influence on the formalism discussed in this section. Thus, the design of homeomorphic families, construction of connected sums, pasting the handles, and the topological balance equations (similar to the equations (22) -- (29)) remain strongly valid [30] upon this change. Hence, the final choice of exact $2D$ images of molecules with (2c,1e) and (3c,2e) bonds is wide. Nevertheless, the simplest pseudomanifolds derived from the bouquets of spheres (with definitive base points and simple invariants m_i and M) remain more effective tools for topological analysis of delocalized molecules.
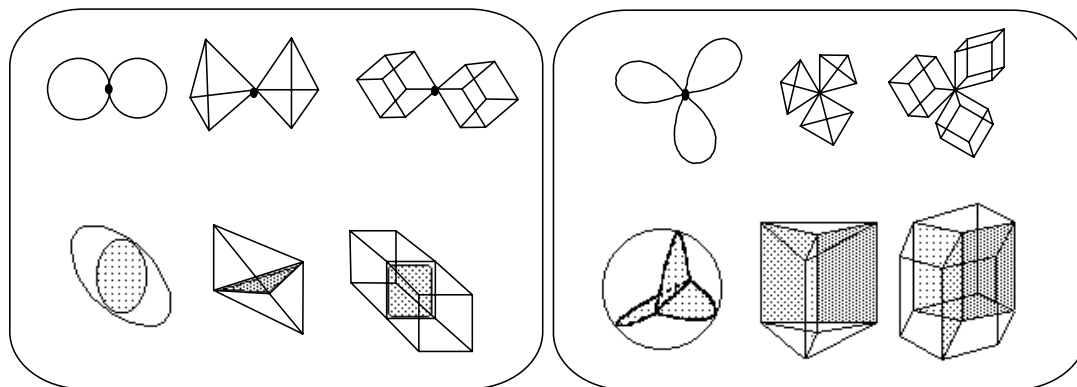

Figure 38. Some examples of topological $2D$ objects with $\chi = 3$ (left) and $\chi = 4$ (right). Shaded e^2 cells are located *inside* the external $2D$ surface. The triangulation of pseudomanifolds (representation of joint spheres by adjacent polyhedrons) helps to clarify how to calculate the χ value.

12. Orientation, Spin, and Nonorientable Surfaces of Free Radicals

Let us clarify how the abstract pasting of holes in molecular topoids is related to the orientability of the resulting surface. Is it possible to join two holes in a cylindrical surface of a biradical in a manner to obtain the Klein bottle instead of handle of a torus?

The hole represents the center of free electron location. Free electron has a certain spin. The recombination of radicals (shifts from the triplet to the singlet states, intermolecular or intramolecular ones) requires opposite spins of interacting electrons. Therefore, it seems reasonable to reflect the sign of a spin by assigning the orientation around the $1D$ boundary of a hole. It may be either clockwise or anti-clockwise. Let us consider the *initial* orientation of boundaries, that is, the spin (Figure 39 A, D), and distinguish it from the *final* orientation of $1D$ boundaries (Figure 39 B, C) in the moment of gluing. (To glue two hemispheres, we need to overturn one of them.) Initial opposite orientation of two holes (case D), favorable for the recombination of radicals, implies the final consonant orientation (case C). On the contrary, initial parallel orientation of holes (case A), forbidden for the recombination of radicals, becomes opposite in the final step of gluing (case B). This is true for the disconnected (a pair of hemispheres) and connected objects (like a cylinder in Figure 39 E -- H). Hence, the concept of forming the electron pair by electrons of opposite spin is nothing else but the topological principle of "true-type gluing" (discussed in Section 2.5 for polygons and surfaces).

We may conclude that the initially opposite orientation around the boundaries of the holes in a cylinder (opposite spins, case H) after pasting via step G may result only in torus, but not in the Klein bottle. However, joining of two holes with initially parallel orientation (equal spins, case E) may be achieved via step F leading to the Klein bottle. Hence, the structure of a triplet biradical (with parallel spins) may be equally presented by either the cylinder (noncompact, open, orientable surface) or by the Klein bottle (compact, closed, nonorientable surface). In other words, the idea of orientation (spin) of open noncompact surface naturally implies the possibility of using closed (although nonorientable) surfaces as images of free radical molecules.

If a biradical is representable by a closed nonorientable surface, what about the analogous $2D$ model of a single radical? The boundary of the single hole in the surface of a methyl radical (or a hydrogen atom) may be "pasted to itself" leading to the closed nonorientable surface, a projective plane. The procedure is simple: take a hole, add an $1D$ boundary (*e.g.*, 2-gon), define an orientation, and apply "false type" of gluing (identifying opposite points of the 2-gon). This is equivalent to the pasting a Möbius band (or a "crossed-cap") to the hemisphere (see Section 2.3 and Figure 4). Let us check that this does not contradict to the model of the triplet biradical as the Klein bottle: the connected sum of two projective planes should be the Klein bottle. The equivalent of connected sum in topoid model is the removal of a pair of hydrogen atoms (one atom from each CH_3 radical) and pasting the holes by a tube (C-C bond). Indeed, the connected sum of two methyl radicals is the triplet ethylene with topology of the Klein bottle.

Molecular modeling of free radicals by closed topological objects is difficult. Therefore, free radicals have been long ignored in the chemical graph theory and classical $2D$ models. As proven above (Section 5), the combinatorial picture becomes

self-consistent only if one considers the topological models of free radicals as the nonclosed objects (the concept of graphoid or topoid with holes). However, it seems possible to sacrifice the orientability in favor of the ability of describing any $2D$ models by closed sets of cells e^0, e^1, and e^2 only. It is essential that such a shift from open to closed surfaces *does not influence* the Euler characteristic. A Möbius band (crossed cap) pasted to the hole decreases the χ value by one, precisely as the hole itself. The closed type of topoids may also be better relating to the concept of spin density surfaces,
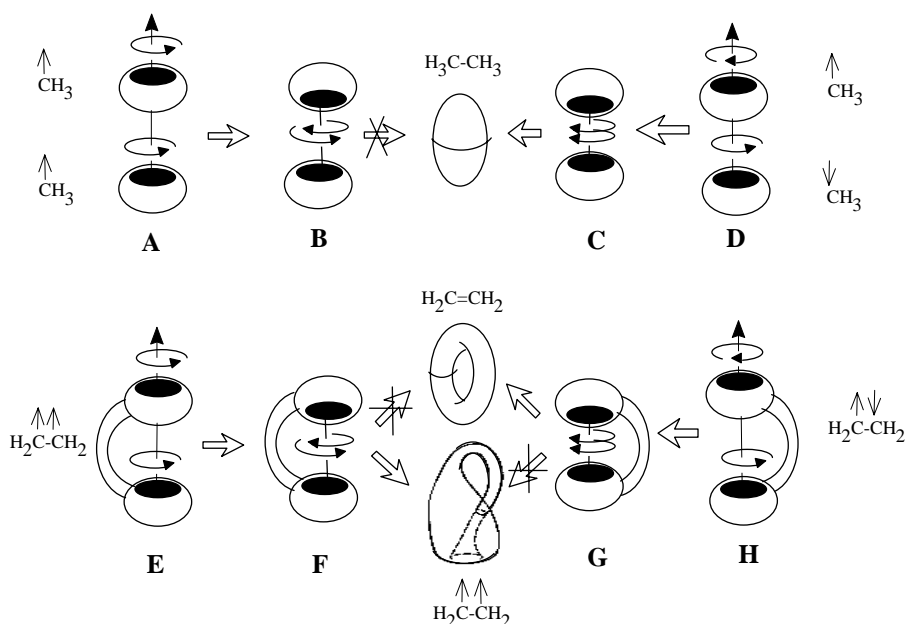

Figure 39. Various possibilities of pasting the holes in the topoids of free radicals (see the text).

although nonorientable surfaces are self crossed in R^3 (but not in R^4). Furthermore, some homeomorphisms of nonorientable surfaces are intriguing. Thus, the structure of triradical and tetraradical species may be represented by the following connected sums:

Triradicals: $N_1 \# N_1 \# N_1 \sim N_1 \# N_2 \sim N_1 \# S_1$, and

Tetraradicals: $N_1 \# N_1 \# N_1 \# N_1 \sim N_1 \# N_1 \# S_1 \sim N_2 \# N_2 \sim N_2 \# S_1$

(Here # is an operation of taking connected sum; N_1 is the projective plane, N_2 is the Klein bottle, S_1 torus, the $\sim$ symbol denotes the homeomorphism.) Attention should be paid to the appearance of a torus S_1 in the connected sum. The formal appearance of a handle for a closed molecular topoid (as we discussed throughout the paper) means some "extra-connectedness". Should an unexpected excess of bonding be observed for highly excited states of molecules?

Conclusion

The questions we put in the beginning of this paper are answered. The model of (hyper)topoids opens an opportunity to relate discrete chemical structures one to another by continuous mapping so that the topological identity (homeomorphism) of molecular $2D$ models corresponds to important types of the chemical similarity. The analysis of "surgery" of such (pseudo)manifolds helps to classify chemical reactions in a new compact way -- from the viewpoint of interchanges of global topological invariants of molecules.

The central feature of the discussed approach is the preservation of the Euler characteristic of molecular $2D$ models upon the formation, destruction, or rearrangement of chemical bonds. It is intriguing that this statement naturally follows from the common invariance of atoms and electrons upon a reaction. One would say, the conservation of mass and charge (that are, physical properties) causes conservation of a topological property. Although we proved this only for a specific type of molecular $2D$ models, there may be an analogous conservation law for the molecules as $3D$ object embedded in space R^3. However, it is still somewhat difficult to treat molecular models (and the molecules themselves) in explicit terms of $3D$ topology: even nowadays the complete classification of $3D$ manifolds is a hard problem of mathematics. According to Mandelbaum [140], it is somewhat ironic that the worlds about which we have the lack of knowledges are just the $3D$ world of physical geometry and $4D$ world of space and time. An increase of these knowledges, therefore, may dramatically influence the field of molecular modeling and its further evolution.

Acknowledgment

References

1. A. T. Balaban. *Chemical Applications of Graph Theory*. Academic Press: London, 1976.

2. N. Trinajstic. *Chemical Graph Theory*. Vols. 1,2. CRC Press: Boca Raton, FL, 1983; 2nd Ed. 1992.

3. *Chemical Applications of Topology and Graph Theory* (A Collection of Papers on a Symposium Held at the University of

Georgia, Athens, Georgia U.S.A.) Ed. R. B. King. Elsevier: Amsterdam, 1983

4. *Applications of Graphs in Chemistry and Physics.* Eds. J. W. Kennedy, L. V. Quintas. North-Holland: Amsterdam, 1988.

5. A. L. Goodson, L. A. Petrov, O. N. Temkin, D. Bonchev, P. Plath, E. Hass. *Graph Theory and Its Application to Chemistry: Kinetics and Reaction Mechanisms* (Graph Theory and Its Application to Chemistry Vol. 2.). Abacus Press / Gordon & Breach: New York, 1989.

6. *Graph Theory and Its Applications to Chemistry: Molecular Structures and Properties* (Graph Theory and Its Applications to Chemistry: Vol. 3). Ed. D. H. Rouvray. Abacus Press / Gordon & Breach: New York, 1989.

7. *Computational Chemical Graph Theory.* Ed. D. H. Rouvray. Nova Science Publ.: Commack, NY, 1990.

8. N. Trinajstic, S. Nikolic, J.V. Knop, W.R. Muller, K. Szymanski. *Computational Chemical Graph Theory: Characterization, Enumeration, and Generation of Chemical Structures by Computer Methods* (Ellis Horwood Series). Horwood: Chichester, 1991.

9. *Chemical Graph Theory : Introduction and Fundamentals* (Mathematical Chemistry, Vol 1). Eds. D. H. Rouvray, D. Bonchev. Abacus Press/Gordon and Beach: New York, 1991.

10. *Graph Theoretical Approaches to Chemical Reactivity* (Understanding Chemical Reactivity, Vol. 9) Eds: D. Bonchev, O. Mekenyan. Kluwer Academic Publ.: Dordrecht-Boston-London, 1994.

11. *Graph Theory and Topology in Chemistry* (Studies in Physical and Theoretical Chemistry, Vol 51) Eds. R. B. King, D. H. Rouvray. Elsevier: Amsterdam, 1987

12. R. E. Merrifield, H. E. Simmons. *Topological Methods in Chemistry.* Wiley Interscience: New York, 1989

13. *From Chemical Topology to Three-Dimensional Geometry* (Topics in Applied Chemistry) Ed. A. T. Balaban. Plenum: New York, 1997.

14. R. B. King. *Applications of Graph Theory and Topology in Inorganic Cluster and Coordination Chemistry.* CRC Press: Boca Raton, FL, 1993

15. I. S. Dmitriev. *Molecules Without Chemical Bonds: Essays on Chemical Topology.* Imported Pubn, 1981. Original: Khimija Publ.: Leningrad, 1980 (in Russian).

16. P. G. Mezey. *Shape in Chemistry : An Introduction to Molecular Shape and Topology.* VCH Publ.: New York, 1993

17. P. E. Schipper. *Symmetry and Topology in Chemical Reactivity.* World Scientific Publ.: Singapour, 1994

18. R. G. Pearson, Symmetry Rules for Chemical Reactions: Orbital Topology and Elementary Processes , J. Wiley and Sons: New York, 1976.

19. D. Bonchev. *Information Theoretic Indices for Characterization of Chemical Structures.* Research Studies Press: Chichester, 1983

20. N. Trinajstic. *Mathematical and Computational Concepts in Chemistry* (Ellis Horwood Series: Mathematics and Its Applications). Horwood: Chichester, 1986

21. P G. Mezey. *Potential Energy Hypersurfaces* (Studies in Physical and Theoretical Chemistry, Vol 53). Elsevier: Amsterdam, 1987

22. *Mathematical Modeling in Chemistry.* Ed. P. G. Mezey VCH Pub.: New York, 1991

23. *Chemical Graph Theory: Reactivity and Kinetics* (Mathematical Chemistry, Vol 2). Eds. D. Bonchev, D. H. Rouvray. Abacus Press/Gordon & Breach: New York, 1992

24. *Chemical Group Theory: Introduction and Fundamentals* (Mathematical Chemistry, Vol 3). Eds. D. Bonchev, D. H. Rouvray. Abacus Press/Gordon & Breach: New York, 1994

25. *Chemical Group Theory: Techniques and Applications* (Mathematical Chemistry, Vol 4) Danail Bonchev, Dennis H. Rouvray Abacus Press/Gordon & Breach: New York, 1995

26. O. N. Temkin, A. V. Zeigarnik, D. Bonchev. *Chemical Reaction Networks: A Graph-Theoretical Approach.* CRC Press: Boca Raton, FL, 1996.

27. *Concepts in Chemistry: A Contemporary Challenge.* Ed. D. H. Rouvray. Research Studies Press / John Wiley & Sons: Taunton, New York, 1997.

28. P. G. Mezey. *Reports in Molecular Theory* **1(2)** (1990) 165.

29. E. V. Babaev, R. Hefferlin in: *Concepts in Chemistry: A Contemporary Challenge.* Ed. D. H. Rouvray. Research Studies Press and John Woley & Sons: New York - Chichester, 1997, pp.41-100.

30. E. V. Babaev, "Chemical Concepts from the Viewpoint of Surfaces' Topology", *6th International Conference on Mathematical Chemistry* (Pitlocry, Scotland, July 10-14, 1995, plenary lecture). Abstract of papers, p.46.

31. E. V. Babaev, in: *Graph Theoretical Approaches to Chemical Reactivity* (Understanding Chemical Reactivity, Vol. 9). Eds. D. Bonchev and O. Mekenyan. Kluwer Academic: Dordrecht-Boston-London, 1994, pp. 209-220.

32. E. V. Babaev, in: *Principles of Symmetry and Systemology in Chemistry.* Ed. N. F. Stepanov. Moscow University Press:

Moscow, 1987, pp. 203-227 (in Russian). [Chem. Abstr. 109: 27902b]

33. E. V. Babaev, in: *Philosophical Problems of Chemistry* (History and Methodology of Natural Sciences, Vol. 35). Ed. A. P. Rudenko, Moscow University Press: Moscow, 1988, pp. 121-140 (in Russian).

34. D. Hilbert, S. Cohn-Vossen. *Ahnsaulische Geometrie* (in German), 1932; [Engl. Translation: *Geometry and the Imagination.* Chelsea: New York, 1967; Russian Translation: Moscow, Nauka Publ., 1981.]

35. G. K. Francis. *A Topological Picturebook*. Springer Verlag, New York - Berlin, 1988.

36. A. T. Fomenko. *Visual Geometry and Topology*. Springer Verlag: Berlin, New York, 1994

37. V. G. Boltyanskii, V. G. Efremovich. *Visual Topology* (in Russian). Nauka Publ.: Moscow, 1982.

38. F. Harary. *Graph Theory*. Addison-Wesley: Reading, MA, 1969.

39. J. L. Gross, T. N. Tucker. *Topological Graph Theory*. Wiley: New York, 1987.

40. A. A. Zykov. *Foundations of Graph Theory* (in Russian). Nauka Publ.: Moscow, 1987.

41. P. J. Giblin. *Graphs, Surfaces and Homology: An Introduction to Algebraic Topology*. Chapman and Hall: London, 1981.

42. H. B. Griffiths. *Surfaces.* Cambridge University Press: Cambridge, 1976.

43. P.A. Firby, C. F. Gardiner. *Surface Topology* (Ellis Horwood Series Mathematics and Its Applications). 2nd Edition. Horwood: Chichester, 1992.

44. F. Morgan. *Amer. Math. Monthly*, **103** (1996) 369.

45. S. Wagon in: *Mathematica in Action*. New York: W. H. Freeman, 1991, pp. 67-91.

46. H. Seifert, W. Trelfall. *Lehrbuch der Topologie*. Dresden, 1934. [Russian Translation: Moscow: GONTI, 1938. English Translation: *A Textbook of Topology.* Pure and Appl. Math. Ser., 1980.]

47. B.A. Dubrovin, A.T. Fomenko, S.P. Novikov. *Modern Geometry-Methods and Applications: Part Ii, the Geometry and Topology of Manifolds* (Graduate Texts in Mathematics, Vol 104). Springer Verlag: Berlin, New York, 1985

48. J. Stillwell. *Classical Topology and Combinatorial Group Theory*. Springer Vertlag: Berlin, 1980.

49. A. T. Fomenko, D. B. Fuchs. *A Course in Homotopy Topology* (in Russian). Nauka Publ.: Moscow, 1989.

50. C. Berge. *Graphes et Hypergraphes* (in French). Dunod, Paris, 1970.

51. A. A. Zykov. *Uspekhi Mathematicheskih Nauk*, **29(6)** (1974) 89 (in Russian).

52. E. V. Babaev. "Lewis Diagrams and Topology". In: *Proceed. of Conference of young scientists* (Moscow University, January 25-28, 1986), Part 1, pp.154-157. [Russian Ref. Journal 6B(1987)1107].

53. E. V. Babaev. "Topological Design of Molecular Structures". In: *Proceed. of 7th All-Union Conference on Application of Computers in Chemical Research and Molecular Spectroscopy* (Riga, October 21-23, 1986), pp.210-212. [Russian Ref. Journal 7A(1987)36].

54. Q. R. Petersen. *J. Chem. Education*, **47** (1970) 24.

57. D. H. Rouvray. *Chem. & Ind.*, **15** (1997) 587.

58. A. R. Leach. *Molecular Modeling: Principles and Applications*. Longmans: Harlow, 1996.

59. W. Gans. *Fundamental Principles of Molecular Modeling*, Plenum: New York, 1996.

60. R. B. Corey, L. Pauling. *Rev. Sci. Instr.*, **24** (1953) 621.

61. *The Chemistry of Alkanes and Cycloalkanes (The Chemistry of Functional Groups).* Eds. S. Patai, Z. Rappoport. Wiley: New York, 1992.

62. A. J. Gordon. *J. Chem. Education*, **47** (1970) 30.

63. M. L. Connolly. *Molecular Surfaces: A Review; Network Science* [On line]. **2**(4) 1996. Available HTTP: http://www.awod.com/netsci/Science/Compchem/feature14.html.

64. Li Xia, N. B. Crane. *Electronic Style: A Guide to Citing Electronic Information*. Mecklermedia: Westport, 1993.

65. W. Heiden, M. Schlenkrich, C.-D. Zachmann, J. Brickmann. in: *Software Development in Chemistry*. Ed. J. Gasteiger. Springer: Berlin - Heidelberg, 1989, p.115.

66. R. J. Zauhar. *J. Computer-Aided Molecular Design*, **9** (1995) 149.

67. B. Lee, F. M. Richards. *J. Mol. Biol.*, **55** (1971) 379.

68. M. L. Connolly. J. Appl. Crystallogr., **16** (1983) 548.

69. M. L. Connolly. Science, **221** (1983) 709.

70. F. Beilstein. *Handbuch der Organischen Chemie*. VOSS: Hamburg - Leipzig, Bd. I, 1888 -- 1890.

71. R. F. W. Bader. *Chem. Rev.* **91** (1991) 993.

72. R. F. W. Bader. *Atoms in Molecules: A Quantum Theory* (The International Series of Monographs on Chemistry, No 22). Oxford University Press: Oxford, 1994

73. R. F. W. Bader, R. J. Gillespie, P. G. Macdougal, in: *From Atoms to Polymers: Isoelectronic Analogies* (Molecular Structure and Energetics, Vol. 11). Eds. J. F. Liebman, A. Greenberg. VCH: New York, 1989, pp. 1-51.

74. U. Burkert, N. L. Allinger. *Molecular Mechanics* (ACS Monograph 177). American Chemical Society: Washington DC, 1982.

75. R. F. Hout, W. J. Pietro, W. J. Hehre. *A pictorial approach to molecular structure and reactivity*. John Wiley & Sons: New York, 1984.

76. A. Streitwieser. *Molecular Orbital Theory for Organic Chemists*. Wiley: New York, 1961.

77. M. J. S. Dewar. *Molecular Orbital Theory of Organic Chemistry*. McGraw Hill: New York, 1969.

78. K. Fukui. *Theory of Orientation and Stereoselection.* Springer: Berlin, 1975.

79. R. Hoffman. *Science*, **211** (1981) 995.

80. N. Trinajstic in: *Semiempirical Methods of Electronic Structure Calculation. Part A: Techniques.* Ed. G. A. Segal. Plenum: New York, 1977, p.1.

81. J. R. Dias. *Molecular Orbital Calculations Using Chemical Graph Theory* (Springer Textbook). Springer: New York, Berlin, 1993

82. H. B. Thompson. *Inorg. Chem.*, **7** (1968) 604.

83. W. C. Herndon, M. L. Ellzey Jr., K. S. Raghuveer, *J. Amer. Chem. Soc.*, **100** (1978) 2645.

84. G. Bieri, J. D. Dill, E. Heilbronner, A. Schmelzer. *Helv.Chim.Acta*, **60** (1977) 2234.

85. R. B. Davidson. *J. Chem. Education*, **54** (1977) 531.

86. J. Fossey, D. Lefort, J. Sorba. *Free Radicals in Organic Chemistry.* John Wiley & Sons: New York.

87. *The Chemistry of Double-Bonded Functional Groups, Part 1* (Chemistry of Functional Groups: Supplement, A) Ed. S. Patai. Volume 2. John Wiley & Sons: New York. 1990

88. *Chemistry of Carbenes and Small-Sized Cyclic Compounds* (Advances in Science and Technology in the USSR. Chemistry Series). Ed. O. M. Nefedov. Imported Publ. 1989.

89. P. A. Schultz, R. P. Messmer. *Phys. Rev. Lett.*, **58** (1987) 2416.

90. R. P. Messmer, P. A. Schultz, R. C. Tatar, H.-J. Freund. *Chem. Phys. Lett.*, **126** (1986) 176.

91. *Valence Bond Theory and Chemical Structure* (Studies in Physical and Theoretical Chemistry, Vol. 64). Eds. D. J. Klein, N. Trinajstic. Elsevier Science: Amsterdam, 1990

92. G. N. Lewis. *J. Amer. Chem. Soc.*, **38** (1916) 762.

93. G. N. Lewis. *Valence and the Structure of Atoms and Molecules*. Dover: New York, 1966.

94. J. W Linnett. *The Electronic Structure of Molecules.* Methuen & Co., London, 1964.

95. I. Langmuir. *J. Amer. Chem. Soc.*, **41** (1919) 868, 1543.

96. R. J. Gillespie, R. S. Nyholm. *Quart. Rev. Chem. Soc.*, **11** (1957) 339.

97. R. J. Gillespie. *Molecular Geometry*. van Nostrand - Reinhold: Princeton, New Jersy, 1972.

98. R. J. Gillespie, I. Hargittai. *The VSEPR Model of Molecular Geometry*. Allyn and Bacon: Boston - London, 1991.

99. M. Creon Levit. "A New Pictorial Approach to Molecular Structure and Reactivity" *First Electronic Molecular Modeling & Graphics Society Conference*, October 1996. [On line]. Available HTTPs: http://science.nas.nasa.gov/~creon/nano/laplace.html and http://science.nas.nasa.gov/~creon/papers/mgms96/

100. G. I. Csonka, N. Anh, I. Kolossváry. "3D visualization of the chemical bonds and properties using the Laplacian of the electron density". *Second Electronic Conference in Computational Chemistry* (ECCC2, November, USA, 1995). [On line]. Available HTTP: http://www.ch.bme.hu/inc/ECCC2/paper5/lapl.html.

101. W. B. Jensen. *The Lewis Acid-Base Concepts: An Overview.* Krieger Publ. Co.: Amsterdam, 1979.

102. J. U. Nef. *Annalen* **288** (1896) 202.

103. I. Ugi, P. Gillespie. *Angew. Chem.*, **83** (1973) 980, 982. [*Angew. Chem., Int. Ed. Engl.,* **10** (1973) 914, 915.]

104. Dugundji, J.; Ugi, I. Top. Curr. Chem. 39 (1973) 19.

105. V. Kwasnicka, *Coll. Czech. Chem. Comm.*, **48** (1983) 2097.

106. S. H. Bertz in Ref. 3, [p. 236 in Russian translation: Moscow: Mir, 1987).

107. H. A. Bent, *J. Chem. Educ.* **43** (4), 170 (1966).

108. H. Shmidbaur, *Fortchr. Chem. Forsh.* **13** (1), 167 (1969)

109. *Carbonium ions*. Eds G. A. Olah, P. v. R. Schleyer. Wiley: New York. Vols. 1 -- 5 (1968 -- 1976).

110. J. March. *Advanced Organic Chemistry. Reactions, Mechanisms, and Structure.* Wiley: New York, 1985.

111. G. A. Olah, G. K. S. Prakash, R. E. Williams, L. D. Field, K. Wade. *Hypercarbon Chemistry*. Wiley: New York, 1987.

112. *Fluorine - Perfluorohalogenoorgano Compounds of Main Group Elements: Handbook of Inorganic and Organometallic Chemistry.* Eds. A. Haas, M.E. Peach, D. Koschel. 8th Edition, Springer Verlag: Berlin, 1995

113. W. d'Arcy Tompson. *On Growth and Forms*. University Press: Cambridge, 1917; 2nd Edn., 1942.

114. E. V. Presnov, V. V. Isaeva. *Topological Surgery in Morphogenesis* (in Russian). Nauka: Moscow, 1985.

115. E. V. Babaev, D. E. Lushnikov, N. S. Zefirov. *J. Amer. Chem. Soc.,* **115** (1993) 2416.

116. Yu. A. Zhdanov. *Homology in Organic Chemistry*. Moscow University Press: Moscow, 1950 (in Russian).

117. *Concepts and Applications of Molecular Similarity*. Eds. M. A. Johnson and G. M. Maggiora, Wiley: New York, 1990.

118. H. Niedenzu, J. W. Dawson. *Boron - Nitrogen Compounds*. Springer: Berlin, 1965.

119. A. W. Johnson, W. C. Kaska. *Ylides and Imines of Phosphorus.* Wiley: New York, 1993.

120. B. M. Trost, L. S. Melvin. *Sulfur Ylides: Emerging Synthetic Intermediates*. Academic Press: London, 1975.

121. V. I. Minkin, M. N. Glukhovtsev, B. Ya. Simkin. *Aromaticity and Antiaromaticity: Electronic and Structural Aspects.* Wiley: New York, 1994.

122. P. J. Garratt. *Aromaticity.* Wiley: New York, 1986.

123. W. N. Lipscomb. *Boron Hydrides.* Benjamin: New York, 1963.

124. R. W. Rudolf. *Acc. Chem. Res.*, **12** (1976) 446.

125. K. Wade. *Adv. Inorg. Chem. Radiochem.*, **18** (1976) 1.

126. R. E. Williams. *Adv. Inorg. Chem. Radiochem.*, **18** (1976) 67;

127. D. M. P. Mingos, R. L. Johnson. *Theoretical Model of Cluster Bonding* (Structure and Bonding). Springer-Verlag: Berlin, 1987, p. 29.

128. D. Nicholls. *Inorganic Chemistry in Liquid Ammonia*. Elsevier: Amsterdam, 1980.

129. E. Flapan. *Private communication* (September, 1997).

130. K. Balasubramanian. *Chem. Rev.*, **85** (1985) 599.

131. S. S. Shaik, P. C. Hiberty, J. M. Lefour, G. Ohanessian. *J. Am. Chem. Soc.*, **109** (1987) 363.

132. K. Jug, A. M. Köster. *J. Am. Chem. Soc.*, **112** (1990) 6772.

133. S. Bauerschmidt, J. Gasteiger. *J. Chem. Inf. Comput. Sci.*, **37** (1997) 705.

134. A. Dietz. *J. Chem. Inf. Comput. Sci.*, **35** (1995) 787.

135. I. Ugi, N. Stein, M. Knauer, B. Gruber, K. Bley, R. Weidinger. *Top. Curr. Chem.*, **166** (1993) 199.

136. J. Shorter. *Nat. Prod. Reports*, **4** (1987) 61.

137. G. A. Olah. *J. Am. Chem. Soc.*, **94** (1972) 808.

138. E. V. Konstantinova, V. A. Skorobogatov. *J. Chem. Inf. Comput. Sci.*, **35** (1995) 472.

139. J. Gasteiger, W. Hanebeck, K. P. Schulz. *J. Chem. Inf. Comput. Sci.*, **32** (1992) 264.

140. R. Mandelbaum. *Four-Dimensional Topology*. University of Rochester Press: Rochester, 1978.